RETURN TO DESK
J82
THE JOHN CRERAR
NOV 17 1948
LIBRARY

JOURNAL OF THE AERONAUTICAL SCIENCES

VOLUME 15 NOVEMBER, 1948 NUMBER 11

CONTENTS

The Transient Reaction of an Airfoil Due to Change in Angle of Attack at Supersonic Speed ..... CHIEH-CHIEN CHANG 635

Vorticity in the Supersonic Flow About Yawing Cones ..... MARK M. LOTKIN 656

The Bending Modulus of Rupture of Round Magnesium Tubing ..... C. H. MORTENSON 661

Unsteady One-Dimensional Flows with Heat Addition or Entropy Gradients ..... A. KAHANE AND LESTER LEES 665

Transonic Separation ..... VERNON OUTMAN AND ARTHUR A. LAMBERT 671

Variational Method in the Theory of Compressible Fluid ..... CHI-TEH WANG 675

The Theoretical Induced Deflection Angle in Cascades Having Wall Boundary Layers ..... GEORGE F. HAUSMANN 686

Surface-Pressure Gradient and Shock-Front Curvature at the Edge of a Plane Ogive with Attached Shock Front ..... M. M. MUNK AND R. C. PRIM 691

Letters to the Editor 655, 664

Published by the

INSTITUTE OF THE AERONAUTICAL SCIENCES, INC.

JOURNAL OF THE AERONAUTICAL SCIENCES

Editor: HUGH L. DRYDEN, *Director of Aeronautical Research, N.A.C.A.*

Associate Editor: ROBERT R. DEXTER *Associate Editor:* BERNEICE H. JARCK

The Institute of the Aeronautical Sciences publishes monthly the JOURNAL OF THE AERONAUTICAL SCIENCES and the AERONAUTICAL ENGINEERING REVIEW.

The JOURNAL OF THE AERONAUTICAL SCIENCES prints papers of scientific and technical interest to Institute members and subscribers. In general, it provides an opportunity for specialists to publish articles disclosing new knowledge and new applications in the field of the aeronautical sciences. The JOURNAL restricts itself to the aeronautical aspects of advances in science and engineering, and papers printed have either been submitted directly to the JOURNAL or have been previously presented at a meeting of the Institute.

The AERONAUTICAL ENGINEERING REVIEW keeps members and subscribers informed regarding the contents of new books and current periodicals in the field of aeronautics. It reviews new developments in the aircraft industry and reports on progress from house organs and catalogs published by aircraft and engine manufacturers and other companies engaged in aeronautical activities. It publishes papers on applied engineering and aircraft production. News of Institute activities is published in the REVIEW.

Statements and opinions expressed in the JOURNAL are to be understood as individual expressions of the authors and not those of the Institute.

SUBSCRIPTION RATES

Journal of the Aeronautical Sciences
Published Monthly

United States and Possessions		Foreign Countries Including Canada (American Currency Rates)	
1 Year	$12.00	1 Year	$13.00
Single Copies	1.50	Single Copies	1.50

Aeronautical Engineering Review
Published Monthly

United States and Possessions		Foreign Countries Including Canada (American Currency Rates)	
1 Year	$3.00	1 Year	$3.50
Single Copies	0.50	Single Copies	0.50

Notices of change of address should be sent to the Institute at least 30 days prior to actual change of address.

Manuscripts for publication, proofs, and all correspondence should be addressed to the Editorial Office of the JOURNAL.

Correspondence regarding subscriptions may be addressed to Publication Office, 20th and Northampton Sts., Easton, Pa., or to the Editorial Office of the JOURNAL OF THE AERONAUTICAL SCIENCES, 2 East 64th Street, New York 21, New York.

Copyright, 1948, by the Institute of the Aeronautical Sciences, Inc.

Entered as Second Class Matter at the Post Office, Easton, Pa., May 1, 1937. Acceptance for mailing at a special rate of Postage provided for in the Act of August 24, 1912. Authorized April 29, 1937.

IN

JOHN K

SMITH J
C. L. J
R. P. L
EARL D

S. PAUL

BENNET

E. E. A
REX B.
LAWREN
WILLIAM
W. A. M
VICTOR

WALTER
FRANK W
RALPH S
KENNETH
R. H. FL
R. PAUL

JOHN R. A
JOHN N. B
FRANK O.
E U. CON
L. C. CRA
DONALD B

E. H. ARN
FRANK W.
SIR GEOFF
JAMES H.
DONALD W

S. E. ALDR
HART O. B
W. A. M. B
E. L. CORD
DONALD W.
SHERMAN

IRA H. ABB
JOHN D. AR
S. E. ALDRI
HARRY G. A
KARL ARNS
J. L. ATWOO
PAUL S. BA
RALPH S. B
P. R. BASSE
WELLWOOD
REX B. BEE
G. M. BELLA
DON R. BER
HENRY A. B
WILLIAM BO
GEORGE W.
LYMAN J. B
W. G. BROM
WILLIAM G.
CHARLES P.
KENNETH CA
CHARLES H.
ALLAN CHIL
FRANKLIN R.
CHARLES H.
KARL T. CO
EMERSON W.
JOHN W. CR
RALPH S. DA
LUIS DE FLO
SMITH J. DE
J. P. DEN H
WALTER S. D
C. S. DRAPE
IVAN H. DRE
WILLIAM K.
C. L. EGTVE
FREDERIC F

INSTITUTE of the AERONAUTICAL SCIENCES

President

JOHN K. NORTHROP

Vice-Presidents

SMITH J. DE FRANCE
C. L. JOHNSON
R. P. LANSING
EARL D. OSBORN

Director

S. PAUL JOHNSTON

Executive Vice-President

BENNETT H. HORCHLER

Past-Presidents

J. C. HUNSAKER
CHARLES L. LAWRANCE
DONALD W. DOUGLAS
GLENN L. MARTIN
CLARK B. MILLIKAN
T. P. WRIGHT
GEORGE W. LEWIS (Deceased)
JAMES H. DOOLITTLE
FRANK W. CALDWELL
HALL L. HIBBARD
HUGH L. DRYDEN
R. H. FLEET
CHARLES H. COLVIN
ARTHUR E. RAYMOND
P. R. BASSETT

Secretary

ROBERT R. DEXTER

Treasurer

SHERMAN M. FAIRCHILD

Controller

JOSEPH J. MAITAN

Counsel

ALLAN D. EMIL

COUNCIL

E. E. ALDRIN
REX B. BEISEL
LAWRENCE D. BELL
WILLIAM BOLLAY
W. A. M. BURDEN
VICTOR E. CARBONARA
FRANK O. CARROLL
CHARLES H. COLVIN
JAMES H. DOOLITTLE
C. C. FURNAS
LEROY R. GRUMMAN
J. A. HERLIHY
JEROME LEDERER
JOHN C. LESLIE
JACK MASON
C. KENNETH RAZAK
L. B. RICHARDSON
RUSSELL G. ROBINSON
GEORGE S. SCHAIRER
ERNEST G. STOUT
A. J. THIEBLOT

ADVISORY COMMITTEE

WALTER BEECH
FRANK W. CALDWELL
RALPH S. DAMON
KENNETH S. M. DAVIDSON
R. H. FLEET
R. PAUL HARRINGTON
R. M. HAZEN
HALL L. HIBBARD
J. C. HUNSAKER
TH. VON KÁRMÁN
THOMAS A. KNOWLES
I. M. LADDON
GROVER LOENING
GLENN L. MARTIN
CLARK B. MILLIKAN
THOMAS A. MORGAN
ARTHUR E. RAYMOND
F. W. REICHELDERFER
LAURANCE S. ROCKEFELLER
T. CLAUDE RYAN
ELMER A. SPERRY, JR.
EDWARD P. WARNER
BURDETTE S. WRIGHT
T. P. WRIGHT

HONORARY MEMBERS

JOHN R. ALISON
JOHN N. BROWN
FRANK O. CARROLL
E. U. CONDON
L. C. CRAIGIE
DONALD B. DUNCAN
HARRY F. GUGGENHEIM
GEORGE C. KENNEY
THEODORE LONNQUEST
JOSEPH J. O'CONNELL, JR.
HOWARD T. ORVILLE
GEORGE B. PEGRAM
E. M. POWERS
ALFRED M. PRIDE
J. LAURENCE PRITCHARD
F. W. REICHELDERFER
DELOS W. RENTZEL
CARL SPAATZ
W. STUART SYMINGTON
J. W. TICE
HOYT S. VANDENBERG

HONORARY FELLOWS

H. H. ARNOLD
FRANK W. CALDWELL
SIR GEOFFREY DE HAVILLAND
JAMES H. DOOLITTLE
DONALD W. DOUGLAS
HUGH L. DRYDEN
W. F. DURAND
SIR RICHARD FAIREY
SIR ROY FEDDEN
J. C. HUNSAKER
SIR MELVILL JONES
GLENN L. MARTIN
GEORGE J. MEAD
SIR FREDERICK HANDLEY PAGE
D. R. PYE
IGOR I. SIKORSKY
SIR GEOFFREY TAYLOR
TH. VON KÁRMÁN
EDWARD P. WARNER
T. P. WRIGHT

BENEFACTORS

E. E. ALDRIN
HART O. BERG (Deceased)
W. A. M. BURDEN
E. L. CORD
DONALD W. DOUGLAS
SHERMAN M FAIRCHILD
SIR RICHARD FAIREY
R. H. FLEET
FLORENCE GUGGENHEIM (Deceased)
C. D. HANSCOM
JOHN P. V. HEINMULLER
ALEXANDER KLEMIN
PAUL KOLLSMAN
BELLA C. LANDAUER
WILLIAM LANDAUER
GROVER LOENING
EDMUND C. LYNCH (Deceased)
F. W. MAGIN
GLENN L. MARTIN
GEORGE J. MEAD
S. A. REED (Deceased)
LAURANCE S. ROCKEFELLER
EDWARD P. WARNER

AMERICAN FELLOWS

IRA H. ABBOTT
JOHN D. ACKERMAN
E. E. ALDRIN
HARRY G. ARMSTRONG
KARL ARNSTEIN
J. L. ATWOOD
PAUL S. BAKER
RALPH S. BARNABY
P. R. BASSETT
WELLWOOD E. BEALL
REX B. BEISEL
G. M. BELLANCA
DON R. BERLIN
HENRY A. BERLINER
WILLIAM BOLLAY
GEORGE W. BRADY
LYMAN J. BRIGGS
W. G. BROMBACHER
WILLIAM G. BROWN
CHARLES P. BURGESS
KENNETH CAMPBELL
CHARLES H. CHATFIELD
ALLAN CHILTON
FRANKLIN R. COLLBOHM
CHARLES H. COLVIN
KARL T. COMPTON
EMERSON W. CONLON
JOHN W. CROWLEY, JR.
RALPH S. DAMON
LUIS DE FLOREZ
SMITH J. DE FRANCE
J. P. DEN HARTOG
WALTER S. DIEHL
C. S. DRAPER
IVAN H. DRIGGS
WILLIAM K. EBEL
C. L. EGTVEDT
FREDERIC FLADER
CHARLES FROESCH
JACK FRYE
GARLAND FULTON
LESTER D. GARDNER
RICHARD C. GAZLEY
MICHAEL E. GLUHAREFF
MELVIN N. GOUGH
LEROY R. GRUMMAN
HAROLD R. HARRIS
R. M. HAZEN
EDWARD H. HEINEMANN
S. D. HERON
HALL L. HIBBARD
L. S. HOBBS
PAUL E. HOVGAARD
WILLIAM HOVGAARD
ROBERT INSLEY
EASTMAN N. JACOBS
C. L. JOHNSON
S. PAUL JOHNSTON
ALEXANDER KARTVELI
PAUL H. KEMMER
CARLETON KEMPER
J. H. KINDELBERGER
OTTO E. KIRCHNER
ARTHUR L. KLEIN
ALEXANDER KLEMIN
W. B. KLEMPERER
PAUL KOLLSMAN
OTTO C. KOPPEN
B. V. KORVIN-KROUKOVSKY
S. M. KRAUS
ARNOLD M. KUETHE
I. M. LADDON
E. S. LAND
CHARLES L. LAWRANCE
JEROME LEDERER
JOHN G. LEE
JOHN C. LESLIE
CHARLES A. LINDBERGH
WILLIAM LITTLEWOOD
GROVER LOENING
ALBERT E. LOMBARD
F. A. LOUDEN
W. RANDOLPH LOVELACE, II
EUGENE E. LUNDQUIST
R. D. MACCART
JOHN R. MARKHAM
ERLE MARTIN
WM. H. MCAVOY
C. J. MCCARTHY
J. S. MCDONNELL
CLARK B. MILLIKAN
ROBERT J. MINSHALL
JOSEPH S. NEWELL
ALFRED S. NILES
JOHN K. NORTHROP
ARTHUR NUTT
SHATSWELL OBER
ROBERT R. OSBORN
W. BAILEY OSWALD
GEORGE A. PAGE, JR.
F. W. PAWLOWSKI
F. W. PENNOYER, JR.
A. A. PRIESTER
ARTHUR E. RAYMOND
F. W. REICHELDERFER
ELLIOTT G. REID
H. J. E. REID
H. C. RICHARDSON
L. B. RICHARDSON
RUSSELL G. ROBINSON
LEONARD E. ROOT
C. E. ROSENDAHL
ADDISON M. ROTHROCK
W. R. SEARS
WILLIAM T. SCHWENDLER
FRANCIS R. SHANLEY
JAMES M. SHOEMAKER
IGOR ALEXIS SIKORSKY
ABE SILVERSTEIN
SELDEN B. SPANGLER
ELMER A. SPERRY, JR.
JOHN STACK
ROBERT M. STANLEY
WILLIAM B. STOUT
HARRY A. SUTTON
C. FAYETTE TAYLOR
EDWARD S. TAYLOR
PHILIP B. TAYLOR
TH. THEODORSEN
T. E. TILLINGHAST
S. TIMOSHENKO
L. B. TUCKERMAN
RALPH H. UPSON
J. PARKER VAN ZANDT
J. G. VINCENT
RICHARD VON MISES
FRANK L. WATTENDORF
P. V. H. WEEMS
FRED E. WEICK
R. D. WEYERBACHER
JOHN B. WHEATLEY
ANDREW V. WILLGOOS
DONALD H. WOOD
ROBERT J. WOODS
JOHN E. YOUNGER
ALBERT F. ZAHM
STEPHEN J. ZAND

CORPORATE MEMBERS

OF THE

INSTITUTE OF THE AERONAUTICAL SCIENCES

ACADEMY OF AERONAUTICS, INC.
CASEY JONES SCHOOL OF AERONAUTICS
AEROJET ENGINEERING CORPORATION
AEROPRODUCTS DIVISION, GENERAL MOTORS CORPORATION
AEROQUIP CORPORATION
AGAWAM AIRCRAFT PRODUCTS, INC.
AIRBORNE INSTRUMENTS LABORATORY, INC.
AIRCHOX COMPANY DIVISION, JOYCE AVIATION, INC.
AIRCRAFT RADIO CORPORATION
AIRESEARCH MANUFACTURING COMPANY, DIVISION OF THE GARRETT CORPORATION
ALLIS-CHALMERS MANUFACTURING COMPANY
ALLISON DIVISION, GENERAL MOTORS CORPORATION
ALUMINUM COMPANY OF AMERICA
AMERICAN AIRLINES SYSTEM
AMERICAN BOSCH CORPORATION
AMERICAN OVERSEAS AIRLINES, INC.
ICELAND AIRPORT CORPORATION (SUBSIDIARY)
AMERICAN PHENOLIC CORPORATION
ASSOCIATED AVIATION UNDERWRITERS
ATLAS SUPPLY COMPANY
BEECH AIRCRAFT CORPORATION
BELL AIRCRAFT CORPORATION
BENDIX AVIATION CORPORATION
BENDIX INTERNATIONAL DIVISION
BENDIX PRODUCTS DIVISION
BENDIX RADIO CORPORATION
ECLIPSE-PIONEER DIVISION
FRIEZ INSTRUMENT DIVISION
PACIFIC DIVISION
SCINTILLA MAGNETO COMPANY
THE BG CORPORATION
BOEING AIRPLANE COMPANY
SEATTLE DIVISION
WICHITA DIVISION
BREEZE CORPORATIONS, INC.
AIRCRAFT STANDARD PARTS COMPANY, INC.
ALDRICH COMPANY
ANDERSON STOVE COMPANY, INC.
FEDERAL LABORATORIES, INC.
FOUNDRY SERVICE, INC.
CAL-AERO TECHNICAL INSTITUTE, A DIVISION OF GRAND CENTRAL AIRPORT COMPANY
CANADAIR, LTD.
CESSNA AIRCRAFT COMPANY
CHANDLER-EVANS DIVISION, NILES-BEMENT-POND COMPANY
CHASE AIRCRAFT COMPANY, INC.
CHASE NATIONAL BANK OF THE CITY OF NEW YORK
THE CLEVELAND GRAPHITE BRONZE COMPANY
THE CLEVELAND PNEUMATIC TOOL COMPANY
AUTOMOTIVE-AIRCRAFT DIVISION
CLIFFORD MANUFACTURING COMPANY, DIVISION OF STANDARD-THOMSON CORPORATION
CONSOLIDATED VULTEE AIRCRAFT CORPORATION
FORT WORTH DIVISION
STINSON AIRCRAFT DIVISION
CONTINENTAL MOTORS CORPORATION
CURTISS-WRIGHT CORPORATION
AIRPLANE DIVISION
PROPELLER DIVISION
WRIGHT AERONAUTICAL CORPORATION DIVISION
DOAK AIRCRAFT COMPANY, INC.
DOUGLAS AIRCRAFT COMPANY, INC.
EL SEGUNDO PLANT
LONG BEACH PLANT
SANTA MONICA PLANT
THE DOW CHEMICAL COMPANY
DZUS FASTENER COMPANY, INC.
EASTERN AIR LINES, INC.
EATON MANUFACTURING COMPANY
DYNAMATIC CORPORATION (SUBSIDIARY)
EATON-WILCOX-RICH LTD. (SUBSIDIARY)
THOMAS A. EDISON, INCORPORATED, INSTRUMENT DIVISION
EDO CORPORATION
ELASTIC STOP NUT CORPORATION OF AMERICA
ELECTROL INCORPORATED
ETHYL CORPORATION
FAIRCHILD CAMERA & INSTRUMENT CORPORATION
FAIRCHILD AERIAL SURVEYS, INC.
FAIRCHILD ENGINE AND AIRPLANE CORPORATION
AL-FIN DIVISION
FAIRCHILD AIRCRAFT DIVISION
FAIRCHILD PERSONAL PLANES DIVISION
FAIRCHILD PILOTLESS PLANE DIVISION
NEPA DIVISION
RANGER AIRCRAFT ENGINES DIVISION
STRATOS CORPORATION (SUBSIDIARY)
FEDERAL TELEPHONE AND RADIO CORPORATION
FEDERAL ELECTRIC MANUFACTURING COMPANY LTD.
FEDERAL TELECOMMUNICATION LABORATORIES, INC. (PARTIAL SUBSIDIARY)
GENERAL ELECTRIC COMPANY
AIRCRAFT GAS TURBINE DIVISION
AVIATION DIVISIONS
GENERAL TIRE AND RUBBER COMPANY OF CALIFORNIA RESEARCH AND DEVELOPMENT DIVISION
THE B. F. GOODRICH COMPANY
THE GOODYEAR TIRE & RUBBER COMPANY
GOODYEAR AIRCRAFT CORPORATION
GRUMMAN AIRCRAFT ENGINEERING CORPORATION
W. & L. E. GURLEY
INSURANCE COMPANY OF NORTH AMERICA COMPANIES
INSURANCE COMPANY OF NORTH AMERICA
THE ALLIANCE INSURANCE COMPANY OF PHILADELPHIA
PHILADELPHIA FIRE AND MARINE INSURANCE COMPANY
INDEMNITY INSURANCE COMPANY OF NORTH AMERICA
THE INTERNATIONAL NICKEL COMPANY, INC.
IRVING AIR CHUTE COMPANY, INC.
JACK & HEINTZ PRECISION INDUSTRIES, INC.
JOHNS-MANVILLE SALES CORPORATION
WALTER KIDDE & COMPANY, INC.
KOLLSMAN INSTRUMENT DIVISION, SQUARE D COMPANY
LAVELLE AIRCRAFT CORPORATION
LEAR INCORPORATED
LINK AVIATION, INC.
THE LIQUIDOMETER CORPORATION
LOCKHEED AIRCRAFT CORPORATION
AIRQUIPMENT COMPANY (SUBSIDIARY)
LOCKHEED AIR TERMINAL (SUBSIDIARY)
LOCKHEED AIRCRAFT OVERSEAS CORPORATION (SUBSIDIARY)
LOCKHEED AIRCRAFT SERVICE, INC. (SUBSIDIARY)
LONGINES-WITTNAUER WATCH COMPANY, INC.
THE GLENN L. MARTIN COMPANY
GLM CHEMICAL DIVISION
ROTAWINGS DIVISION
WARREN McARTHUR CORPORATION
McDONNELL AIRCRAFT CORPORATION
MINNEAPOLIS-HONEYWELL REGULATOR COMPANY
BROWN INSTRUMENT COMPANY (SUBSIDIARY)
MOORE DROP FORGING COMPANY
NATIONAL CITY BANK OF NEW YORK
NATIONAL CREDIT OFFICE, INC.
NORTH AMERICAN AVIATION, INC.
NORTH AMERICAN AVIATION, INC., OF TEXAS
NORTHROP AIRCRAFT, INC.
NORTHWEST AIRLINES, INC.
OWENS-CORNING FIBERGLAS CORPORATION
PAN AMERICAN WORLD AIRWAYS SYSTEM
THE PARKER APPLIANCE COMPANY
PESCO PRODUCTS DIVISION, BORG-WARNER CORPORATION
PHILLIPS PETROLEUM COMPANY
PURE OIL COMPANY
RADIOPLANE COMPANY
REPUBLIC AVIATION CORPORATION
A. V. ROE CANADA LIMITED
JOHN A. ROEBLING'S SONS COMPANY
ROHR AIRCRAFT CORPORATION
RYAN AERONAUTICAL COMPANY
SHELL OIL COMPANY, INC.
SIMMONDS AEROCESSORIES, INC.
SOCONY-VACUUM OIL COMPANY, INC.
SOLAR AIRCRAFT COMPANY
SPERRY GYROSCOPE COMPANY, DIVISION OF THE SPERRY CORPORATION
SQUARE D COMPANY
STANDARD OIL COMPANY OF CALIFORNIA
STANDARD OIL COMPANY (INDIANA)
STANDARD OIL COMPANY OF NEW JERSEY
THE TEXAS COMPANY
THOMPSON PRODUCTS, INC.
TINNERMAN PRODUCTS, INC.
UNION CARBIDE AND CARBON CORPORATION
BAKELITE CORPORATION
ELECTRO METALLURGICAL COMPANY
HAYNES STELLITE COMPANY
THE LINDE AIR PRODUCTS COMPANY
NATIONAL CARBON COMPANY, INC.
UNITED AIR LINES, INC.
UNITED AIRCRAFT CORPORATION
CHANCE VOUGHT AIRCRAFT DIVISION
HAMILTON STANDARD PROPELLERS DIVISION
PRATT & WHITNEY AIRCRAFT DIVISION
SIKORSKY AIRCRAFT DIVISION
UNITED AIRCRAFT EXPORT CORPORATION
UNITED AIRCRAFT SERVICE CORPORATION
UNITED STATES AVIATION UNDERWRITERS, INC.
UNITED STATES RUBBER COMPANY
DOMINION RUBBER COMPANY, LTD.
VICKERS, INC.
WARNER AIRCRAFT CORPORATION
THE WEATHERHEAD COMPANY
ANGOLO, INDIANA DIVISION
COLUMBIA PRODUCTS DIVISION
HOUMA DIVISION
THE WEATHERHEAD COMPANY OF CANADA (SUBSIDIARY)
WESTINGHOUSE ELECTRIC CORPORATION
AVIATION GAS TURBINE DIVISION
INDUSTRIAL ELECTRONICS DIVISION
MARINE & AVIATION SALES DEPARTMENT
SMALL MOTOR DIVISION, AVIATION SALES
WESTON ELECTRICAL INSTRUMENT CORPORATION
WYMAN-GORDON COMPANY
YOUNG RADIATOR COMPANY

JOURNAL OF THE AERONAUTICAL SCIENCES

VOLUME 15 NOVEMBER, 1948 NUMBER 11

The Transient Reaction of an Airfoil Due to Change in Angle of Attack at Supersonic Speed*

CHIEH-CHIEN CHANG†

The Johns Hopkins University

SUMMARY

Near the destination of a flying guided missile, it is sometimes necessary to change the angle of attack of the wing or any control surface from one value to another in a short interval of time so that the trajectory can be modified to intersect the target. In order to calculate such a trajectory accurately, the transient reaction of the lift, moment, and wave drag of the wing has to be evaluated as a function of time.

For the preliminary investigation, it is assumed that the angle of attack of an airfoil moving at constant supersonic speed starts, at a certain instant, to increase linearly with time until it reaches a specific value, after which it stays constant. For the analysis, both the angle of attack and its changing rate are expressed in the form of Fourier integrals.

The linearized differential equation for the unsteady flow of a compressible fluid is used along with Possio's solution for a simple source. Unlike the solution of a harmonically oscillating airfoil where numerical integrations of finite integrals of the Bessel functions of the zero and first order are necessary, the lift and moment of this case can be explicitly expressed in a closed form as a function of time. Some examples are shown.

As expected, the lift, wave drag, and moment will be reduced to Ackeret's results of steady two-dimensional supersonic flow as soon as the transient reaction damps out after the change in angle of attack ceases.

The problem is also approached by finding the unit solution of an arbitrary change in angle of attack of constant rate with time. By superposition of a proper number of such unit solutions, the pressure, lift, and moment can be evaluated for the angle of attack with any arbitrary function of time. Some integrals are derived in the general case if the second derivative of the angle of attack with respect to time is continuous.

Presented at the Aerodynamics Session, Sixteenth Annual Meeting, I.A.S., New York, January 26–29, 1948.

* This investigation was initiated at The Glenn L. Martin Company last year. The author wishes to express his deep appreciation to Prof. Francis H. Clauser for his discussions and suggestions. His thanks are also due to Misses Vivian O'Brien and Patricia Clarken for completing the numerical calculations, drawings, and topographical work. Acknowledgment should be made to Prof. H. Ashley and Mr. G. Zartarian of M.I.T. for their advice on some of the misprints in the I.A.S. Preprint No. 134 of this paper.

† Associate Professor of Aeronautics.

(1) INTRODUCTION

THE THEORY OF THE NONSTATIONARY MOTION of an airfoil has many important applications in flight, such as flutter and wing loading due to gust. There have been many investigations in this field. In incompressible cases, notable work has been accomplished by Birnbaum, Glauert, Wagner, Kussner, Theodorsen, Jones, Reissener, von Kármán, and Sears. In the two-dimensional subsonic cases, some of the pioneers are Possio, Borbely, and Kussner. As an extension of the subsonic cases, Possio,[1] von Borbely,[3] Garrick and Rubinow,[2] Miles,[8] Temple and Jahn,[14] Schwarz,[4] and Hönl[13] have treated the supersonic cases. Both in the subsonic and supersonic cases, the theory is based on the linearized concept of the thin wing where the local downwash is small in comparison to the flight speed and/or sound velocity. Except for the case of vertical gust which was treated by Kussner and von Kármán and Sears[9] in incompressible cases and Schwarz[4] in supersonic cases, most of the theoretical investigations have treated the case of steady harmonic oscillations with respect to time in a number of degrees of freedom.

There is another application of the theory to the calculation of the transient reaction on an airfoil due to change in angle of attack or to deflection of the control surface attached to it. Although not treated much in incompressible or subsonic cases, the application certainly becomes increasingly important in the supersonic case.

The present treatment investigates the transient reaction of a two-dimensional wing in supersonic flight when the angle of attack of the wing changes from one fixed value to another according to a given function of time. This is based upon certain current needs in the design of supersonic guided missiles and pilotless aircraft.

In the performance of a guided missile flying near its moving or stationary target, its trajectory must be precisely predetermined as a function of time in order to reach its destination accurately. Sometimes, however, after the missile is fired, certain unexpected factors may spoil the scheduled trajectory, and some correction of the path of the missile may be found necessary, particularly during flight near the target. One feasible means of performing such a correction is to deflect the wing or any other control surface to another appropriate angle of attack during the course of time in such a manner that the missile will not miss the target. In a certain sense, this may be considered as an analogy of von Kármán and Sears'[9] case of a sharp-edged gust in incompressible flow, although the methods of approach in the two cases are entirely different.

In the linearized two-dimensional theory of supersonic nonsteady flow, the vortex theory can no longer be applied because the flow in the wake cannot influence the pressure on the wing. However, Possio's[1] solution of acoustic sources can be used with interesting results. In the two-dimensional case the strength of the acoustic source at any point on the surface is linearly dependent on the downwash at that point and at that instant and is independent of the downwash of the neighboring points. Furthermore, as shown by von Kármán,[11] to the approximation of the linearized theory, the effect of the vertical displacement from the neutral plane on the downwash at the solid boundary may be neglected if the vertical displacement is small in comparison to the airfoil chord. Consequently, the downwash can be considered to occur in the plane of the undeflected thin wing where the corresponding source strength is distributed to replace the airfoil. Besides, the disturbance due to an acoustic source lies entirely in the downstream Mach cone and cannot be beyond it. These facts make the linearized theory simpler in the supersonic than in the subsonic case.

The present treatment is based on the superposition of Possio's solution of simple sources. The angle of attack is first constant, then changes linearly with time for a short time interval t_i, and then remains constant. A Fourier integral is used for the downwash to evaluate the velocity potential. In contrast to the case of harmonic oscillation, in which numerical integrations of finite integrals of Bessel functions are involved, the pressure, lift, and moment can be expressed explicitly as a function of time.

If the angle of attack is an arbitrary function of time, it is shown that the pressure, lift, and moment can be obtained approximately by superimposing a number of the downwashes that linearly increase with time. If the second derivative of the angle of attack is a continuous function of time, the lift and moment can be expressed as a group of integrals.

(2) Nomenclature

C = wing chord
C_D = transient wave drag coefficient
C_L = transient lift coefficient
C_{L_0} = two-dimensional lift coefficient in steady case
C_M = transient moment coefficient about x_0
C_{M_0} = two-dimensional moment coefficient in steady case
C_p = $2(p - p_1)/\rho_1 U^2$, pressure coefficient
C_{p_0} = $2\alpha_1/(M^2 - 1)^{1/2}$
c = sound velocity in free stream
$F(\ )$ = function concerning the lift coefficient
$f(\ )$ = function concerning the pressure coefficient
$G(\ )$ = function concerning the moment coefficient
$J_0(\ )$ = Bessel function of the zero order
M = Mach Number
m = $(M^2 - 1)/M$, parameter of Mach Number
p_1 = static pressure in free stream
r = $\dfrac{\sqrt{(x-\xi)^2 - (M^2-1)[(y-\eta)^2 + (z-\zeta)^2]}}{(M^2-1)}$
r' = $\sqrt{(x-\xi)^2 - (M^2-1)(y-\eta)^2}/(M^2-1)$
t = time
t' = $t/\tilde{t}$, nondimensional time
$\tilde{t}$ = C/U
t_x = $(x - x_0)/U$
t_ξ = $(\xi - x_0)/U$
w = z-component of velocity
U = free-stream velocity
u = x-component of velocity
v = y-component of velocity
x = axis along chord direction
x' = x/C per cent of chord
x_0 = axis of rotation of the entire airfoil
x_0' = x_0/C
y = vertical axis
z = spanwise axis
α = angle of attack
α_1 = total increment of angle of attack from t_0 to t_1
ζ = source location along z-axis
η = source location along y-axis
λ = $(x - \xi)/c(M^2 - 1)$
μ' = $t' - \tau'$
ν_i = $x/U(t - t_i) = x'/(t' - t_i')$
ν_{i_0} = $x_0/U(t - t_i) = x_0'/(t' - t_i')$
ν_{i_∞} = $C/U(t - t_i) = 1/(t' - t_i')$
ξ = source location along x-axis
ρ_1 = free-stream density
τ = time interval
τ' = $\tau/\tilde{t}$; nondimensional time
Φ = $\phi/[-\alpha_1/(M^2 - 1)^{1/2}]$
ϕ = velocity potential
ϕ_0 = velocity potential of a simple source line
ω = frequency parameter as an integration variable

(3) Statement of the Problem

The present problem is to find, at any time, the force and moment acting on a thin airfoil in a supersonic stream of constant velocity, when the angle of attack changes as follows: (a) After being constant for a long period of time, it increases linearly for a short time interval and then remains constant; (b) it changes arbitrarily with time.

The assumptions are: (1) The flow is isentropic and consequently irrotational; (2) the fluid is nonviscous; and (3) the angle of attack and its rate of change are

sufficiently small that the downwash is small in comparison to the sound velocity.

(4) Linearized Differential Equations and Elementary Solutions

Under the above assumptions 1 and 2, the differential equation for unsteady three-dimensional flow can be obtained and is nonlinear. Little is known about its solution for any particular case. However, if the disturbance velocities are sufficiently small compared to the sound velocity and to the difference between the free velocity and the sound velocity that their squares can be neglected, the differential equation can be linearized as

$$\phi_{yy} + \phi_{zz} = (M^2 - 1)\phi_{xx} + \frac{2M}{c}\phi_{xt} + \frac{1}{c^2}\phi_{tt} \quad (4.1)$$

where $M = U/c$, c is the sound velocity of the free stream, and ϕ is the velocity potential such that $\nabla\phi = (U + u)\bar{i} + v\bar{j} + w\bar{k}$, where $\bar{i}$, $\bar{j}$, $\bar{k}$ are unit vectors in x, y, and z directions, respectively. Through this process, three advantages are gained. First, the particular solution of a simple source or of a simple doublet is rather easy to derive by means of the classical mathematical analysis. Second, being linear, its solutions are superimposable. Third, the general solution consists of one or both of two parts, odd and even. The even part of the solution can be uniquely determined by superposition of simple sources and the odd part by superposition of simple doublets. Thus, we can superimpose the particular solutions to fit particular required boundary conditions. Then, the whole problem is reduced to determining the strength of the source and/or of the doublet with the given boundary conditions.

To find such a simple solution, we consider the effect at a point P caused by an acoustic source at Q in the presence of a supersonic flow with uniform velocity U. The points P and Q have coordinates x, y, z and ξ, η, ζ which are fixed in space. Fig. (1a) shows the view on a plane which passes through P and Q and which is parallel to the supersonic stream. As a sound pulse issues from the source, the spherical waves moving with the fluid will increase in diameter with acoustic velocity c while being transported downstream with velocity U. The envelope of such a system of spherical waves is the stationary Mach cone. If P is outside of the Mach cone—i.e., in the so-called forbidden region—the velocity potential at P must be zero. However, if P is inside, there are two spherical waves simultaneously passing P at time t. Both issued from Q at earlier times. These time intervals can be determined from the cosine law.

$$\tau_1'' = \frac{M}{c}\frac{x-\xi}{M^2-1} - \frac{r}{c}, \qquad \tau_2'' = \frac{M}{c}\frac{x-\xi}{M^2-1} + \frac{r}{c} \quad (4.2)$$

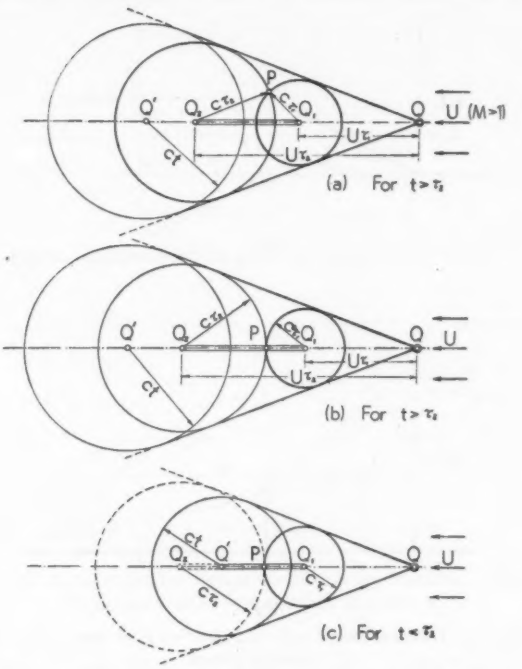

Fig. 1. A point P and an acoustic source Q are both in a uniform flow of supersonic velocity U. The strength of Q is zero when $t < 0$. The acoustic waves which are issued by Q and blown downstream reach P simultaneously at t as shown
(a) P and Q are on parallel streamlines.
(b) P and Q are on the same line.
(c) P and Q are on the same line.

where

$$r = \frac{1}{M^2-1}\sqrt{(x-\xi)^2 - (M^2-1)[(y-\eta)^2 + (z-\zeta)^2]} \quad (4.3)$$

It has been shown by Garrick and Rubinow[7] that the velocity potential at P due to a source at Q whose strength, A, varies with time is

$$\phi_0'(x, y, z, t) = \frac{A(\xi, \eta, \zeta, t - \tau_2'') + A(\xi, \eta, \zeta, t - \tau_1'')}{r} \quad (4.4)$$

This can be extended to give the potential for a two-dimensional line source by summing up the potential of sources uniformly distributed along a line ξ = constant, η = constant—i.e., by integrating Eq. (4.4) with respect to ζ holding ξ and η fixed.

$$\phi_0(x, y, z, t) = \int_{-\infty}^{\infty} \phi_0' d\zeta$$

In this integration, τ_1'', τ_2'', and r are, of course, functions of ζ. Points on the line source whose Mach cones do not contain P cannot affect the potential at P. Consequently, the integration may be carried out along the source line only between the two points:

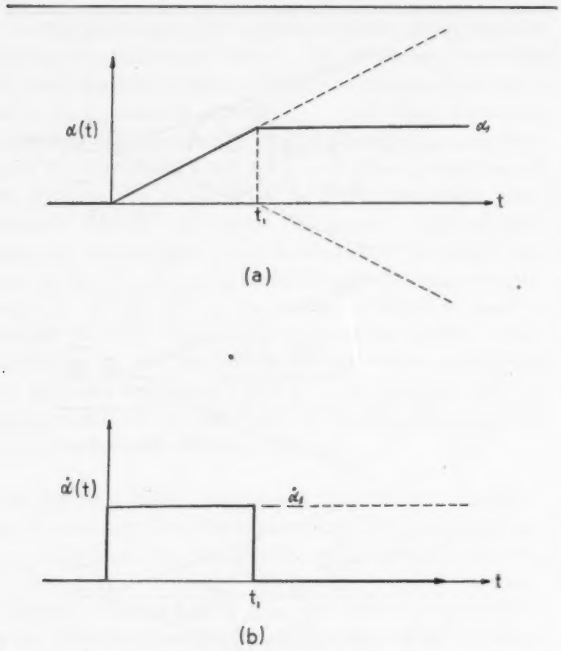

FIG. 2. Distribution of $\alpha(t)$ and $\dot{\alpha}(t)$ vs. t for any point on a straight airfoil.

$$\zeta_1 = z - \sqrt{[(x-\xi)^2/(M^2-1)] - y^2}$$

and

$$\zeta_2 = z + \sqrt{[(x-\xi)^2/(M^2-1)] - y^2}$$

If we use these two limits and assume that at a given time the pulses emanating from the line source are everywhere of the same strength, then this integral becomes Possio's solution, which is

$$\phi_0(x, y, t) = \int^{\tau_2} \frac{A(\xi, \eta, t-\tau)}{\sqrt{c^2\tau^2 - (x-\xi-U\tau)^2 - (y-\eta)^2}}\, d\tau \quad (4.5)$$

where

$$\tau_1 = \frac{M(x-\xi)}{c(M^2-1)} - \frac{r'}{c}, \qquad \tau_2 = \frac{M(x-\xi)}{c(M^2-1)} + \frac{r'}{c} \quad (4.6)$$

where

$$r' = \frac{1}{M^2-1}\sqrt{(x-\xi)^2 - (M^2-1)(y-\eta)^2}$$

τ_1 and τ_2 are now the shorter and longer time intervals for the cylindrical waves to travel from the line source at $Q(\xi, \eta)$ to the point $P(x, y)$. [See Fig. (1a).]

We see that in the two-dimensional case, the spherical waves of an infinitely long acoustic line source scatter over the whole of the Mach wedge of the source. Therefore, P is affected not only by the pulses emitted at previous times τ_1 and τ_2 but also by all pulses between these times.

With the principle of superposition, the total potential at P due to an infinite source sheet on the positive x-axis can be obtained by integrating the potential of the above source lines with respect to ξ

$$\phi(x, y, t) = \int_0^{\xi_1} \phi_0 d\xi \quad (4.7)$$

where $\xi_1 = x - y\sqrt{M^2-1}$ is the nearest element of the source sheet whose disturbances will reach the point P.

To facilitate the integration, we can substitute $c^2 \times (M^2-1)(\tau-\tau_1)(\tau_2-\tau)$ for $c^2\tau^2 - (x-\xi-Ut)^2 - y^2$. Expressing Eq. (4.7) in another form we have

$$\phi(x, y, t) = \frac{1}{c\sqrt{M^2-1}} \int_0^{\xi_1} \int_{\tau_1}^{\tau_2} \frac{A(\xi, +0, t-\tau)}{\sqrt{(\tau-\tau_1)(\tau_2-\tau)}}\, d\tau\, d\xi \quad (4.8)$$

This expression has been given by Possio[1] and Garrick and Rubinow.[2] Now the problem is how to determine the source strength from the boundary conditions. For the two-dimensional case, it is known[2] that

$$A(x, \pm 0, t) = \mp(c/\pi)v(x, \pm 0, t) \quad (4.9)$$

where v is the vertical velocity immediately above or below the source sheet. Thus, the negative sign of v is to be used as y approaches zero from the positive side, and the positive sign of v is to be used as y approaches zero from the negative side. It is interesting to note that, if the lower wing surface is equivalent to a positive source sheet, the upper surface corresponds to a negative source sheet of the same strength. Each side can be considered independently as a source sheet for the present problem, because the influences of the two will not meet except in the region behind the trailing edge with which we are not concerned in this problem. If the flow behind the wing were considered, the problem would have to be treated as a doublet sheet of finite chord length.

Substituting Eq. (4.9) into Eq. (4.8), we have the velocity potential on the upper half plane, which is

$$\phi(x, y, t) = \frac{-1}{\pi} \frac{1}{(M^2-1)^{1/2}} \int_0^{\xi_1} \int_{\tau_1}^{\tau_2} \frac{v(\xi, t-\tau)}{\sqrt{(\tau-\tau_1)(\tau_2-\tau)}}\, d\tau\, d\xi \quad (4.10)$$

If the point considered is on the airfoil but below the surface, Eq. (4.10) becomes

$$\phi(x, -0, t) = \frac{+1}{\pi} \frac{1}{(M^2-1)^{1/2}} \int_0^{x} \int_{\tau_1}^{\tau_2} \frac{v(\xi, t-\tau)}{\sqrt{(\tau-\tau_1)(\tau_2-\tau)}}\, d\tau\, d\xi \quad (4.11)$$

where

$$\tau_1 = \frac{x-\xi}{c}\left(\frac{1}{M+1}\right) = \frac{x-\xi}{U+c}$$

$$\tau_2 = \frac{x-\xi}{c}\left(\frac{1}{M-1}\right) = \frac{x-\xi}{U-c}, \qquad \xi_1 = x \quad (4.12)$$

(5) The Downwash Distribution

Assume that the angle of attack and its rate of change are both zero at $t \leq 0$ and that the rate of change of the angle of attack remains constant from time $+0$ to t_1. Beyond this time interval t_1, the angle of attack is kept at a constant value α_1. Figs. (2a) and (2b) show the distribution of the angle of attack $\alpha(t)$ and its derivative $\dot{\alpha}(t)$ at a fixed point $(x, +0)$. With Dirichlet's integral it can be shown that

$$\dot{\alpha}(t) = \frac{\dot{\alpha}_1}{\pi}\int_0^\infty \frac{\sin \omega t - \sin \omega(t-t_1)}{\omega} d\omega$$

$$= \frac{\dot{\alpha}_1}{2i\pi}\int_0^\infty \frac{d\omega}{\omega}\left[e^{i\omega t}(1-e^{-i\omega t_1}) - e^{-i\omega t}(1-e^{+i\omega t_1})\right] \quad (5.1)$$

where $\dot{\alpha}(t) = d\alpha(t)/dt$ and $\dot{\alpha}_1 = \alpha_1/t_1$. It can be shown easily that this equation satisfies the proposed physical condition at any instant of time, positive or negative. Similarly, we can express $\alpha(t)$ as

$$\alpha(t) = \frac{\dot{\alpha}_1 t_1}{2} - \frac{\dot{\alpha}_1}{\pi}\int_0^\infty \frac{d\omega}{\omega^2}\left(\cos\omega|t| - \cos\omega|t-t_1|\right)$$

$$= \frac{\dot{\alpha}_1 t_1}{2} - \frac{\dot{\alpha}_1}{2\pi}\int_0^\infty \frac{d\omega}{\omega^2}\left[e^{i\omega t}(1-e^{-i\omega t_1}) + e^{-i\omega t}(1-e^{+i\omega t_1})\right] \quad (5.2)$$

where $\dot{\alpha}_1 t_1$ is introduced for α_1. In order to represent $\alpha(t)$ as specified, the absolute values of both t and $t - t_1$ are introduced.

No loss in generality is occasioned by taking the angle of attack before deflection to be zero. Because of the linear character of lift and moment, any steady state contribution can be added to the transient values computed here. The effect on the wave drag will be considered later. In case of constant $\dot{\alpha}_0$ (i.e., $\dot{\alpha}$ at $t < 0$) and $\dot{\alpha}_0 \neq 0$, the above equations are still true if $\dot{\alpha}_1$ is replaced by $\dot{\alpha}_1 - \dot{\alpha}_0$, $\dot{\alpha}$ by $\Delta\dot{\alpha}$, and α by $\Delta\alpha$. In other words, only the increment in $\dot{\alpha}$ at $t = 0$ is considered.

From Fig. 3, we see that, within the limits of our approximations, the vertical velocity of any point of a flat plate airfoil can be expressed in terms of α and $\dot{\alpha}$ as follows:

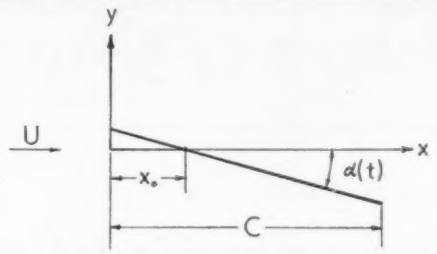

Fig. 3. Geometry of the airfoil at time t $(0 < t < t_1)$.

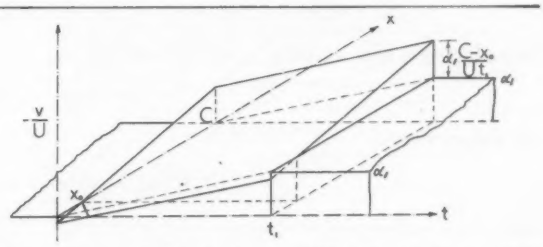

Fig. 4. Downwash distribution $(-v/U)$ in the t-x plane. Note the discontinuities of downwash at t_0 and t_1.

$$v(x, t) = -\{U[\alpha(t)] + (x - x_0)[\dot{\alpha}(t)]\} \quad (5.3a)$$

where x_0 is the location of the hinge axis about which the wing rotates.

If we put $(x - x)_0/U = t_x$, then, approximately,

$$v(x, 0, t)/U = -\alpha(x, y_e, t) - t_x[\dot{\alpha}(x, y_e, t)] \quad (5.3b)$$

Introducing Eqs. (5.1) and (5.2) into Eq. (5.3b), we can obtain

$$\frac{-\pi}{\dot{\alpha}_1}\frac{v(x, 0, t)}{U} = \frac{\pi t_1}{2} + \int_0^\infty \frac{d\omega}{\omega^2}(\cos\omega|t-t_1| - \cos\omega|t|) + t_x\int_0^\infty \frac{d\omega}{\omega}[\sin t - \sin(t-t_1)]$$

$$= \frac{\pi t_1}{2} + \frac{1}{2}\int_0^\infty \frac{d\omega}{\omega^2}\left\{e^{i\omega t}\left[\left(\frac{\omega t_x}{i} - 1\right)(1 - e^{-i\omega t_1})\right] - e^{-i\omega t}\left[\left(\frac{\omega t_x}{i} + 1\right)(1 - e^{i\omega t_1})\right]\right\} \quad (5.4)$$

Fig. 4 shows the proposed downwash in the t-x plane.

(6) Calculation of the Velocity Potential

The velocity potential will be used to determine the pressure distribution on the airfoil. For this purpose, only the t and x derivatives at $y = 0$ are necessary. Since y can be placed equal to zero before or after differentiating t and x, we simplify the work by using ϕ evaluated at the airfoil. From Eq. (4.11), we have

$$\phi(x, -0, t) = \frac{1}{\pi(M^2-1)^{1/2}}\int_0^x \int_{\tau_1}^{\tau_2} \frac{v(\xi, t-\tau)}{\sqrt{(\tau-\tau_1)(\tau_2-\tau)}}\, d\xi\, d\tau$$

Substituting $t - \tau$ for t and ξ for x in Eq. (5.4), we have

$$-\frac{\pi}{\dot{\alpha}_1}\frac{v(\xi, t-\tau)}{U} = \frac{\pi t_1}{2} + \frac{1}{2}\int_0^\infty \frac{d\omega}{\omega^2} e^{i\omega t} e^{-i\omega\tau}\left(\frac{\omega t_\xi}{i} - 1\right)(1 - e^{-i\omega t_1}) - \frac{1}{2}\int_0^\infty \frac{d\omega}{\omega^2} e^{i\omega\tau}\left[\left(\frac{\omega t_\xi}{i} + 1\right)(1 - e^{i\omega t_1})e^{-i\omega t}\right] \quad (6.1)$$

where $t_\xi = (\xi - x_0)/U$. Then

$$\phi(x-0, t) = \frac{-1}{\pi(M^2-1)^{1/2}}\frac{U\dot{\alpha}_1}{2\pi}\left\{\pi t_1 \int_0^x \int_{\tau_1}^{\tau_2} \frac{d\xi d\tau}{\sqrt{(\tau-\tau_1)(\tau_2-\tau)}} + \int_0^x \int_0^\infty \frac{da}{\omega^2}\left[e^{i\omega t}\left(\frac{\omega t_\xi}{i} - 1\right)(1 - e^{-i\omega t_1})\right] \times \right.$$
$$\left. \int_{\tau_1}^{\tau_2} \frac{e^{-i\omega\tau} d\tau d\xi}{\sqrt{(\tau-\tau_1)(\tau_2-\tau)}} - \int_0^x \int_0^\infty \frac{d\omega}{\omega^2}\left[e^{-i\omega t}\left(\frac{\omega t_\xi}{i} + 1\right)(1 - e^{i\omega t_1})\right] \int_{\tau_1}^{\tau_2} \frac{e^{+i\omega\tau} d\tau d\xi}{\sqrt{(\tau-\tau_1)(\tau_2-\tau)}}\right\} \quad (6.2)$$

Introducing a new variable θ, which is defined by

$$2\tau = (\tau_2 - \tau_1)\cos\theta + (\tau_2 + \tau_1) \quad (6.3)$$

we can evaluate[6]

$$\int_0^x \int_{\tau_1}^{\tau_2} d\xi d\tau / \sqrt{(\tau-\tau_1)(\tau_2-\tau)} = \int_0^x \int_0^\pi d\theta d\xi = \pi x \quad (6.4)$$

and

$$\int_{\tau_1}^{\tau_2} \frac{e^{\pm i\omega\tau} d\tau}{\sqrt{(\tau-\tau_1)(\tau_2-\tau)}} = e^{\pm i\omega[(\tau_2+\tau_1)/2]} \int_0^\pi e^{\pm i[\omega[(\tau_2-\tau_1)/2]]\cos\theta} d\theta = \pi e^{\pm i\omega\lambda M} J_0(\lambda\omega) \quad (6.5)$$

where $\lambda = (\tau_2 - \tau_1)/2 = (x - \xi)/c(M^2 - 1)$ and then

$$(\tau_2 + \tau_1)/2 = (x - \xi)M/c(M^2 - 1) = M\lambda \quad (6.6)$$

Substituting Eqs. (6.4) and (6.5) into Eq. (6.2)

$$\phi(x, -0, t)\left[\frac{-\dot{\alpha}_1}{(M^2-1)^{1/2}}\right]^{-1} = \frac{Uxt_1}{2} + \frac{U}{2\pi}\int_0^x d\xi \int_0^\infty \frac{d\omega}{\omega^2}\left[e^{i\omega(t-M\lambda)}\left(\frac{\omega t_\xi}{i} - 1\right)(1 - e^{-i\omega t_1}) - e^{-i\omega(t-M\lambda)} \times \right.$$
$$\left. \left(\frac{\omega t_\xi}{i} + 1\right)(1 - e^{i\omega t_1})\right] J_0(\lambda\omega) \quad (6.7)$$

For convenience of future integration, we can express the above equation in terms of trignometrical functions and change ξ to λ. Then

$$\phi(x, -0, t)\left[\frac{-\dot{\alpha}_1}{(M^2-1)^{1/2}}\right]^{-1} = \frac{Uxt_1}{2} + \frac{Uc(M^2-1)}{\pi}\int_0^{x/c(M^2-1)} d\lambda \int_0^\infty \frac{d\omega}{\omega^2}(\cos\omega|t - t_1 - M\lambda| - \cos\omega|t - M\lambda|) \times$$
$$J_0(\lambda\omega) + \frac{Uc(M^2-1)}{\pi}\int_0^{x/c(M^2-1)} (t_x - m\lambda)d\lambda \int_0^\infty \frac{d\omega}{\omega}[\sin\omega(t - M\lambda) - \sin\omega(t - t_1 - M\lambda)]J_0(\lambda\omega) \quad (6.8)$$

where $t_\xi = (\xi - x_0)/U = t_x - m\lambda$, and $m = (M^2 - 1)/M$. The integration of the above equation is carried out in Appendix A where the velocity potential is discontinuous along certain lines in the domain of the t-x plane.

In order to understand those lines of discontinuities some explanation of the physical relation of the distribution of the source and the velocity potential ϕ should be treated before the analytic expressions of ϕ are given.

(*a*) *Zone of Influence.*—The acoustic disturbance due to the source Q (which is proportional to downwash) at any point x on the airfoil at time t influences the pressure or the velocity potential at other points on the airfoil behind x at a time later than t. This can be expressed in the t-x plane as shown in the shaded downstream wedge in Fig. 5a. This wedge vertex is at the source $Q(x, t)$, and the slopes of the wedge sides are $(U - c)$ and $(U + c)$. Outside of this wedge, the disturbance at Q no longer influences the pressure. This wedge area may be called the zone of influence of Q in the t-x plane, and it is similar to the downstream Mach cone in the steady supersonic flow.

(*b*) *Zone of Action.*—Conversely, the potential at any point x on the airfoil at time t is obtained by a surface integral [Eq. (4.11)], which sums up the sources that have occurred at a point forward of x and at a time previous to t. These sources are contained in the

shaded upstream wedge in Fig. 5b. This wedge is at the point $P(t, x)$ and the slopes of the two sides are also $(U - c)$ and $(U + c)$. Outside of this area, the acoustic source produces no action on the potential at P. Therefore, this area may be called the zone of action upon P, and it is similar to the upstream Mach cone in the steady supersonic flow.

Now for the present problem, the downwash is zero for $x < 0$ and $t < 0$, and, consequently, the downwash distribution in Fig. 4 is discontinuous along $x = 0$ and $t = 0$. At $t = 0$, an abrupt increment in $\dot{\alpha}$ (i.e., $\dot{\alpha}_1$) is made, and $\dot{\alpha}_1$ remains constant hereafter. We want to know the effect of this change on the velocity potential of a point x on the airfoil at different times. First, if $0 < t < x/(U + c)$, the zone of action upon P_3 is shown by the shaded area in Fig. 5c. Later, if $x/(U + c) \leq t \leq x/(U - c)$, the zone of action upon P_2 is shown by the shaded area in the figure. Furthermore, if $t > x/(U - c)$, the zone of action upon P_1 is shown by the shaded triangular area. The potential at x, being a surface integral of the shaded area, must be different in nature for differently shaped areas. This may be considered as one reason for the discontinuities of the velocity potential in the t-x plane.

Furthermore, the strength of the source at $t = 0$ and $x = 0$ is discontinuous both in t and x. The zone of influence of this point source is a wedge with side lines $t = (U - c)x$ and $t = (U + c)x$. The two lines divide the region bound by $x > 0$ and $t > 0$ into three zones, called I-1, I-2, and I-3 as shown in Fig. 6a. Here I refers to the first region produced by an increment in $\dot{\alpha}$ (i.e., $\dot{\alpha}_1$) at $t = 0$. In zone I-3, the leading edge exerts no influence, and, consequently, the potential at P_3 is the same as though an airfoil extending to infinity ahead of x had started abruptly to rotate. In zone I-2, the influence of both the abrupt start in the rotation and the effect of the leading edge is present. In zone I-1, the potential is the same as though a finite airfoil were undergoing a steady rotation. The leading edge effect is present but not the abrupt start in rotation. Thus in each zone, the source strength is different in nature and the potential is different in expression accordingly.

The above physical picture occurs because there is an abrupt change in $\dot{\alpha}$ at $t = 0$ (i.e., $\Delta\dot{\alpha} = \dot{\alpha}_1$), and $\dot{\alpha}_1$ remains constant for $t > 0$, as shown by the dotted line of Fig. 2b. Now at $t = t_1$ another change in $\dot{\alpha}$ (i.e., $\Delta\dot{\alpha} = \dot{\alpha}_2 - \dot{\alpha}_1 = -\dot{\alpha}_1$, $\dot{\alpha}_2$ being zero) is made as shown by the solid line from the dotted line. The second change in $\dot{\alpha}$ can be treated like the first one. Thus region II, where $t - t_1 > 0$, can be introduced. Three zones II-1, II-2, and II-3 can be similarly defined.

Introducing the new parameters $\nu_0 = x/U(t - t_0)$ (t_0 being 0) and $\nu_1 = x/U(t - t_1)$, we can show that, in region I, zone I-1 corresponds to $0 \leq \nu_0 \leq 1 - (1/M)$; zone I-2 corresponds to $1 - (1/M) \leq \nu_0 \leq 1 + (1/M)$; and zone I-3 corresponds to $1 + (1/M) \leq \nu_0$.

Similarly, in region II, zone II-1 corresponds to $0 \leq \nu_1 \leq 1 - (1/M)$; zone II-2 corresponds to $1 - (1/M) \leq \nu_1 \leq 1 + (1/M)$; and zone II-3 corresponds to $1 + (1/M) \leq \nu_1$.

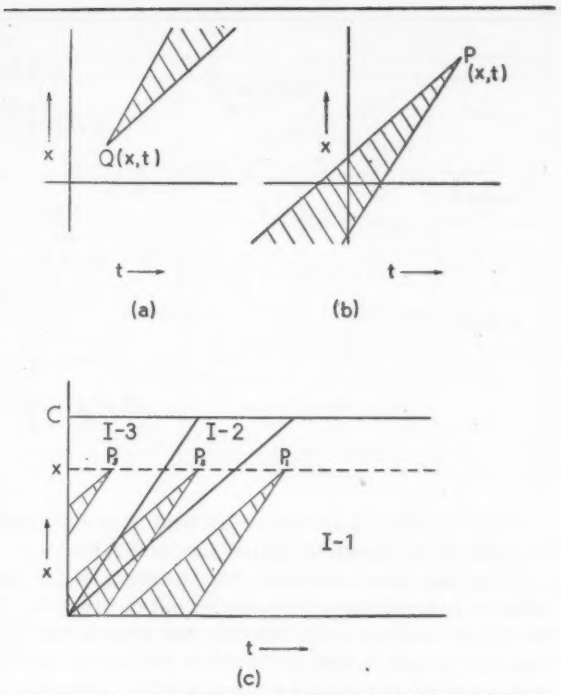

FIG. 5. (a) Zone of influence of source Q. (b) Zone of action upon P. (c) Zones of action upon P_1, P_2, and P_3 due to $\dot{\alpha}_1 = \frac{1}{2}\dot{\alpha}_0$ at $t = 0$. Each zone of action is different in shape from the other.

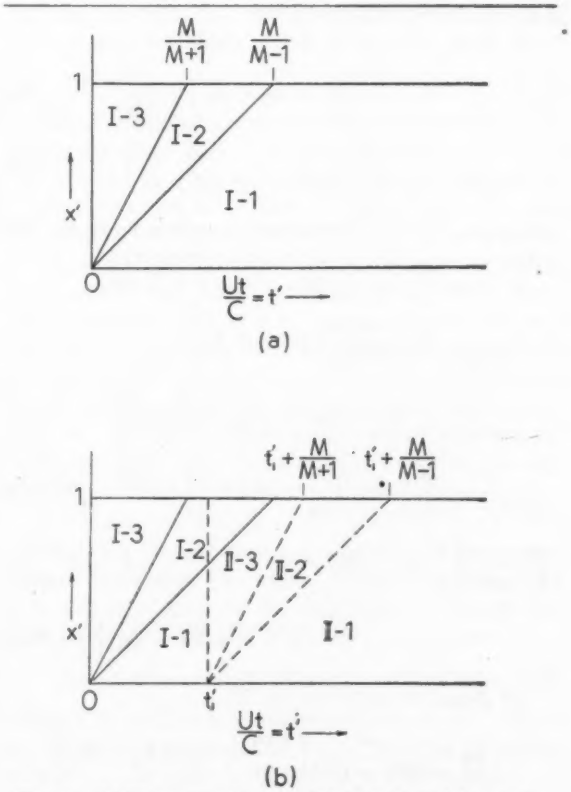

FIG. 6. (a) Three zones in region I ($t > 0$) formed due to $\dot{\alpha}_1 - \dot{\alpha}_0$ at $t_0 = 0$. (b) Region II ($t > t_1$) overlaps region I. Region II is due to $\dot{\alpha}_2 - \dot{\alpha}_1$ at t_1.

TABLE 1

ϕ vs. ν_0 and ν_1

Range of ν_1 \ Range of ν_0	$0 \leqq \nu_0 \leqq 1 - \frac{1}{M}$	$1 - \frac{1}{M} \leqq \nu_0 \leqq 1 + \frac{1}{M}$	$1 + \frac{1}{M} \leqq \nu_0 \leqq \infty$
Region I: $t - t_1 < 0$	(I-1) $\phi = \phi_{01}$	(I-2) $\phi = \phi_{02}$	(I-3) $\phi = \phi_{03}$
Regions I + II: $0 \leqq \nu_1 \leqq 1 - \frac{1}{M}$	(I-1) + (II-1) $\phi = \phi_{01} + \phi_{11} = \frac{-Ux\alpha_1}{(M^2-1)^{1/2}}$	Impossible	Impossible
Regions I + II: $1 - \frac{1}{M} \leqq \nu_1 \leqq 1 + \frac{1}{M}$	(I-1) + (II-2) $\phi = \phi_{01} + \phi_{12}$	(I-2) + (II-2) $\phi = \phi_{02} + \phi_{12}$	Impossible
Regions I + II: $1 + \frac{1}{M} \leqq \nu_1 \leqq \infty$	(I-1) + (II-3) $\phi = \phi_{01} + \phi_{13}$	(I-2) + (II-3) $\phi = \phi_{02} + \phi_{13}$	(I-3) + (II-3) $\phi = \phi_{03} + \phi_{13} = -\alpha_1(M^2-1)^{1/2}c(x - x_0)$

Zones in region I are shown by solid lines and zones in region II are shown by dotted lines in Fig. 6b.

Using the above concepts, the integrations for the velocity potential have been carried out in Appendix A. It is clear that, once the velocity potential of the first region is obtained, the contribution due to the second region can be written down immediately. In region I, ϕ_{01}, ϕ_{02}, and ϕ_{03} are introduced to represent the velocity potentials in zones I-1, I-2, and I-3, respectively. From Appendix A, if Eqs. (A10), (A11), and (A13) are substituted into Eq. (A3), the velocity potential in each zone can be written as follows:

(*a*) *Zone I-1*, $0 \leqq \nu_0 \leqq 1 - (1/M)$.

$$\phi_{01} = \frac{-\dot{\alpha}_1}{(M^2-1)^{1/2}}\left(\frac{Uxt_1}{2} + \Phi_{01} + \Phi_{11}\right) = \frac{-2\dot{\alpha}_1}{(M^2-1)^{1/2}}\Phi_{01}$$

$$= \frac{-\dot{\alpha}_1 x^2}{(M^2-1)^{1/2}}\left[\frac{1-\nu_{00}}{\nu_0} - \frac{1}{2(M^2-1)}\right] \qquad (6.9)$$

where Eq. (A14) is introduced to reduce Φ_{11} to Φ_{01}, and where $\nu_{00} = x_0/U(t - t_0)$ (x_0 being arbitrary).

(*b*) *Zone I-2*, $1 - (1/M) \leqq \nu_0 \leqq 1 + (1/M)$.

$$\phi_{02} = \frac{-\dot{\alpha}_1}{(M^2-1)^{1/2}}\left(\frac{Uxt_1}{2} + \Phi_{02} + \Phi_{11}\right)$$

$$= \frac{-\dot{\alpha}_1}{(M^2-1)^{1/2}}(\Phi_{01} + \Phi_{02}) = \frac{-\dot{\alpha}_1 x^2}{(M^2-1)^{1/2}}\left(\left[\frac{1-\nu_{00}}{\nu_0} - \frac{1}{2(M^2-1)}\right]\left[\frac{1}{\pi}\sin^{-1}\left(\frac{m}{\nu_0} - M\right) + \frac{1}{2}\right] - \frac{(M^2-1)^{1/2}}{M} \times \left\{\frac{\nu_0 - \nu_{00}}{\nu_0^2}\left[\frac{1}{\pi}\sin^{-1}M(1-\nu_0) - \frac{1}{2}\right] - \frac{1}{2\pi\nu_0^2}\left(\frac{1}{M} + \frac{\nu_0}{m}\right) \times \sqrt{1 - M^2(1-\nu_0)^2}\right\}\right) \qquad (6.10)$$

(*c*) *Zone I-3*, $\nu_0 \geqq 1 + (1/M)$.

$$\phi_{03} = \frac{-\dot{\alpha}_1}{(M^2-1)^{1/2}}\left(\frac{Uxt_1}{2} + \Phi_{03} - \Phi_{01} + \Phi_{11}\right)$$

$$= \frac{-\dot{\alpha}_1}{(M^2-1)^{1/2}}\Phi_{03} = \frac{-\dot{\alpha}_1 x^2}{M}\left(\frac{\nu_0 - \nu_{00}}{\nu_0^2}\right) \qquad (6.11)$$

It is easy to show that, for $t < 0$ (i.e., $\nu < 0$), the velocity potential is zero from Eq. (A3). This checks with the given condition.

Similarly in region II, the contribution to the velocity potential due to the second change in $\dot{\alpha}$ (i.e., $\Delta\dot{\alpha} = \dot{\alpha}_2 - \dot{\alpha}_1 = -\dot{\alpha}_1$, $\dot{\alpha}_2$ being zero) can be shown to be $\phi_{1j} = -\phi_{0j}$, where ν_0 and ν_{00} in ϕ_{0j} are replaced by ν_1 and ν_{10} in ϕ_{1j} ($j = 1, 2$ or 3). Here, $\nu_{10} = x_0/U(t - t_1)$.

With the above relations and Appendix A, a table can be formulated to represent ϕ for all cases in Eq. (A-3) (see Table 1).

An important feature of Table 1 is that in the overlapping regions $\phi = \phi_{0k} + \phi_{1m}$ corresponds exactly to the overlapping zones (I-k) + (II-m), where $k, m = 1, 2, 3$. Since ϕ_{0k} is the velocity potential in zone I-k due to change in $\dot{\alpha}$ at $t = 0$ and ϕ_{1m} in zone II-m due to change in $\dot{\alpha}$ at $t = t_1$, we see that ϕ can be obtained by superimposing the solutions ϕ_{0k} and ϕ_{1m} for $t > t_1$.

In the overlapping zone (I-1) + (II-1), α becomes constant at α_1, and all of the transient effect damps out. The velocity potential becomes identical to Ackeret's solution of the steady case

It is apparent that the effect of the first change in $\dot{\alpha}$ and α at $t = 0$ cannot influence the pressure for $t < 0$; therefore $\phi_0 = 0$ for $t < 0$. Similarly $\phi_1 = 0$ for $t < t_1$ in the second change at $t = t_1$.

When the zone II-3 overlaps the zone I-3, the potential is again independent of time. This means that the influence of $\dot{\alpha}$ discontinuity ($\Delta\dot{\alpha} = \dot{\alpha}_1$) at $t = 0$ just counterbalances that at $t = t_1$($\Delta\dot{\alpha} = -\dot{\alpha}_1$) and this potential must be equivalent to that of an infinite chord airfoil at constant α_1.

(7) Pressure Distribution

To the approximation of the linearized theory, the pressure coefficient C_p is connected to the derivative of the velocity potential ϕ as follows:

$$C_p = \frac{p - p_1}{\rho_1 U^2/2} = -\frac{2}{U}\frac{d\phi}{dt} = -\frac{2}{U^2}\frac{\partial\phi}{\partial t} - \frac{2}{U}\frac{\partial\phi}{\partial x} \qquad (7.1)$$

where ϕ is given in Table 1 for various regions and zones. For region I ($t > 0$) the pressure coefficient in

TABLE 2
C_p vs. ν_0 and ν_1

	Range of ν_0 → / Range of ν_1 ↓	$0 \leq \nu_0 \leq 1 - \frac{1}{M}$	$1 - \frac{1}{M} \leq \nu_0 \leq 1 + \frac{1}{M}$	$1 + \frac{1}{M} \leq \nu_0 \leq \infty$
Region I	$\nu_1 < 0$	(I-1) $C_p = C_{p01}$	(I-2) $C_p = C_{p02}$	(I-3) $C_p = C_{p03}$
Regions I + II	$0 \leq \nu_1 \leq 1 - \frac{1}{M}$	(I-1) + (II-1) $C_p = C_{p01} + C_{p11} = \frac{2\alpha_1}{(M^2-1)^{1/2}}$	Nonexisting	Nonexisting
	$1 - \frac{1}{M} \leq \nu_1 \leq 1 + \frac{1}{M}$	(I-1) + (II-2) $C_p = C_{p01} + C_{p12}$	(I-2) + (II-2) $C_p = C_{p02} + C_{p12}$	Nonexisting
	$1 + \frac{1}{M} \leq \nu_1 \leq \infty$	(I-1) + (II-3) $C_p = C_{p01} + C_{p13}$	(I-2) + (II-3) $C_p = C_{p02} + C_{p13}$	(I-3) + (II-3) $C_p = C_{p03} + C_{p13} = \frac{2\alpha_1}{M}$

each zone can be defined as

$$C_{p0j} = -(2/U)(d\phi_{0j}/dt) \qquad (j = 1, 2, 3) \qquad (7.2)$$

$$C_{p0j} = (\dot{\alpha}_1 - \dot{\alpha}_0)(x/U) f_j(\nu_0, \nu_{00})$$

where $\dot{\alpha}_1 - \dot{\alpha}_0$ is introduced to replace $\dot{\alpha}_1$ in order to extend the result to a more general case, $\dot{\alpha}_0$ being zero. Here f_j can be obtained by differentiating Eqs. (6.9), (6.10), and (6.11),

$$(\nu_0, \nu_{00}) = \frac{-2}{(\dot{\alpha}_1 - \dot{\alpha}_0)x}\frac{d\phi_{01}}{dt}$$

$$= \frac{2}{(M^2-1)^{1/2}}\left(\frac{1-\nu_{00}}{\nu_0} + \frac{M^2-2}{M^2-1}\right),$$

$$\text{for } 0 < \nu_0 \leq 1 - \frac{1}{M} \qquad (7.3)$$

$$f_2(\nu_0, \nu_{00}) = \frac{-2}{(\dot{\alpha}_1 - \dot{\alpha}_0)x}\frac{d\phi_{02}}{dt} = \frac{2}{(M^2-1)^{1/2}} \times$$

$$\left\{\left(\frac{1-\nu_{00}}{\nu_0} + \frac{M^2-2}{M^2-1}\right)\left[\frac{1}{2} + \frac{1}{\pi}\sin^{-1}\left(\frac{m}{\nu_0} - M\right)\right] + \right.$$

$$\frac{(M^2-1)^{1/2}}{\pi M}\left(\frac{1-\nu_{00}}{\nu_0} + 1\right)\cos^{-1} M(1-\nu_0) +$$

$$\left.\frac{2M^2-1}{\pi\nu_0(M^2-1)^{1/2}M^2}\left[1 - M^2(1-\nu_0)^2\right]^{1/2}\right\},$$

$$\text{for } 1 - \frac{1}{M} \leq \nu_0 \leq 1 + \frac{1}{M} \qquad (7.4)$$

and

$$f_3(\nu_0, \nu_{00}) = \frac{-2}{(\dot{\alpha}_1 - \dot{\alpha}_0)x}\frac{d\phi_{03}}{dt}$$

$$= \frac{2}{M}\left(\frac{1-\nu_{00}}{\nu_0} + 1\right), \qquad \text{for } \nu_0 \geq 1 + \frac{1}{M} \qquad (7.5)$$

Similarly, in the region II, $(t > t_1)$, we can define the pressure coefficient as

$$C_{p1j} = -(2/U)(d\phi_{1j}/dt)$$

$$= (\dot{\alpha}_2 - \dot{\alpha}_1)(x/U) f_j(\nu_1, \nu_{10}) \qquad (j = 1, 2, 3) \qquad (7.6)$$

where $f_j(\nu_1, \nu_{10})$ are the same as $f_j(\nu_0, \nu_{00})$ given in Eqs. (7.3), (7.4), and (7.5) except ν_0, ν_{00} are replaced by ν_1 and ν_{10}.

In Eqs. (7.3) and (7.4), it is easy to verify that, at $\nu_i = 1 - (1/M)$ and at the same time,

$$f_1(\nu_i, \nu_{i0}) = f_2(\nu_i, \nu_{i0}) \qquad (i = 0, 1) \qquad (7.7a)$$

In Eqs. (7.4) and (7.5) we can get at $\nu_i = 1 + (1/M)$ and at the same time,

$$f_2(\nu_i, \nu_{i0}) = f_3(\nu_i, \nu_{i0}) \qquad (i = 0, 1) \qquad (7.7b)$$

Therefore along the two boundary lines of the zones of the t-x plane [i.e., $\nu_i = 1 - (1/M)$ and $\nu_i = 1 + (1/M)$] the C_p's are continuous in value, but are discontinuous in the derivatives. This is true for any one of a number of regions (i.e., ith region) as shown later.

Therefore the pressure coefficient $C_p(t, x)$ can be evaluated if the point is located in one of the three zones in region I where $0 < t$ as shown in the first row in Table 2. Of course, only the increment in $\dot{\alpha}$ at $t = 0$ is considered. Now if the point (t, x) lies in both regions I and II, where $t > t_1$, the increments in $\dot{\alpha}$ both at $t = 0$ and $t = t_1$ will influence the pressure coefficient, and both should be considered accordingly. This is clearly shown in Table 2 when $t \geq t_1$.

For ease of treatment, a new time unit $\bar{t} = C/U$ is introduced. $\bar{t}$ is the time required for the free-stream flow to travel a chord length. A nondimensional time $t' = t/\bar{t}$ can be used for the time scale. With the new time unit, Eqs. (7.2) and (7.6) can be written as

$$C_{pij} = (\dot{\alpha}_{i+1} - \dot{\alpha}_i)x' f_j(\nu_i, \nu_{i0}) \qquad (i = 0, 1) \qquad (7.8)$$

where $x' = x/C$, $\dot{\alpha}_i$ is $\dot{\alpha}$ immediately ahead of t_i', $\dot{\alpha}_{i+1}$ is $\dot{\alpha}$ immediately after t_i', and $\dot{\alpha}_{i+1} - \dot{\alpha}_i$ is the increment of $\dot{\alpha}$ at t_i'. In Table 2, this new time unit is used.

In the table $\nu_0 < 0$, $(t < 0)$, $C_p = 0$. In the overlapped zone (I-1) + (II-1) where the transient reaction

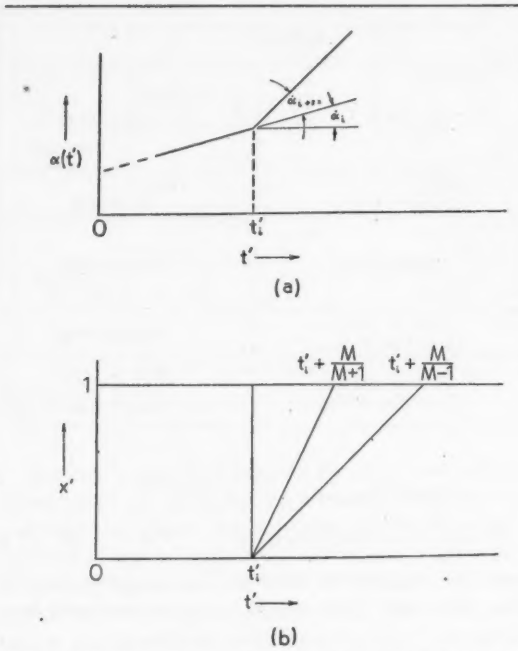

FIG. 7. Three zones formed in region $i+1 (t > t_i)$ due to $\dot{\alpha}_{i+1} - \dot{\alpha}_i$ at t_i'.

damps out, $C_p = 2\alpha_1/(M^2-1)^{1/2}$ checks with Ackeret's result. It is interesting that $C_p = 2\alpha_1/M$ in the overlapped zone (I-3) + (II-3). Note the superposition of the parts of C_p contributed by region I and region II.

(8) Lift, Moment, and Wave Drag

It is generally known that the lift coefficient of an airfoil with a chord C is

$$C_L(t) = \frac{1}{C}\int_0^C dx[C_p(-0) - C_p(+0)] = \frac{2}{C}\int_0^C dx C_p \qquad (8.1a)$$

where $C_p(-0) = C_p(x, -0, t)$ and $C_p(+0) = C_p(x, +0, t)$. They are equal in magnitude but opposite in sign. $C_p = C_p(x, -0, t)$ is introduced in the latter equation. The moment coefficient is

$$C_M(t)' = \frac{2}{C^2}\int_0^C (x - x_0)dx C_p = \frac{2}{C^2}\int_0^C x\,dx\,C_p - x_0' C_L \qquad (8.2a)$$

The wave drag coefficient is

$$C_D(t) = (2/C)\int_0^C dx\; C_p\alpha \qquad (8.3)$$

where $\alpha = \alpha(x, t)$. For a flat plate

$$C_D(t) = \alpha C_L \qquad (8.3a)$$

Therefore, as soon as C_L is known, it becomes a simple matter to calculate C_D, and, consequently, C_D will not be treated in this paper. However, in the case of $\alpha_0 = \alpha_b \neq 0$, $C_p + 2\alpha_b/(M^2-1)^{1/2}$ and $\alpha + \alpha_b$ should replace C_p and α, respectively, in Eq. (8.3).

(A) *Lift and Moment for the Present Case*

Now we may study C_L and C_M in region I due to $\dot{\alpha}_1 - \dot{\alpha}_0$ at $t_0' = 0$. As C_p is conveniently expressed in terms of $\nu_0 = x'/(t' - t_0')$ and $\nu_{00} = x_0'/(t' - t_0')$, we may transform Eqs. (8.1) and (8.2) into the forms

$$C_{L1}(t') = \frac{2}{\nu_{0C}}\int_0^{\nu_{0C}} d\nu_0 C_p = 2(t' - t_0')\int_0^{1/(t'-t_0')} C_p d\nu_0 \qquad (8.1b)$$

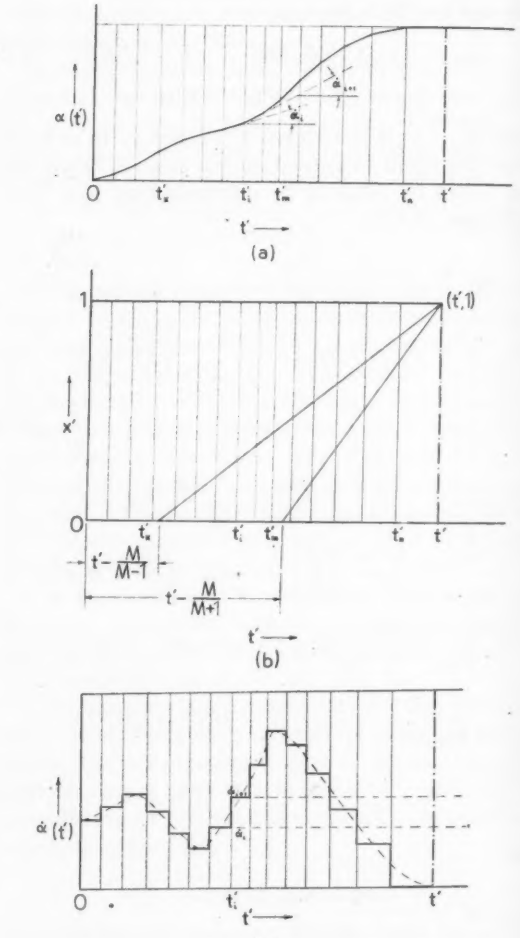

FIG. 8. (a) Arbitrary $\alpha(t')$ vs. t' approximated by a series of tangent line elements. (The curve is omitted.)

(b) All the overlapped regions ahead of t' are divided into three groups: first group, 0 to t_k'; second group, t_{k+1}' to t_m'; and third group, t_{m+1}' to t_n'.

(c) Corresponding $\dot{\alpha}$ vs. t' curve (dotted) approximated by steps.

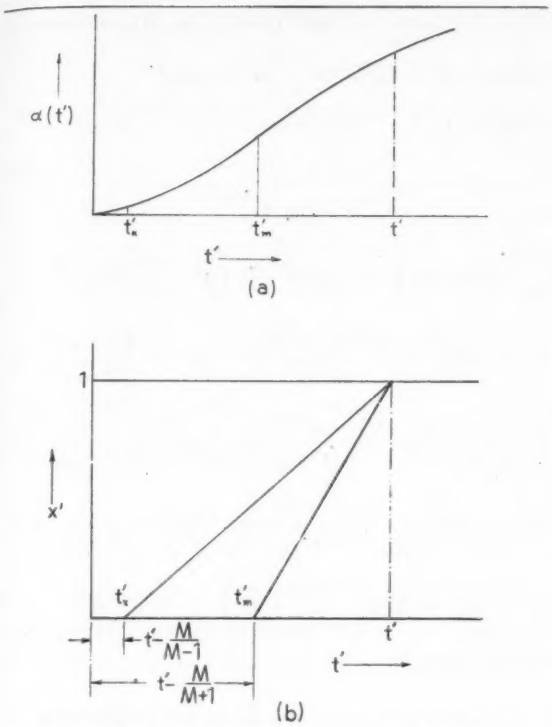

FIG. 9. (a) α vs. t' ($\dot{\alpha}$ being continuous). (b) Three characteristic integration intervals shown: first interval from 0 to t_k'; second interval from t_k' to t_m'; third interval from t_m' to t'.

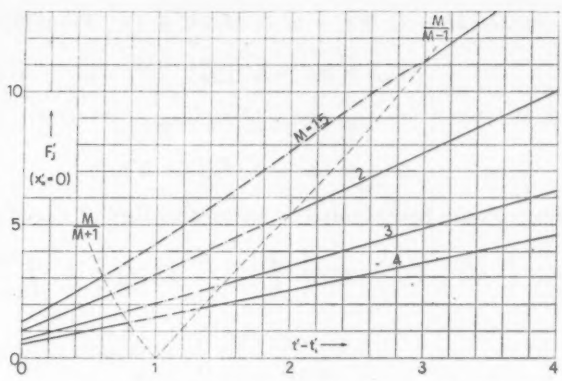

FIG. 10a. F_j' vs. $t - t_i'$ at $M = 1.5, 2, 3, 4$. Left solid lines—F_3' vs. $t' - t_i'[t - t_i' \leq M/(M+1)]$. Center dotted lines—$F_2'$ vs. $t' - t_i'[M/(M+1) \leq t' - t_i' \leq M/(M-1)]$. Right solid lines—$F_1'$ vs. $t' - t_i'[M/(M-1) \leq t' - t_i']$.

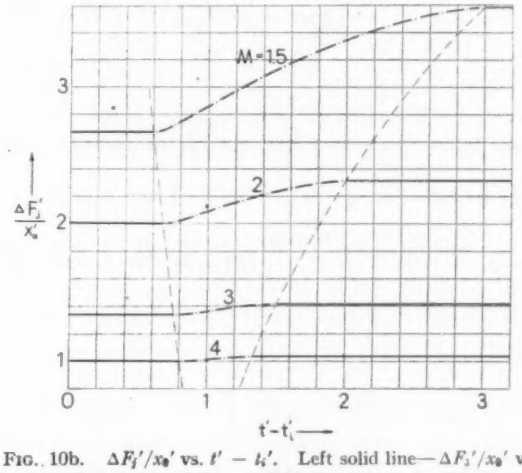

FIG. 10b. $\Delta F_j'/x_0'$ vs. $t' - t_i'$. Left solid line—$\Delta F_3'/x_0'$ vs. $t' - t_i'$. Center dotted line—$\Delta F_2'/x_0'$ vs. $t' - t_i'$. Right solid line—$\Delta F_1'/x_0'$ vs. $t' - t_i'$.

where $\nu_{0C} = 1/(t' - t_0')$.

$$C_{M1}(t') = \frac{2}{(\nu_{0C})^2}\int_0^{\nu_{0C}} \nu_0 d\nu_0 C_p - x_0' C_L$$

$$= 2(t' - t_0')^2 \int_0^{1/(t'-t_0')} \nu_0 d\nu_0 C_p - x_0' C_L \quad (8.2b)$$

where C_{L1} and C_{M1} are lift and moment coefficients in the region I due to $\dot{\alpha}_1 - \dot{\alpha}_0$ at t_0'.

As shown before, C_p is discontinuous along two lines, $\nu_0 = 1 - (1/M)$ and $\nu_0 = 1 + (1/M)$ in the t'-x' plane. The above integrals have to be split up once if $\nu_0 > 1 - (1/M)$ and twice if $\nu_0 > 1 + (1/M)$. Therefore, there are three possibilities: (a) $t' - t_0' \geq M/(M-1)$; (b) $M/(M+1) \leq t' - t_0' \leq M/(M-1)$, where one discontinuity $\nu_0 = 1 - (1/M)$ will be encountered; and (c) $0 \leq t' - t_0' \leq M/(M+1)$ where two discontinuities will be encountered.

(a) $t' - t_0' \geq M/(M-1)$. From Eqs. (7.4) and (8.1) and Table 2,

$$C_{L11}(t') = 2(t' - t_0')\int_0^{1/(t'-t_0')} (\dot{\alpha}_1 - \dot{\alpha}_0) x' f_1(\nu_0) d\nu_0$$

Substituting ν_0 for x', we have

$$C_{L11} = 2(t' - t_0')^2(\dot{\alpha}_1 - \dot{\alpha}_0)\int_0^{1/(t'-t_0')} \nu_0 d\nu_0 f_1(\nu_0) = (\dot{\alpha}_1 - \dot{\alpha}_0) F_1(t' - t_0') \quad (8.4)$$

where C_{L1} means the contribution of C_L due to $\dot{\alpha}_1 - \dot{\alpha}_0$ and C_{L11} refers to C_{L1} when $t' - t_0' \geq M/(M-1)$. With Eq. (7.4) we can show

$$F_1(t' - t_0') = 2(t' - t_0')^2 \int_0^{1/(t'-t_0')} \nu_0 d\nu_0 f_1(\nu_0) = \frac{4}{(M^2-1)^{1/2}}\left[t' - t_0' + \frac{M^2 - 2}{2(M^2-1)} - x_0'\right] = F_1' - \Delta F_1' \quad (8.5)$$

where $F_1' = F_1$ when $x_0' = 0$ and where $\Delta F_1'$ is the contribution of x_0' to F_1.

(*b*) $M/(M-1) \geqq t'-t_0' \geqq M/(M+1)$. From Eqs. (7.4), (7.5), and (8.1) and Table 2, the lift coefficient is

$$\begin{aligned} C_{L12} &= 2(t'-t_0')\left[\int_0^{1-(1/M)} x'(\dot{\alpha}_1-\dot{\alpha}_0)f_1(\nu_0)d\nu_0 + \int_{1-(1/M)}^{1/(t'-t_0')} x'(\dot{\alpha}_1-\dot{\alpha}_0)f_2(\nu_0)d\nu_0\right] \\ &= 2(t'-t_0)^2(\dot{\alpha}_1-\dot{\alpha}_0)\left[\int^{1-(1/M)} \nu_0 d\nu_0 f_1(\nu_0) + \int_0^{1/(t'-t_0')} \nu_0 f_2(\nu_0)d\nu_0\right] \\ &= (\dot{\alpha}_1-\dot{\alpha}_0)F_2(t'-t_0') \end{aligned} \tag{8.6}$$

where F_2 can be evaluated by integrating Eqs. (7.4) and (7.5).

$$\begin{aligned} F_2(t'-t_0') = 2(t'-t_0')^2\left[\int_0^{1-(1/M)} \nu_0 d\nu_0 f_1(\nu_0) + \int_{1-(1/M)}^{1/(t'-t_0')} \nu_0 f_2(\nu_0)d\nu_0\right] = \frac{4}{(M^2-1)^{1/2}}\left(\left[\frac{t'-t_0'}{2} + \right.\right. \\ \left.\frac{M^2-2}{4(M^2-1)}\right]\left\{1+\frac{2}{\pi}\sin^{-1}[m(t'-t_0')-M]\right\} + \frac{(M^2-1)^{1/2}}{4M^2\pi}\left(t'-t_0'+\frac{5M^2-3}{M^2-1}\right)\times \\ \sqrt{(t'-t_0')^2-M^2(t'-t_0'-1)^2} + \frac{(M^2-1)^{1/2}}{M\pi}\left[t'-t_0'+\frac{1}{2}+\frac{(t'-t_0')^2}{4M^2}\right]\cos^{-1}M\left(1-\frac{1}{t'-t_0'}\right)\Bigg) - \\ \frac{4x_0'}{(M^2-1)^{1/2}}\left(\frac{1}{2}\left\{1+\frac{2}{\pi}\sin^{-1}[m(t'-t_0')-M]\right\} + \frac{(M^2-1)^{1/2}}{M\pi}\cos^{-1}M\left(1-\frac{1}{t'-t_0'}\right) + \right. \\ \left.\frac{(M^2-1)^{1/2}}{M^2\pi}\sqrt{(t'-t_0')^2-M^2(t'-t_0'-1)^2}\right) = F_2' - \Delta F_2' \end{aligned} \tag{8.7}$$

where $F_2' = F_2$ when $x' = 0$; $\Delta F_2'$ is the part of F_2 contributed by $x_0' \neq 0$.

(*c*) $0 \leqq t'-t_0' \leqq M/(M+1)$. From Eqs. (7.4), (7.5), (7.6), and (8.1) and Table 2, the lift coefficient is

$$\begin{aligned} C_{L13} &= 2(t'-t_0')\left[\int_0^{1-(1/M)} (\dot{\alpha}_1-\dot{\alpha}_0)x'd\nu_0 f_1(\nu_0) + \int_{1-(1/M)}^{1+(1/M)} (\dot{\alpha}_1-\dot{\alpha}_0)x'd\nu_0 f_2(\nu_0) + \right. \\ &\qquad \left. \int_{+(1/M)}^{1/(t'-t_0')} (\dot{\alpha}_1-\dot{\alpha}_0)x'd\nu_0 f_3(\nu_0)\right] \\ &= 2(\dot{\alpha}_1-\dot{\alpha}_0)(t'-t_0')^2\left[\int^{1-(1/M)} \nu_0 d\nu_0 f_1(\nu_0) + \int_{1-(1/M)}^{1+(1/M)} \nu_0 d\nu_0 f_2(\nu_0) + \int_{1+(1/M)}^{1/(t'-t_0')} \nu_0 d\nu_0 f_3(\nu_0)\right] \\ &= (\dot{\alpha}_1-\dot{\alpha}_0)F_3(t'-t_0') \end{aligned} \tag{8.8}$$

where

$$\begin{aligned} F_3(t'-t_0') &= 2(t'-t_0')^2\left[\int_0^{1-(1/M)} \nu_0 d\nu_0 f_1(\nu_0) + \int_{1-(1/M)}^{1+(1/M)} \nu_0 d\nu_0 f_2(\nu_0) + \int_{1+(1/M)}^{1/(t'-t_0')} \nu_0 d\nu_0 f_3(\nu_0)\right] \\ &= \frac{1}{M^3}(t'-t_0')^2 + \frac{4}{M}(t'-t_0') + \frac{2}{M} - \frac{4x_0'}{M} = F_3' - \Delta F_3' \end{aligned} \tag{8.9}$$

where $F_3' = F_3$ when $x_0' = 0$ and $\Delta F_3'$ is the part of F_3 contributed by $x_0' \neq 0$. If we introduce $j = 1, 2, 3$, F_j' and $\Delta F_j'/x_0'$ are given in the above equations. F_j' and $\Delta F_j'/x_0'$ vs. $t'-t_1'$ are plotted in Fig. 10 for $M = 1.5$, 2, 3, and 4.

(*d*) *Similarly, we can have the moment coefficient for the three cases.*

$$G_{M1j} = (\dot{\alpha}_1-\dot{\alpha}_0)[G_j(t'-t_0') - x_0'F_j(t'-t_0')] \qquad (j = 1, 2, 3) \tag{8.10}$$

When $t'-t_0' \geq M/(M-1)$, $j = 1$,

$$G_1(t'-t_0') = 2(t'-t_0')^3\int_0^{1/(t'-t_0')} \nu_0^2 d\nu_0 f_1(\nu_0) = \frac{4}{(M^2-1)^{1/2}}\left[\frac{1}{2}(t'-t_0') + \frac{M^2-2}{3(M^2-1)} - \frac{x_0'}{2}\right] = G_1' - \Delta G_1' \tag{8.11}$$

When $M/(M+1) \leqq t'-t_0' \leqq M/(M-1)$, $j = 2$,

$$G_2(t'-t_0') = 2(t'-t_0')^3\left[\int_0^{1-(1/M)} v_0^2 dv_0 f_1(v_0) + \int_{1-(1/M)}^{1/(t'-t_0')} v_0^2 dv_0 f_2(v_0)\right] = \frac{4}{(M^2-1)^{1/2}}\left(\left[\frac{t'-t_0'}{4} + \frac{M^2-2}{6(M^2-1)}\right]\left\{1+\frac{2}{\pi}\sin^{-1}[m(t'-t_0')-M]\right\} + \frac{(M^2-1)^{1/2}}{M\pi}\left[\frac{1}{12M^2}(t'-t_0')^2 + \frac{t'-t_0'}{2} + \frac{1}{3}\right]\cos^{-1}M \times \left(1-\frac{1}{t'-t_0'}\right) + \frac{(M^2-1)^{1/2}}{9M^2\pi}\left[\frac{M^2-4}{4M^2}(t'-t_0')^2 + \frac{t'-t_0'}{4} + \frac{7M^2-4}{M^2-1}\right]\sqrt{(t'-t_0')^2 - M^2(t-t_0'-1)^2}\right) - \frac{4x_0'}{(M^2-1)^1}\left(\frac{1}{4}\left\{1+\frac{2}{\pi}\sin^{-1}[m(t'-t_0')-M]\right\} + \frac{(M^2-1)^{1/2}}{M\pi}\left[\frac{1}{2} - \frac{(t'-t_0')^2}{4M^2}\right]\cos^{-1}M\left(1-\frac{1}{t'-t_0'}\right) + \frac{(M^2-1)^{1/2}}{4M^2\pi}(t'-t_0'+1)\sqrt{(t'-t_0')^2 - M^2(t'-t_0'-1)^2}\right) = G_2' - \Delta G_2' \quad (8.12)$$

When $t'-t_0' \leqq M/(M+1)$, $j=3$,

$$G_3(t'-t_0') = 2(t'-t_0')^3\left]\int_0^{1-(1/M)} v_0^2 dv_0 f_1(v_0) + \int_{1-(1/M)}^{1+(1/M)} v_0^2 dv_0 f_2(v_0) + \int_{1+(1/M)}^{1/(t'-t_0')} v_0^2 dv_0 f_3(v_0)\right]$$
$$= \left[\frac{1}{3M^3}(t'-t_0')^3 + \frac{2}{M}(t'-t_0') + \frac{4}{3M}\right] - x_0'\left[-\frac{1}{M^3}(t'-t_0')^2 + \frac{2}{M}\right]$$
$$= G_3' - \Delta G_3' \quad (8.13)$$

In the above, it should be noted that $G_j' = G_j$ when $x_0' = 0$ and $\Delta G_j'$ is the part of G_j contributed by $x_0' \neq 0$ ($j = 1, 2, 3$). G_j' and $\Delta G_j'/x_0'$ vs. $(t'-t_i')$ are plotted in Fig. 11 for $M = 1.5$, 2, 3, and 4.

It is interesting and useful to note that $\Delta F_j/x_0'$ and $\Delta G_j/x_0'$ can be used to calculate C_L and C_M of an airfoil or a wing that starts suddenly to descend at constant vertical velocity $\dot{\bar{h}}$. The procedure is: Let $x_0' = 1$ in the above expressions of ΔF_j and ΔG_j. Then $\Delta F_j = C_{Lj}/(\dot{\bar{h}}/U)$ and $\Delta G_j = C_{Mj}/(\dot{\bar{h}}/U)$ of the wing because of the flapping degree of freedom. Of course, some integral relations may be easily formulated for the case of $\dot{\bar{h}}$ being an arbitrary function of time. The details will be discussed in a later paper.

(e) *Decomposition of C_{L1} into three parts.*—Physically $C_{L1}(t')$ can be decomposed into three parts—namely, ΔC_{LA}, ΔC_{LB}, and ΔC_{LC}. ΔC_{LA} is the contribution of instant angle of attack $\Delta\alpha = (\dot{\alpha}_1 - \dot{\alpha}_0)(t'-t_0')$ and can be calculated from Ackeret's formula

$$C_{LA} = 4\Delta\alpha/(M^2-1)^{1/2} \quad (8.14)$$

The second part ΔC_{LB} is the contribution due to rotating velocity $\dot{\alpha}_1 - \dot{\alpha}_0$ and is proportional to $\dot{\alpha}_1 - \dot{\alpha}_0$ but independent of t'. Its value can be shown as

$$\Delta C_{LB} = C_{L11} - \Delta C_{LA} = C_{L11} - \frac{4(\dot{\alpha}_1-\dot{\alpha}_0)(t'-t_0')}{(M^2-1)^{1/2}}$$
$$= (\dot{\alpha}_1-\dot{\alpha}_0)\left[F_1 - \frac{4(t'-t_0')}{(M^2-1)^{1/2}}\right]$$
$$= \frac{4}{(M^2-1)^{1/2}}\left[\frac{M^2-2}{2(M^2-1)} - x_0'\right](\dot{\alpha}_1-\dot{\alpha}_0) \quad (8.15)$$

The third part ΔC_{LC} is the contribution due to transient effect that occurs when $0 \leqq t'-t_0' \leqq M/(M-1)$ If $0 \leqq t'-t_0' \leqq M/(M+1)$,

$$\Delta C_{LC} = C_{L13} - C_{L11} = (\dot{\alpha}_1-\dot{\alpha}_0)(F_3-F_1) \quad (8.16a)$$

and if $M/(M+1) \leqq t'-t_0' \leqq M/(M-1)$,

$$\Delta C_{LC} = C_{L12} - C_{L11} = (\dot{\alpha}_1-\dot{\alpha}_0)(F_2-F_1) \quad (8.16b)$$

where F_1, F_2, and F_3 are functions of $t'-t_0'$ and are given in Eqs. (8.5), (8.7), and (8.9).

Similarly, C_{MA} can also be decomposed into three parts,

$$\Delta C_{MA} = [4\Delta\alpha/(M^2-1)^{1/2}][(1/2) - x_0'] \quad (8.17)$$

which can be evaluated from Ackeret's formula if the instant increment of α is used.

$$\Delta C_{MB} = \frac{4(\dot{\alpha}_1-\dot{\alpha}_0)}{(M^2-1)^{1/2}}\left[\frac{M^2-2}{3(M^2-1)} - \frac{x_0'}{2}\right] - x_0'\Delta C_{LB} \quad (8.18)$$

which is proportional to $(\dot{\alpha}_1 - \dot{\alpha}_0)$ but is independent of time, and the transient part is

$$\Delta C_{MC} = C_{M1} - \Delta C_{MA} - \Delta C_{MB} \quad (8.19)$$

$$\Delta C_{MC} = (\dot{\alpha}_1-\dot{\alpha}_0)[G_2 - G_1 - x_0'(F_2-F_1)]$$

if $M/(M+1) \leqq t'-t_0' \leqq M/(M-1)$ or

$$\Delta C_{MC} = (\dot{\alpha}_1-\dot{\alpha}_0)[G_3 - G_1 - x_0'(F_3-F_1)]$$

if $0 \leqq t'-t_0' \leqq M/(M+1)$. The discussion of the results will be treated later.

TABLE 3

$C_L/\dot{\alpha}_1$ and $(C_M + x_0'C_L)/\dot{\alpha}_1$ as functions of $t' - t_0'$ and $t' - t_1'$

Region I $t' \geq 0$	Range of $t' - t_0'$	$t' - t_0' \geq \frac{M}{M-1}$	$\frac{M}{M+1} \leq t' - t_0' \leq \frac{M}{M-1}$	$0 \leq t' - t_0' \leq \frac{M}{M+1}$
	Zones crossed	I-1	I-1 and I-2	I-1, I-2, and I-3
	$C_L/\dot{\alpha}_1 =$	$F_1(t' - t_0')$	$F_2(t' - t_0')$	$F_3(t' - t_0')$
	$(C_M + x_0'C_L)/\dot{\alpha}_1 =$	$G_1(t' - t_0')$	$G_2(t' - t_0')$	$G_3(t' - t_0')$
Regions I + II $t' \geq t_1'$	Range of $t' - t_0'$	$t' - t_0' \geq \frac{M}{M-1}$	$t' - t_0' \geq \frac{M}{M-1}$	$t' - t_0' \geq \frac{M}{M-1}$
	Range of $t' - t_1'$	$t' - t_1' \geq \frac{M}{M-1}$	$\frac{M}{M+1} \leq t' - t_1' \leq \frac{M}{M-1}$	$0 \leq t' - t_1' \leq \frac{M}{M+1}$
	Zones crossed	I-1 and II-1	I-1, II-1, and II-2	I-1, II-1, II-2, and II-3
	$C_L/\dot{\alpha}_1 =$	$F_1(t' - t_0') - F_1(t' - t_1') = \frac{4t_1}{(M^2-1)^{1/2}}$	$F_1(t' - t_0') - F_2(t' - t_1')$	$F_1(t' - t_0') - F_2(t' - t_1')$
	$(C_M + x_0'C_L)/\dot{\alpha}_1 =$	$G_1(t' - t_0') - G_1(t' - t_1') = \frac{2t_1}{(M^2-1)^{1/2}}$	$G_1(t' - t_0') - G_2(t' - t_1')$	$G_1(t' - t_0') - G_2(t' - t_1')$
	Range of $t' - t_0'$	$\frac{M}{M+1} \leq t' - t_0' \leq \frac{M}{M-1}$	$\frac{M}{M+1} \leq t' - t_0' \leq \frac{M}{M-1}$	$0 \leq t' - t_0' \leq \frac{M}{M+1}$
	Range of $t' - t_1'$	$\frac{M}{M+1} \leq t' - t_1' \leq \frac{M}{M-1}$	$0 \leq t' - t_1' \leq \frac{M}{M+1}$	$0 \leq t' - t_1' \leq \frac{M}{M+1}$
	Zones crossed	I-1, I-2, II-1, and II-2	I-1, I-2, II-1, II-2, and II-3	I-1, I-2, I-3, II-1, II-2, and II-3
	$C_L/\dot{\alpha}_1 =$	$F_2(t' - t_0') - F_2(t' - t_1')$	$F_2(t' - t_0') - F_3(t' - t_1')$	$F_3(t' - t_0') - F_3(t' - t_1')$
	$(C_M + x_0'C_L)/\dot{\alpha}_1 =$	$G_2(t' - t_0') - G_2(t' - t_1')$	$G_2(t' - t_0') - G_3(t' - t_1')$	$G_3(t' - t_0') - G_3(t' - t_1')$

(f) The second region of the given downwash.—In the case of another change in α slope at t_1' (i.e., $\dot{\alpha}_2 - \dot{\alpha}_1$), another new region, II, is formulated. If $t' > t_1'$, both regions will contribute to lift and moment. As the contribution due to $\dot{\alpha}_1 - \dot{\alpha}_0$ on lift and moment has been given above, the additional contribution due to $\dot{\alpha}_2 - \dot{\alpha}_1$ in region II is

$$C_{L2j}(t') = (\dot{\alpha}_2 - \dot{\alpha}_1)F_j(t' - t_1') \qquad (j = 1, 2, 3) \quad (8.20)$$

$$C_{M2j}(t') = (\dot{\alpha}_2 - \dot{\alpha}_1)[G_j(t' - t_1') - x_0'F_j(t' - t_1')] \quad (8.21)$$

where $F_j(t' - t_1')$ and $G_j(t' - t_1')$ are the same as given in Eqs. (8.5), (8.7), (8.9), (8.11), (8.12), and (8.13) except t_0' is replaced by t_1'.

For the case $\dot{\alpha}_0 = \dot{\alpha}_2 = 0$, the result is given in Table 3. There are a number of interesting points.

(1) In region I ($0 \leq t \leq t_1'$) where disturbance due to the second change in $\dot{\alpha}$ at $t = t_1$ has not started, C_L and C_M are due only to the first change in $\dot{\alpha}$ at $t' = 0$, and it is obvious that the second change can contribute nothing.

(2) In regions (I + II), ($t' \leq t_1'$), changes of $\dot{\alpha}$ at both $t' = 0$ and at $t' = t_1'$ contribute to lift and moment. The contribution of the second change in $\dot{\alpha}$, however, may be considered as independent of that due to the first change. In regions (I + II), one contribution superimposes on the other. This shows that the principle of superposition can apply not only to the velocity potential in a linear differential equation but also to its derivatives or to the finite integrals of its derivatives such as C_L and C_M.

(3) If the chord crosses the zones I-1 and II-1, the transient effect dies out and the angle of attack is α_1. $C_L = 4\alpha_1/(M^2 - 1)^{1/2}$ and $C_M = 2\alpha_1/(M^2 - 1)^{1/2}$ check with Ackeret's formulas for the steady case.

(B) *Extension to an Arbitrary Change in $\dot{\alpha}$ at t_1'*

Suppose that at t_i' there is a sudden change in α slope—i.e., $\dot{\alpha}_{i+1} - \dot{\alpha}_i$ as shown in Fig. 7— and then α slope remains constant at $\dot{\alpha}_{i+1}$ after t_i'. From the above analysis, it is not difficult to see that the contribution to C_L and C_M due to $\dot{\alpha}_{i+1} - \dot{\alpha}_i$ at t_i' must be of the same kind as that due to $\dot{\alpha}_1 - \dot{\alpha}_0$ at t_0' in region I. Similarly, we can write

$$[C_{L i(j+1)}(t')]_j = (\dot{\alpha}_{i+1} - \dot{\alpha}_i)F_j(t' - t_i') \quad (8.22)$$

and

$$[C_{M i(j+1)}(t')]_j = (\dot{\alpha}_{i+1} - \dot{\alpha}_i)[G_j(t' - t_i') - x_0'F_j(t' - t_i')] \quad (8.22a)$$

where $j = 1$, when $t' - t_i' > M/(M-1)$; $j = 2$, when $M/(M+1) \leq t' - t_i' \leq M/(M-1)$; and $j = 3$ when $0 \leq t' - t_i' \leq M/(M+1)$. $F_j(t' - t_i')$ and $G_j(t' - t_i')$ are the same as $F_j(t' - t_0')$ given in Eqs. (8.5), (8.7), and (8.9) and $G_j(t' - t_0')$ given in Eqs. (8.11), (8.12), and (8.13), respectively, except t_i' replaces t_0'. Obviously, the contribution of $\dot{\alpha}_{i+1} - \dot{\alpha}_i$ to C_L and C_M is zero if $t' < t_i'$.

(C) *Total Lift and Moment at t' for a Given $\dot{\alpha}(t')$*

Before extending known results to this general case, some behavior of $\alpha(t')$ and $\dot{\alpha}(t')$ curves must be clearly understood.

(1) $\alpha(t')$ vs. t' is decomposible into elements linear with time. For a given $\alpha(t')$ where α is a continuous function of t', the curve can be approximated with a series of infinitely small tangent line elements. If we extend those line elements in the downstream direction, a series of wedge areas is formed. As an example, $\Delta\alpha(t' - t_i')$ starts at the conjunction t_i' as shown by the dotted lines. The contribution of this $\Delta\alpha(t' - t_i')$ to the force or moment must be proportional to that $\alpha(t')$ in region I of Fig. 2. In that case, its contribution is independent of later changes in $\dot{\alpha}$. Similarly, its contribution is also independent of early changes in $\dot{\alpha}$. $\alpha(t')$ at any time can be obtained by summing up all of the wedge elements.

(2) $\dot{\alpha}(t')$ vs. t' is decomposible into step functions of time. The corresponding $\dot{\alpha}(t')$ vs. t' and its approximation step curves are plotted in Fig. (8b) It is also decomposible into a series of step curves which extend to infinity at constant value as shown in $\Delta\dot{\alpha}_i = \dot{\alpha}_{i+1} - \dot{\alpha}_i$ at t_i'.

(3) There are three types of regions ahead of t'. Suppose we are interested in C_L and C_M at t'. Two lines can be drawn from the trailing edge of the chord at t', one with slope $M/(M-1)$ and the other $M/(M+1)$ as shown in Fig. (8c). It has been learned from earlier results that any region ahead of time $t' - M/(M-1)$ is covered by the chord in only one zone of type I-1. Similarly, any region between $t' - M/(M-1)$ and $t' - M/(M+1)$ is covered by the chord in two zones of types I-1 and I-2, and any region between $t' - M/(M-1)$ and t' is covered in three zones of types I-1, I-2, and I-3.

From above, we know that the contribution of each change in $\dot{\alpha}$ (say $\Delta\dot{\alpha}_i = \dot{\alpha}_{i+1} - \dot{\alpha}_i$) can be treated independently of changes in $\dot{\alpha}$ behind or ahead of t_i. The total contribution must be the sum of the individual contributions. If $t' > M/(M-1)$, the regions ahead of t' are divided into three groups as follows:

First group: $k+1$ regions with only one zone covered by chord at t'.

$$t_k' < t' - [M/(M-1)] < t_{k+1}'$$

Second group: $m - k$ regions with two zones covered.

$$t_m' < t' - [M/(M+1)] < t_{m+1}'$$

Third group: $n - m$ regions with three zones covered.

$$t_n' \leq t' \leq t_{n+1}'$$

Based upon the principle of superposition, we have the following three categories:

(a) $t' > M/(M-1)$. Subscript III refers to existence of all three groups.

$$C_L(t')_{III} = \sum_{i=1}^{k+1} C_{L\text{I}} + \sum_{i=k+2}^{m+1} C_{L\text{II}} + \sum_{i=m+2}^{n+1} C_{L\text{III}}$$

$$= \sum_{i=0}^{k} (\dot{\alpha}_{i+1} - \dot{\alpha}_i)F_1 + \sum_{i=k+1}^{m} (\dot{\alpha}_{i+1} - \dot{\alpha}_i)F_2 + \sum_{i=m+1}^{n} (\dot{\alpha}_{i+1} - \dot{\alpha}_i)F_3 \tag{8.23a}$$

where all F's are functions of $t' - t_i'$ as given in Eqs. (8.5), (8.7), and (8.9). Similarly,

$$C_M(t')_{III} = \sum_{i=1}^{k+1} C_{M\text{I}} + \sum_{i=k+2}^{m+1} C_{M\text{II}} + \sum_{i=m+2}^{n+1} C_{M\text{III}}$$

$$= \sum_{i=0}^{k} (\dot{\alpha}_{i+1} - \dot{\alpha}_i)G_1 + \sum_{i=k+1}^{m} (\dot{\alpha}_{i+1} - \dot{\alpha}_i)G_2 + \sum_{i=m+1}^{n} (\dot{\alpha}_{i+1} - \dot{\alpha}_i)G_3 - x_0' C_L(t')_{III} \tag{8.24a}$$

(b) $M/(M-1) \geq t' > M/(M+1)$. In this case, the regions in the first group do not exist, and it can be shown that

$$C_L(t')_{II} = \sum_{i=0}^{m} (\dot{\alpha}_{i+1} - \alpha_i)F_2 + \sum_{i=m+1}^{n} (\dot{\alpha}_{i+1} - \dot{\alpha}_i)F_3 \tag{8.23b}$$

$$C_M(t')_{II} = \sum_{i=0}^{m} (\dot{\alpha}_{i+1} - \dot{\alpha}_i)G_2 + \sum_{i=m+1}^{n} (\dot{\alpha}_{i+1} - \dot{\alpha}_i)G_3 - x_0' C_L(t')_{II} \tag{8.24b}$$

where the subscript II refers to the existence of only two groups.

(c) $M/(M+1) \geq t' > 0$. In this case, the regions in both the first and the second groups do not exist, and

$$C_L(t')_I = \sum_{i=0}^{n} (\dot{\alpha}_{i+1} - \dot{\alpha}_i)F_3 \tag{8.23c}$$

$$C_M(t')_I = \sum_{i=0}^{n} (\dot{\alpha}_{i+1} - \dot{\alpha}_i)G_3 \tag{8.24c}$$

Now for the case where $\alpha(t')$ is continuous to the second derivative, the above can be expressed in terms of integrals. If the number of the tangent line elements increases indefinitely and each decreases to infinitely small length, we find in the limits, $t_k' \to t' - [M/(M-1)]$, $t_m' \to t' - [M/(M+1)]$, and except $\dot\alpha_1 - \dot\alpha_0$ at $t = 0$, which is discontinuous, all $\dot\alpha_{i+1} - \dot\alpha_i$ can be approximated by $\ddot\alpha_i \Delta t_i'$ (where $\Delta t_i' = t_{i+1}' - t_i'$). Thus, corresponding to the above three cases, we have:

(*d*) $t' > M/(M-1)$.

$$C_L(t')_{III} = (\dot\alpha_1 - \dot\alpha_0)F_1(t') + \int_0^{t'-[M/(M-1)]} \ddot\alpha(\tau')F_1(t'-\tau')d\tau' + \int_{t'-[M/(M-1)]}^{t'-[M/(M+1)]} \ddot\alpha(\tau')F_2(t'-\tau')d\tau' + \int_{t'-[M/(M+1)]}^{t'} \ddot\alpha(\tau')F_3(t'-\tau')d\tau' \quad (8.25a)$$

where τ' is introduced to replace t_i'.

$$C_M(t')_{III} = (\dot\alpha_1 - \dot\alpha_0)G_1(t') + \int_0^{t'-[M/(M-1)]} \ddot\alpha(\tau')G_1(t'-\tau')d\tau' + \int_{t'-[M/(M-1)]}^{t'-[M/(M+1)]} \ddot\alpha(\tau')G_2(t'-\tau')d\tau' + \int_{t'-[M/(M+1)]}^{t'} \ddot\alpha(\tau')G_3(t'-\tau')d\tau' - x_0'C_L(t')_{III} \quad (8.26a)$$

(*e*) $M/(M+1) < t' \leq M/(M-1)$.

$$C_L(t')_{II} = (\dot\alpha_1 - \dot\alpha_0)F_2(t') + \int_0^{t'-[M/(M+1)]} \ddot\alpha(\tau')F_2(t'-\tau')d\tau' + \int_{t'-[M/(M+1)]}^{t'} \ddot\alpha(\tau')F_3(t'-\tau')d\tau' \quad (8.25b)$$

$$C_M(t')_{II} = (\dot\alpha_1 - \dot\alpha_0)G_2(t') + \int_0^{t'-[M/(M+1)]} \ddot\alpha(\tau')G_2(t'-\tau')d\tau' + \int_{t'-[M/(M+1)]}^{t'} \ddot\alpha(\tau')G_3(t'-\tau')d\tau' - x_0'C_L(t')_{II} \quad (8.26b)$$

where in the first term $F_2(t')$ and $G_2(t')$ replace $F_1(t')$ and $G_1(t')$, respectively.

(*f*) $M/(M+1) \geq t' > 0$.

$$C_L(t')_I = (\dot\alpha_1 - \dot\alpha_0)F_3(t') = \int^{t'} \ddot\alpha(\tau')F_3(t'-\tau')d\tau' \quad (8.25c)$$

$$C_M(t')_I = (\dot\alpha_1 - \dot\alpha_0)G_3(t') = + \int_0^{t'} \ddot\alpha(\tau')G_3(t'-\tau')d\tau' - x_0'C_L(t')_I \quad (8.26c)$$

It is easy to see that $C_L(t'=0)$ and $C_M(t'=0)$ are not zero in general but

$$C_L(0) = (\dot\alpha_1 - \dot\alpha_0)F_3(0) \quad (8.25d)$$

$$C_M(0) = (\dot\alpha_1 - \dot\alpha_0)G_3(0) - x_0'C_L(0) \quad (8.26d)$$

The above integrals are similar to Duhamel's integral[10] or to Carson's integral.

All the above formulas are true if $\dot\alpha_0 = 0$ for a length of time $\geq C/(U-c)$ ahead of $t' = 0$, because the past transient effect will die out before $t = 0$. α_0 is not necessarily zero; its contribution to C_L is $4\alpha_0/(M^2-1)^{1/2}$ and to C_M is $2\alpha_0/(M^2-1)^{1/2}$. Both should be added to the above if $\alpha_0 \neq 0$.

In case of $\ddot\alpha$ being continuous except at a finite number of discontinuities in $\dot\alpha$, the above can also be applied.

The above analysis shows one important physical principle. If the solution of an elementary boundary condition is known and if the given boundary condition can be obtained by superimposing the elementary boundary condition, the general solution can then be obtained by superimposing the elementary solution.

(*D*) *Some Applications*

As shown before, Eqs. (8.5), (8.7), and (8.9) can be applied to determine the contribution to C_L due to $\dot\alpha_{i+1} - \dot\alpha_i$ at t_i'. For this purpose, Fig. (10a) shows F_j' vs. $t' - t_i'$ for $M = 1.5, 2, 3$, and 4. Here $j = 1$, when $t' - t_i' \geq M/(M-1)$; $j = 2$, when $M/(M+1) \leq t' - t_i' \leq M/(M-1)$; and $j = 3$, when $0 \leq t' - t_i' \leq M/(M+1)$. From the definition $F_j' = C_{Lij}/(\dot\alpha_{i+1} - \dot\alpha_i)$ if $x_0' = 0$. If x_0' is not zero, $\Delta F_j'/x_0'$ vs. $t' - t_i'$ is given in Fig. (10b). Similarly, G_j and $\Delta G_j/x_0'$ in Eqs. (8.11), (8.12), and (8.13) are plotted in Fig. 11. Both figures are useful for calculating C_L and C_M for an arbitrary $\alpha(t')$ which is continuous and can be approximated by straight line elements.

As an example, the following case of the downwash distribution in Fig. 2 is illustrated:

$C = 6$ ft.	$c = 1000$ ft. per sec.
$M = 1.5$	$\dot\alpha_0 = \dot\alpha_2 = 0$
$t_1 = 0.02$ sec. ($t_1' = 5$)	$x_0' = 0$ and $x_0' = 0.5$

Figs. 12, 13, and 14 show C_L/C_{L0}, C_M/C_{L0}, and center of pressure from the leading edge vs. $(t' - t_0')$. For illustration, the steady lift coefficient $C_{L0} = 4\alpha_1/(M^2 -$

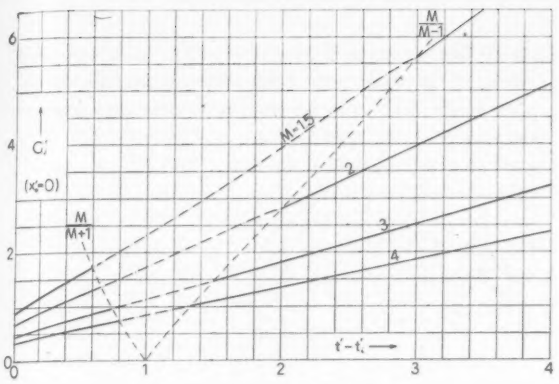

FIG. 11a. G_j' vs. $t' - t_i'$ ($x_0' = 0$).

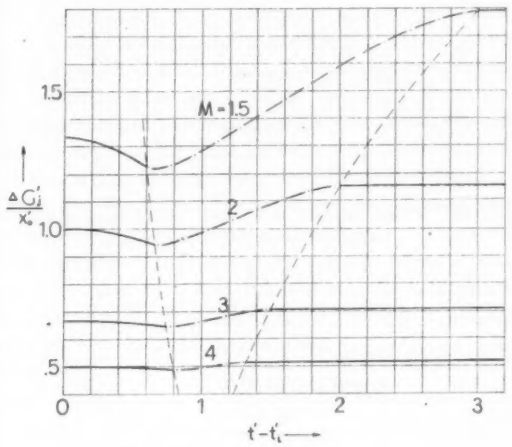

FIG. 11b. $\Delta G'/x_0'$ vs. $t' - t_i'$.

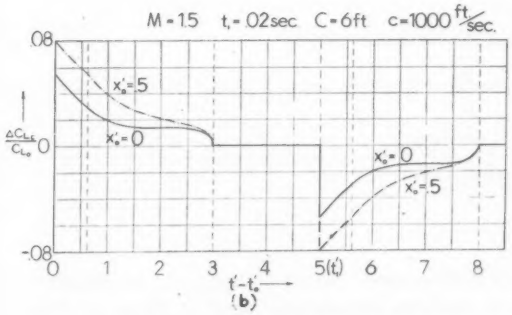

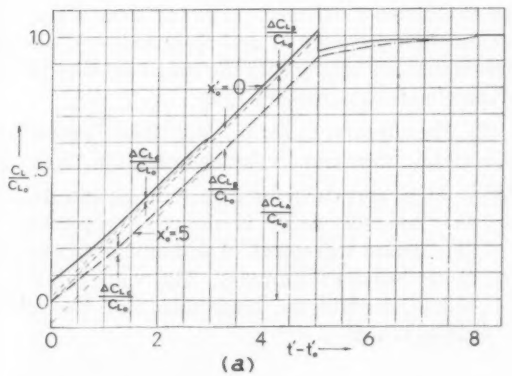

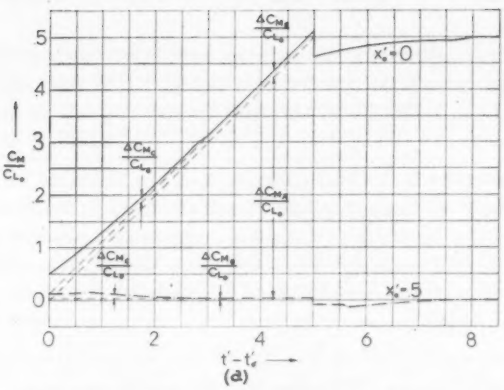

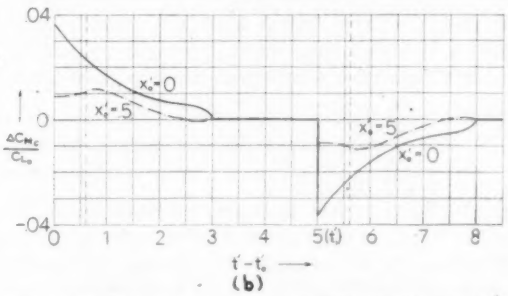

FIG. 13. (a) C_M/C_{L0} vs. $t' - t_0'$ corresponding to the case in Fig. 11. (b) $\Delta C_{MC}/C_{L0}$ vs. $t' - t_0'$.

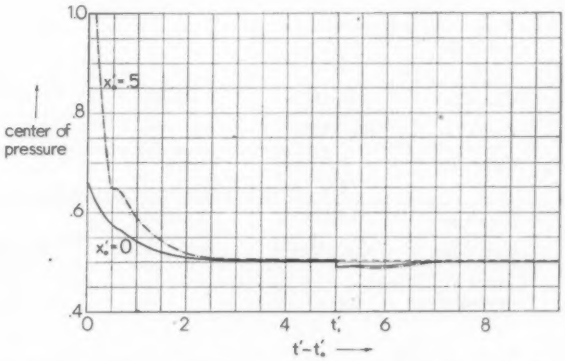

FIG. 14. Center of pressure from leading edge vs. $t' - t_i'$. Initial angle of attack is assumed to be zero.

FIG. 12. (a) C_L/C_{L0} vs. $t' - t_0'$ for the case $\alpha(t')$ as shown in Fig. 2. $M = 1.5$, $t_1 = 0.02$ sec., $C = 6$ ft., $c = 1{,}000$ ft. per sec. Solid line—$x_0' = 0$. Dotted line—$x_0' = 0.5$. NOTE: $\Delta C_{LA}/C_{L0}$, $\Delta C_{LB}/C_{L0}$, and $\Delta C_{LC}/C_{L0}$ in both $x_0' = 0$ and $x_0' = 0.5$.

(b) $\Delta C_{LC}/C_{L0}$ vs. $t' - t_0'$. NOTE: $\Delta C_{LC}/C_{L0}$ at $t' - t_0'$ is equal and opposite to $\Delta C_{LC}/C_L$ at $t' - t_1'$, if $t' - t_0' = t' - t_1''$.

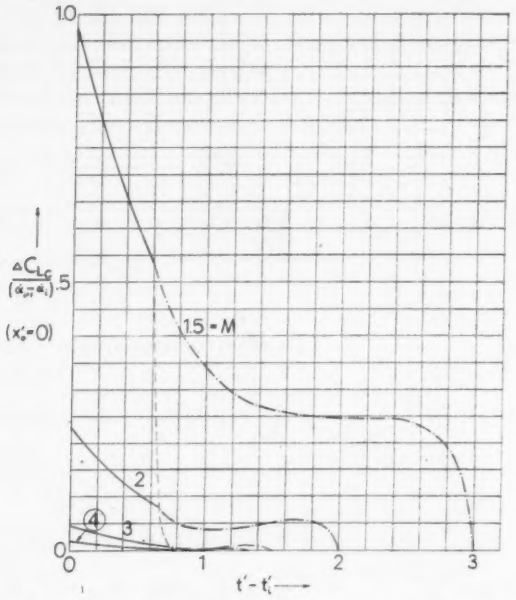

FIG. 15a. $\Delta C_{LC}/(\dot{\alpha}_{i+1} - \dot{\alpha}_i)$ vs. $t' - t_i'$ at $x_0' = 0$ for $M = 1.5$, 2, 3, 4. Solid curves—$0 \leq t' - t_i' \leq M/(M + 1)$. Dotted curves—$M/(M + 1) \leq t' - t_i' \leq M/(M - 1)$.

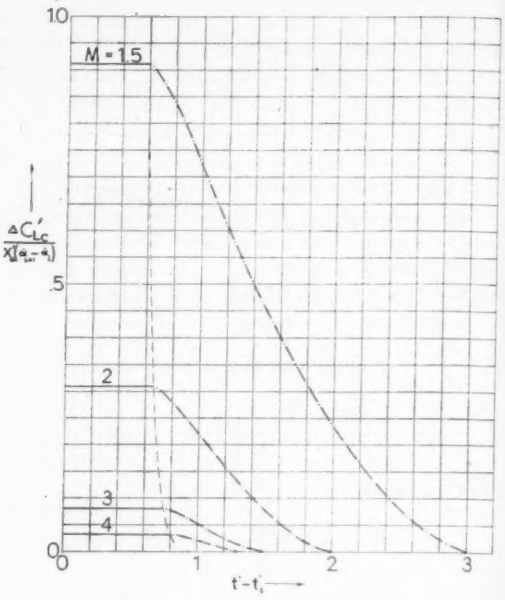

FIG. 15b. $\Delta C_{LC}'/x_0'(\dot{\alpha}_{i+1} - \dot{\alpha}_i)$ vs. $t' - t_i'$ ($\Delta C_{LC}'$ is additional contribution of ΔC_{LC} due to x_0').

TABLE 4
Some general features in Figs. 12, 13, and 14

	Region 1, $0 \leq t' < t_1'$		Region I + II, $t' \geq t_1'$	
x_0'	0	0.5	0	0.5
C_{LA}/C_{L0}	$\frac{t'}{t_1'}$	$\frac{t'}{t_1'}$	1	1
C_{LB}/C_{L0}	0.02	−0.08	0	0
C_{LC}/C_{L0}	Fig. (12b)	Fig. (12b)	$C_{LC}(t' - t_1') = -C_{LC}(t' - t_0')$	$C_{LC}(t' - t_1') = -C_{LC}(t' - t_0')$
C_{MA}/C_{L0}	$\frac{1}{2}\frac{t'}{t_1'}$	0	$\frac{1}{2}$	0
C_{MB}/C_{L0}	0.0133	0.003333	0	0
C_{MC}/C_{L0}	Fig. (13c)	Fig. (13c)	$C_{MC}(t' - t_1') = -C_{MC}(t' - t_0')$	$C_{MC}(t' - t_1') = -C_{MC}(t' - t_0')$
Center of pressure	← Fig. 14 →			

1) is substituted for $\dot{\alpha}_1$ so that this result can be used for any α_1. Of course, this result is equivalent to $C_L/\dot{\alpha}_1$ and $C_M/\dot{\alpha}_1$ with $\dot{\alpha}_1 = 15.625$ rad. per sec. A more complete explanation will be found in Table 4, and some discussion will be given in the conclusion. Fig. (15a) shows $\Delta C_{LC}/(\dot{\alpha}_{i+1} - \dot{\alpha}_i)$ as a function of $t' - t_i'$ for $M = 1.5$, 2, 3, and 4 for $x_0' = 0$. Fig. (15b) gives the additional contribution to ΔC_{LC} due to $x_0' \neq 0$, and this additional contribution may be called $\Delta C_{LC}'$.

(9) Conclusions

(1) For an airfoil in a flow of constant supersonic speed, the transient reaction will damp out in a time period $C/(U - c)$ immediately after the change in angle of attack ceases. After that period, the lift, wave drag, and moment become the same as given by Ackeret in the two-dimensional case. The transient reaction becomes more pronounced and lasts longer if the free-stream velocity approaches the sound velocity or if the Mach Number approaches 1.

(2) The effect on C_L (or C_M) due to an increment of $\dot{\alpha}$ at a certain time can be decomposed into three parts: ΔC_{LA}, ΔC_{LB}, and ΔC_{LC} (or ΔC_{MA}, ΔC_{MB}, and ΔC_{MC}).

(a) ΔC_{LA} or ΔC_{MA} is directly proportional to the instant increment in α and can be evaluated from Ackeret's formula. The value of ΔC_{LA} is independent of the hinge axis, but the value of ΔC_{MA} is not.

(b) ΔC_{LB} or ΔC_{MB} is directly proportional to $\Delta\dot{\alpha}$ and independent of time. The value of ΔC_{LB} decreases linearly with increase of x_0', the hinge axis. (c) ΔC_{LC} or ΔC_{MC}, the transient part, is proportional to $\Delta\dot{\alpha}$ but is a complicated function of time and Mach Number. ΔC_{LC} decreases linearly with increase of x_0'. ΔC_{MC} decreases with increase of x_0' but not linearly. The effect of Mach Number on ΔC_{LC} or ΔC_{MC} is more pronounced as M approaches 1. (See Fig. 15.) For extremely large Mach Numbers, the contribution of ΔC_{LC} or ΔC_{MC} is small and may be neglected in certain cases.

(3) Immediately after increasing $\dot{\alpha}(t)$, C_L and C_M are greater than the values that are linear with time, and immediately after decreasing $\dot{\alpha}(t)$, C_L and C_M are less. (Refer to Figs. 12 and 13.) Besides, the center of pressure moves backward after increasing $\dot{\alpha}(t)$ and moves forward after decreasing $\dot{\alpha}(t)$. The smaller the lift, the more pronounced the shift. (See Fig. 14.) From this analysis, $\dot{\alpha}(t)$ should be kept small at the beginning and at the end of changing α, so that the travel in the center of pressure may not impair the stability of the missile.

(4) In the linearized theory, there is a unique relationship between $C_L(t)$ [or $C_M(t)$] and $\alpha(t)$. The present analysis shows that in the case of $\alpha(t)$ being a complicated function of t, this relation can be established through superposition of solutions of a simple boundary condition—i.e., $\Delta\dot{\alpha}(t)$ being constant.

(5) It is not difficult to calculate the lift and moment for the case of an airfoil in harmonic oscillation by means of the generalized integrals of C_L and C_M. It will be treated later.

(6) This result can be applied to study of the transient reaction of the deflecting control surface if the main wing remains stationary. With the principle of superposition, the present analysis can be readily applied to more degrees of freedom. The details will be given in a later report.

(7) With this analysis, the lift and moment of an airfoil can be calculated for any arbitrary $\alpha(t)$ without difficulty. More treatment seems necessary for the case with more degrees of freedom, the case of a wing with finite span, and the case with accelerated flow.

(8) This analysis is based upon the linearized theory. It cannot be applied when M is near 1, and when M is larger than $|U/v|$.

(9) It is obvious that the result can be applied to an infinite swept wing if the leading edge is ahead of the Mach line. In that case M should be replaced by $M\cos\gamma$ and α by $\alpha/\cos\gamma$ in all of the above equations. (γ = swept angle.)

(10) The expressions of ΔF_j and ΔG_j can be easily used to calculate C_L and C_M of a wing due to flapping degree of freedom.

Appendix A

Derivation of the Velocity Potential

With the aid of reference 6, it is not difficult to show that the following integrals are true:

$$\int_0^\infty \frac{d\omega}{\omega^2}(1-\cos b\omega)J_0(a\omega) = \begin{cases} b\sin^{-1}(b/|a|) + \sqrt{a^2-b^2} - |a| & \text{for } |a| \geq |b| \\ (\pi/2)|b| - |a| & \text{for } |a| \leq |b| \end{cases} \tag{A1}$$

and

$$\int_0^\infty \frac{d\omega}{\omega}\sin b\omega J_0(a\omega) = \begin{cases} \sin^{-1} b/|a| & \text{for } |a| \geq |b| \\ (\pi/2)(b/|b|) & \text{for } |a| \leq |b| \end{cases} \tag{A2}$$

With Eqs. (A1) and(A2), we can integrate Eq. (6.8) to the form

$$\phi(x,-0,t)\left[\frac{-\dot{\alpha}_1}{\sqrt{M^2-1}}\right]^{-1} =$$

$$\frac{Uxt_1}{2} + \frac{Uc(M^2-1)}{\pi}\int_0^{\pi/c(M^2-1)} d\lambda \times \begin{cases} \left(t + t_x - \dfrac{2M^2-1}{M}\lambda\right)\sin^{-1}\left(\dfrac{t}{\lambda} - M\right) + \sqrt{\lambda^2 - (t-M\lambda)^2} & \text{when } \left|\dfrac{t}{\lambda} - M\right| \leq 1 \\ \dfrac{\pi}{2}|t-M\lambda|\left(1 + \dfrac{t_x - m\lambda}{t-M\lambda}\right) & \text{when } \left|\dfrac{t}{\lambda} - M\right| \geq 1 \end{cases}$$

$$-\frac{Uc(M^2-1)}{\pi}\int_0^{x/c(M^2-1)} d\lambda \times \begin{cases} \left(t-t_1+t_x-\dfrac{2M^2-1}{M}\lambda\right)\sin^{-1}\left(\dfrac{t-t_1}{\lambda}-M\right)+ \\ \sqrt{\lambda^2-(t-t_1-M\lambda)^2} & \text{when } \left|\dfrac{t-t_1}{\lambda}-M\right| \leqq 1 \\ \dfrac{\pi}{2}\left|t-t_1-M\lambda\right|\left(1+\dfrac{t_x-m\lambda}{t-t_1-M\lambda}\right) & \text{when } \left|\dfrac{t-t_1}{\lambda}-M\right| \leq 1 \end{cases} \quad \text{(A3)}$$

where two substitutions are used—namely, $\lambda = (x-\xi)/c(M^2-1)$ and $t_x - m\lambda = t_\xi$. If t is replaced by $t - t_1$ in the first integral, the first integral becomes the second with opposite sign. Eq. (A3) is a discontinuous integral. The integration can be carried out only between points of discontinuity.

For convenience of integration, introduce I_U for the upper line of the first integral with indefinite limit, I_L for the lower; II_U for the upper line of the second integral with indefinite limit, and II_L for the lower in the above equation. It is easy to show that the values of the indefinite integrals are:

$$I_U = \left(t+t_x-\frac{2M^2-1}{M}\lambda\right)\lambda\sin^{-1}\left(\frac{t}{\lambda}-M\right) - \frac{t(t_x)_\lambda}{(M^2-1)^{1/2}}\sin^{-1}\left[M-\frac{(M^2-1)\lambda}{t}\right] + \frac{t^2}{2(M^2-1)^{1/2}}\left(\frac{1}{M}+\frac{\lambda}{t}\right)\sqrt{1-\left[M-\frac{(M^2-1)\lambda}{t}\right]^2} \quad \text{for } \frac{t}{M+1} \leqq \lambda \leqq \frac{t}{M-1} \quad \text{(A4)}$$

$$II_U = -I_{1U} \text{ if } t \text{ is replaced by } t-t_1 \qquad \text{for } \frac{t-t_1}{M+1} \leqq \lambda \leqq \frac{t-t_1}{M-1} \quad \text{(A5)}$$

$$I_L = +\frac{\pi}{2}\left(t+t_x-\frac{2M^2-1}{M}\lambda\right)\lambda \qquad \text{for } \lambda < \frac{t}{M+1} \text{ and } t > 0 \quad \text{(A6)}$$

$$II_L = -I_{1L} \text{ if } t \text{ is replaced by } t-t_1 \qquad \text{for } \lambda < \frac{t-t_1}{M-1} \text{ and } t-t_1 > 0 \quad \text{(A7)}$$

Introducing

$$I_L' = -I_L \qquad \text{for } \lambda > \frac{t}{M-1},\ t < 0 \quad \text{(A8)}$$

$$II_L' = -II_L \qquad \text{for } \lambda > \frac{t-t_1}{M-1},\ t-t_1 < 0 \quad \text{(A9)}$$

In order to express ϕ more explicitly, we introduce Φ_{ij} ($i = 0, 1$, and $j = 1, 2, 3$) to denote the definite integrals in different cases of Eq. (A3). Thus,

$$\Phi_{01} = \frac{cU(M^2-1)}{\pi}\left\{I_L\right\}_0^{\lambda_2 = x/c(M^2-1)} = \frac{x^2}{2}\left[\frac{1-\nu_{00}}{\nu_0}-\frac{1}{2(M^2-1)}\right] \qquad \text{for } \nu_0 > 0 \quad \text{(A10)}$$

where $\nu_0 = x/U(t-t_0)$ and $\nu_{00} = x_0/U(t-t_0)$ (t_0 being zero). Note that as $t \to 0$, $\nu_0 \to \infty$ and as $t \to \infty$, $\nu_0 \to 0$.

$$-\Phi_{01} = \frac{cU(M^2-1)}{\pi}\left\{I_L'\right\}_0^{\lambda_2 = x/c(M^2-1)} \qquad \text{for } \nu_0 < 0 \quad \text{(A11)}$$

$$\Phi_{02} = \frac{cU(M^2-1)}{\pi}\left\{[I_L]_0^{\lambda_1 = t/(M+1)} + [I_U]_{t/(M+1)}^{\lambda_2 = x/c(M^2-1)}\right\} = \frac{x^2}{\pi}\left(\left[\frac{1-\nu_{00}}{\nu_0}-\frac{1}{2(M^2-1)}\right]\sin^{-1}\left(\frac{m}{\nu}-M\right) - \frac{1}{(M^2-1)^{1/2}}\frac{1}{\nu_0}\left\{m\left(1-\frac{\nu_{00}}{\nu_0}\right)\left[\sin^{-1}M(1-\nu_0)-\frac{\pi}{2}\right] + \frac{1}{2}\left(1+\frac{m}{M\nu_0}\right)\sqrt{1-M^2(1-\nu_0)^2}\right\}\right) \quad \text{(A12)}$$

where $\lambda = t/(M+1)$ is a point of discontinuity.

$$\Phi_{03} - \Phi_{01} = \frac{cU(M^2-1)}{\pi}\left[\left\{I_L\right\}_0^{\lambda_1 = t/(M+1)} + \left\{I_U\right\}_{t/(M+1)}^{\lambda_2 = t/(M-1)} + \left\{I_L'\right\}_{t/(M-1)}^{\lambda_2 = x/c(M^2-1)}\right] = \frac{(M^2-1)^{1/2}}{M}\frac{x^2}{\nu_0}\left(1-\frac{\nu_{00}}{\nu_0}\right) - \frac{x^2}{2t_1}\left\{\frac{1-\nu_{00}}{\nu_0}-\frac{1}{2(M^2}\right\} \qquad \text{for } 1+\frac{1}{M} \leqq \nu_0 \leqq \infty$$

where $\lambda = t/(M+1)$ and $\lambda = t/(M-1)$ are points of discontinuity and

$$\Phi_{03} = [(M^2-1)^{1/2}/M](x^2/\nu_0)[1-(\nu_{00}/\nu_0)] \quad \text{(A13)}$$

Similarly, we can evaluate Φ_{11}, Φ_{12}, and Φ_{13} by replacing $t - t_0$ by $t - t_1$. Let $\nu_1 = x/U(t - t_1)$ and $\nu_{10} = x_0/U(t - t_1)$. In those cases $\nu_0 \to \nu_1$, and $\nu_{00} \to \nu_{10}$. A useful relation may be noted:

$$\Phi_{01} = \Phi_{11} + (Uxt_1/2) \tag{A14}$$

References

[1] Possio, C., *L'azione aerodinamica sul profilo oscillante alle velocita ultrasonore*, Acta, Pont. Acad. Sci., Vol. 1, No. 11, pp. 93–105, 1937.

[2] Garrick, I. E., and Rubinow, S. I., *Flutter and Oscillating Air-Force Calculations for an Airfoil in a Two-dimensional Supersonic Flow*, N.A.C.A. T.N. No. 1158, October, 1946.

[3] von Borbely, S., *Aerodynamic Forces on A Harmonically Oscillating Wing at Supersonic Velocity (2-Dimensional Case)*, R.T.P. Translation No. 2019, British Ministry of Aircraft Production (from Z.A.M.M., Bd. 22, Heft 4, pp. 190–205, August, 1942).

[4] Schwarz, L., *Ebene instationare Theorie der Tragfläche bei Überschallgeschwindigkeit*, Jahrb. 1943 der deutschen Luftfahrtforschung, IAOIO, Stephan Geibel & Co. (Altenburg/Thur), pp. 1-8 (available as Translation No. F-TS-934-RE, Air Materiel Command, Wright Field, Dayton, Ohio, March, 1947).

[5] Kussner, H. G., *General Airfoil Theory*, N.A.C.A. T.M. No. 979, 1941.

[6] Watson, G. N., *A Treatise on the Theory of Bessel Functions*, 2nd Ed.; The MacMillan Company, New York, 1944.

[7] Garrick, I. E., and Rubinow, S. I., *Theoretical Study of Air Forces on an Oscillating or Steady Thin Wing in a Supersonic Main Stream*, N.A.C.A. T.N. No. 1383, July, 1947.

[8] Miles, J. W., *The Aerodynamic Forces on an Oscillating Airfoil at Supersonic Speeds*, Journal of the Aeronautical Sciences, Vol. 14, No. 6, pp. 351–358, June, 1947.

[9] von Kármán, Th., and Sears, W. R., *Airfoil Theory for Non-Uniform Motion*, Journal of the Aeronautical Sciences, Vol. 5, No. 10, pp. 379–389, August, 1938.

[10] von Kármán, Th., and Biot, M. A., *Mathematical Methods in Engineering;* McGraw-Hill Book Company, Inc., New York, 1940.

[11] von Kármán, Th., *Supersonic Aerodynamics—Theory and Application*, Journal of Aeronautical Sciences, Vol. 14, No. 7, pp. 373–409, July, 1947.

[12] Ackeret, J., *Luftkräfte auf Flügel die mit grösserer als Schallgeschwindigkeit bewegt werden*, Z.F.M., Vol. 16, pp. 72–74, 1925.

[13] Hönl, H., *Zweidimensionale Tragflächentheorie im Überschallgebiet*, Forschungsbericht Nr. 1903, Deutsche Luftfahrtforschung (Göttingen), 1944.

[14] Temple, G., and Jahn, H. A., *Flutter at Supersonic Speeds, Part 1. Mid-Chord Derivative Coefficients for a Thin Airfoil at Zero Incidence*, Rept. No. S.M.E. 3314, British R.A.E., April, 1945.

Letter to the Editor

Dear Sir:

Professor Alan Pope ("Letter to the Editor," JOURNAL OF THE AERONAUTICAL SCIENCES, Vol. 15, No. 8, p. 496, August, 1948) recently gave a simplified calculation for the power-saving obtainable by sucking off the boundary layer and accelerating it up to free-stream conditions. The result of his simplified calculation was a net saving of 50 per cent of the power required.

A more realistic calculation was indicated in the article by Professor Goldstein ("Low Drag and Suction Airfoils," JOURNAL OF THE AERONAUTICAL SCIENCES, Vol. 15, No. 4, p. 209, April, 1948). Carrying this through for a flat plate is easily done and yields much less favorable results.

Thus, if δ is the height of the boundary layer; u_0, the free-stream velocity; u, the velocity in the boundary layer; and ρ, the constant density, then the drag of the plate (two sides) is

$$D = 2\rho \int_0^S u(u_0 - u)dy$$

and the power required to overcome this drag is

$$P = 2\rho u_0 \int_0^\delta u(u_0 - u)dy$$

If the boundary-layer air is accelerated up to free-stream conditions, the rate of kinetic energy increase will equal the power required to accelerate the air, and the rate of momentum increase will yield a thrust equal to the drag. The power thus required (assuming a lossless system) is

$$P' = 2(\rho/2) \int_0^\delta u(u^2_0 - u^2)dy$$

If we now assume that the boundary layer profile is given by

$$u/u_0 = (y/\delta)^n$$

Then

$$P = 2\rho u_0{}^3\delta[n/(n + 1)(2n + 1)]$$
$$P' = \rho u_0{}^3\delta[2n/(n + 1)(3n + 1)]$$

so that

$$\frac{P'}{P} = \frac{2n + 1}{3n + 1} = \frac{2 + (1/n)}{3 + (1/n)}$$

For a crude approximation to the laminar boundary layer take $n = 1$. Then $P'/P = 0.75$ or a power saving of 25 per cent. For the turbulent boundary layer take $n = 1/7$, whence $P'/P = 0.9$ or a power saving of only 10 per cent. Professor Goldstein mentions comparable savings of 21 and 8 per cent, respectively.

It is gratifying that at least at one point in the boundary-layer control system a net gain is possible. Probably this gain will be more than cancelled by duct losses, etc.

It can further be noted that the relatively small gain obtained by pumping off the turbulent boundary layer is typical. Suction of airfoils with predominantly turbulent (but unseparated) boundary layers will yield relatively small decreases in the profile drag. The large gains generally pictured as obtainable by boundary-layer control are possible only by delaying transition to far aft chord positions.

ABRAHAM FIUL
Aerodynamics Engineer
Northrop Aircraft, Inc.

Vorticity in the Supersonic Flow About Yawing Cones

MARK M. LOTKIN*

Ballistic Research Laboratories

ABSTRACT

A comparison is made between Stone's and Sauer's methods of calculation of the supersonic flow about a slightly yawing cone. It is shown that the neglect of vorticity, while having only a small effect on the ratio of shock yaw to cone yaw, may lead to erroneous values of the normal force coefficient.

INTRODUCTION

SEVERAL METHODS dealing with the flow of air about a slightly yawing cone have been developed. We shall concern ourselves here with the treatment of this problem as given by Stone[1] and compare it with that advanced by Sauer.[2] Of these two methods, Stone's is the more exact one, since it assumes only—among other things—isentropy along streamlines; whereas Sauer bases his deductions on the premise of irrotationality, and, hence, isentropy, in the whole region of flow. A comparison, then, is of interest mainly because it permits the estimation of the error introduced in the assumption of potential flow.

Following brief outlines of both theories, the comparison mentioned above is made by an evaluation of two quantities obtainable by both methods—namely, the ratio of shock yaw to cone yaw, and the coefficient of the normal force acting on the head of the cone.

NOTATION

D	= diameter of the base of the circular cone
K_N	= coefficient of the normal force on the cone
M_1	= Mach Number of the free stream
N	= normal force of the cone
S	= entropy of the flow
S_0	= entropy of the flow in the nonyaw case
T	= absolute temperature
X, Y, Z	= components of the velocity vector q^* in the direction of r, θ, ω, respectively, measured in units of c
$U(\theta), V(\theta)$	= components of q^* in the nonyaw case
a	= local speed of sound in the nonyaw case, measured in units of c
c	= speed of efflux into vacuum
d_1	= variation of entropy in the plane of yaw
p	= local pressure of flow
q^*, q	= local velocity, speed of flow, respectively
r	= radial distance from the vertex of the cone
x_1, y_1	= perturbations of X, Y in the plane of yaw
z_1	= perturbation of Z normal to the plane of yaw
$\Delta\alpha, \Delta K$	= error in α, K_N, respectively
θ	= polar angle in the system of spherical coordinates
θ_0	= semiapex angle of the cone
θ_w	= shock wave angle in the nonyaw case
Φ	= potential function of the oblique flow
α_1	= yaw of the shock wave
β	= angle of attack
γ	= ratio of the specific heats of air
δ	= shock wave angle
ϵ	= angle of yaw of the cone
η_1	= perturbation of p in the plane of yaw
ν	= angle of rotation of the cone in Sauer's theory
ξ_1	= perturbation of ρ in the plane of yaw
ρ	= density of the flow
φ	= potential function of the flow in the nonyaw case
ω	= azimuthal angle in the system of spherical coordinates

Received May 10, 1948.

* Ordnance Department, Aberdeen Proving Ground.

STONE'S THEORY

In his theory of the yawing cone Stone makes the following basic assumptions:

(a) The Mach Number M_1 of the free stream is sufficiently large, and the semiapex angle θ_0 of the cone is sufficiently small for the (conical) shock wave in the nonyaw case to be attached to the vertex of the cone.

(b) The flow is steady and independent of the distance r from the vertex of the cone. Then, velocity q^* of the flow, pressure p, density ρ, etc., are constant along radial lines through the vertex.

(c) The flow is adiabatic along each streamline. It follows that the entropy S is constant along each streamline but generally assumes different values for different streamlines.

(d) The angle ϵ of yaw of the cone is so small that ϵ^2 and higher powers of ϵ may be neglected.

Since the vorticity $\nabla \cdot q^*$ and the entropy gradient ∇S are related by

$$(\nabla \cdot q^*) \cdot q^* = T \nabla S \tag{1}$$

where T denotes the absolute temperature, it is seen that, by virtue of assumption (c), the flow is necessarily rotational.

Let now X, Y, Z be the components of the velocity q^* in a system of spherical coordinates r, θ, ω, and let $\omega = 0$ be the plane of yaw (see Fig. 1). For the case of axial flow ($\epsilon = 0$), Taylor and Maccoll[3] have shown that $X = U(\theta)$, $Y = V(\theta) = U'(\theta)$, $(U' \equiv dU/d\theta)$, $Z = 0$, and that U, V satisfy the ordinary differential equation

$$(U'' + U)(V^2 - a^2) = a^2(U + V \cot \theta) \tag{2}$$

with

$$a^2 = (1/2)(\gamma - 1)(1 - q_0^2), \qquad q_0^2 = U^2 + V^2 \tag{3}$$

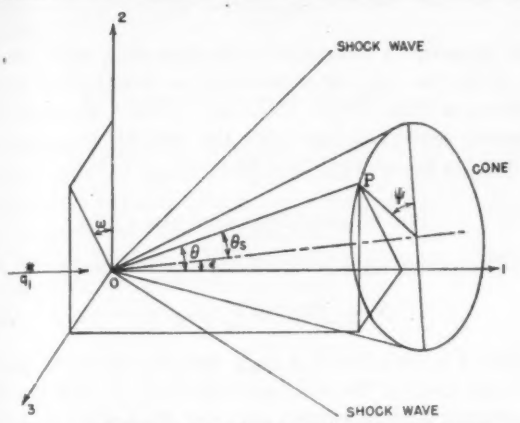

FIG. 1. Systems of coordinates used in Stone's theory.

if the velocity components are measured in terms of the speed c of efflux into a vacuum. For later considerations [see Eq. (16)] we mention here that always $V < 0$.

Further,

$$S_0 = \log p_0/\rho_0^{\gamma} \tag{4}$$

is constant everywhere.

Because of assumptions (b) and (d) it is reasonable to expect that X, Y, Z, ρ, p are expressible in the form

$$X - U = f(\theta, \omega, \epsilon) \tag{5}$$

$$Y - V = g(\theta, \omega, \epsilon), \text{ etc.} \tag{6}$$

where f, g are small functions. Since they must be periodic in ω with the period 2π, f, g can be expanded in Fourier series

$$f(\theta, \omega, \epsilon) = \Sigma_0^{\infty}[x_n(\theta, \epsilon) \cos n\omega + u_n(\theta, \epsilon) \sin n\omega], \qquad u_0 = 0$$

$$g(\theta, \omega, \epsilon) = \Sigma_0^{\infty}[y_n(\theta, \epsilon) \cos n\omega + v_n(\theta, \epsilon) \sin n\omega], \qquad v_0 = 0$$

here x_n, u_n, y_n, v_n are small for small ϵ. The same reasoning leads to

$$\delta - \theta_w = \Sigma[\alpha_n(\epsilon) \cos n\omega + A_n(\epsilon) \sin n\omega], \qquad A_0 = 0$$

for the equation of the shock wave, θ_w denoting the angle of the shock wave in the nonyaw case and α_n, A_n again being small.

Since, further, the components of ∇S in the r, θ, ω directions are $S_r(S_r \equiv \partial S/\partial r)$, $(1/r)S_\theta$, , $[(1/r) \sin \theta]S_\omega$, it follows from assumption (c) that

$$0 = q^* \nabla S = XS_r + YS_\theta/r + ZS_\omega/r \sin \theta$$

Here $S_r = 0$, and Z, S_ω are small if ϵ is small, so that ZS_ω is of the same order as ϵ^2. The result, then, is

$$S_\theta = 0, \qquad \text{i.e., } S = S(\omega, \epsilon)$$

whence it may be deduced, as above, that

$$S - S_0 = \Sigma[d_n(\epsilon) \cos n\omega + D_n \sin n\omega] \tag{7}$$

Finally, the equation of the cone, by virtue of assumption (d), turns out to be

$$\theta = \theta_s + \epsilon \cos \omega \tag{8}$$

Now the flow must be of such a nature as to have a vanishing velocity component in the direction normal to the surface of the cone. By means of the Taylor expansion of Y about $\theta = \theta_s$: $Y = Y_s + Y_s'(\theta - \theta_s)$, Eqs. (8) and (6), this requirement may be seen to result in

$$y_1 = 2\epsilon U \tag{9}$$

$$y_n = 0, \qquad \text{for } n \neq 1, v_n = 0 \text{ for all } n \tag{10}$$

for $\theta = \theta_s$. As shown in reference 1, these conditions (9) and (10), in conjunction with the equation of motion, the continuity equation, and the equation of state, necessitate the vanishing of all the quantities u_n, v_n, and of x_n, y_n, etc., except for $n = 1$, leaving as unknowns the functions $d_1(\epsilon)$, $\alpha_1(\epsilon)$, $x_1(\epsilon, \theta)$, y_1, z_1, and the density and pressure perturbations ξ_1 and η_1. Furthermore, $d_1(\epsilon)/\epsilon$, etc., turn out to be independent of ϵ, if terms of order ϵ^2 are neglected. With the introduction of $d_1/\epsilon = d$, $\alpha_1/\epsilon = \alpha$, etc., where d and α are now constants, and x, y, z, ξ, η are functions of θ, Eqs. (5), (6), etc., finally become

$$\left.\begin{aligned} X - U &= \epsilon x \cos \omega \\ Y - V &= \epsilon y \cos \omega \\ Z &= \epsilon z \sin \omega \\ \rho - \rho_0 &= \epsilon \xi \cos \omega \\ p - p_0 &= \epsilon \eta \cos \omega \\ S - S_0 &= \epsilon d \cos \omega \\ \delta - \theta_w &= \epsilon \alpha \cos \omega \end{aligned}\right\} \tag{11}$$

The last equation, in particular, shows that the disturbed shock surface is again a circular cone of semi-angle θ_w. The yaw α_1 of the conical shock surface—i.e., the angle between its symmetry axis and the free stream velocity vector q_1^*—is given by

$$\alpha_1 = \epsilon\alpha \tag{12}$$

THE DIFFERENTIAL EQUATIONS

For the determination of the six quantities x, y, z, ξ, η, d the equations of motion, continuity, and state [Eq. (7)] supply these five differential equations:

$$\left.\begin{aligned} y - x' &= 0 \\ Vy' + (U'' + U)y + Vx + (\eta'/\rho_0) - (\xi p_0'/\rho_0^2) &= 0 \\ V_s' + (U + V \cot \theta)z - [\eta/(\rho_0 \sin \theta)] &= 0 \\ y' + (\cot \theta + \rho_0'/\rho_0)y + 2x + z \csc \theta + V(\xi/\rho_0)' &= 0 \\ (\eta/p_0) - (\gamma\xi/\rho_0) &= d \end{aligned}\right\} \tag{13}$$

These equations are to be solved subject to the usual boundary conditions, which require the fulfillment of the Rankine-Hugoniot equations at the shock and the vanishing of the normal velocity component at the cone.

Of the five conditions thus obtainable at the shock, we mention here only the one containing α:

$$\alpha = -x \cot \theta/(U + V \cot \theta) \tag{14}$$

System (13) of differential equations is now reducible to one differential equation in $x(\theta)$, as follows: Elimination in Eq. (13.2)—by Eq. (13.2) is meant the second equation of the system (13)—of y and ξ by Eqs. (13.1) and (13.5) and integration show that

$$Vx' + Ux + (\eta/\rho_0) + dp_0/(\gamma - 1)\rho_0 = 0 \tag{15}$$

since the constant of integration may be shown to vanish. Now expressing in Eq. (13.3) η/ρ_0 by means of Eq. (15), we get this differential equation for the quantity $t = x + z \sin \theta$:

$$Vt' = Ut + [dp_0/(\gamma - 1)\rho_0] = 0$$

Its solution is

$$t = \frac{d}{\gamma - 1}(-V\rho_0 \sin \theta)^{1/2} \int_{\theta_w}^{\theta} \frac{p_0 d\theta}{-V\rho_0(-V\rho_0 \sin \theta)^{1/2}} \tag{16}$$

Finally, insertion of Eqs. (13.1), (13.5), (15), and (16) in Eq. (13.4) lead to the following equation:

$$(x/d)'' + A(x/d)' + B(x/d) + C = 0 \tag{17}$$

where

$$A = \cot \theta + \lambda[2U + 3V \cot \theta + (\gamma + 1)\lambda V(U + V \cot \theta)]$$
$$B = 1 - \cot^2 \theta + \lambda[-V \cot^2 \theta + (\gamma - 1)\lambda U(U + V \cot \theta)]$$
$$C = (1 + \lambda V)(t/d) \csc^2 \theta$$

and $\lambda = V/E$, $E = a^2 - V^2$. The conditions at the shock may be condensed into

$$\left.\begin{aligned} \frac{x}{d} &= \frac{-a^2}{\gamma(\gamma - 1)(U + V \cot \theta)} \\ \left(\frac{x}{d}\right)' &= \frac{2a^2 \cot \theta(2U - V \cot \theta)}{\gamma(\gamma^2 - 1)(U + V \cot \theta)^2} \end{aligned}\right\} \tag{18}$$

If we introduce the expression for λ into A, B, C, we obtain

$$\left.\begin{aligned} A_1 \equiv AE &= a^2 \cot \theta + [2a^2 + (\gamma - 1)V^2] \times (V/E)(U + V \cot \theta) \\ B_1 \equiv BE &= -a^2 \cot^2 \theta + E + (\gamma - 1) \times (UV^2/E)(U + V \cot \theta) \\ C_1 \equiv CE &= a^2(t/d) \csc^2 \theta \end{aligned}\right\} \tag{19}$$

and

$$E(x/d)'' + A_1(x/d)' + B_1(x/d) + C_1 = 0 \tag{20}$$

for Eq. (17).

Once this equation has been integrated, the quantity d can be calculated from Eq. (9) written in the form

$$d(x/d)_s' = 2U_s \tag{21}$$

the subscript s indicating evaluation at $\theta = \theta_s$; then z, η/p_0, ξ/ρ_0 may be determined as functions of θ by means of Eqs. (19.3), (15), and (13.5). We shall be mainly concerned here with the quantities α and η_s; these can be obtained from Eqs. (14) and (15).

The Normal Force on the Cone

The normal force N on a finite cone is given by

$$N = \int p_s \cos \theta_s \cos \psi \, d\sigma \tag{22}$$

where ψ is the azimuthal angle measured from the plane of yaw around the cone axis (see Fig. 1), and the integration is to be carried out over the surface σ of the cone. Now by Eq. (11.5), $p = p_0 + \epsilon\eta \cos \omega$. For a point on the cone, then,

$$p_s = (p_0)_s + \epsilon\eta_s \cos \omega$$

or

$$p_s = (p_0)_s + \epsilon\eta_s \cos \psi \tag{23}$$

since $\cos \omega = \cos \psi$ to the accuracy considered here. Introducing Eq. (23) into Eq. (22) leads to

$$N = (1/8)\pi D^2 \cot \theta_s \epsilon\eta_s \tag{24}$$

D being the diameter of the base of the cone.

The normal force coefficient K_N is defined by

$$K_N = N[\rho_1 q_1^2 D^2 \sin \epsilon]^{-1}$$

By Eqs. (24) and (15), then,

$$K_N = -\frac{\pi}{8}\frac{(\rho_0)_s}{\rho_1}\frac{\cot \theta_s}{q_1^2} U_s x_s \left[1 + \frac{1 - U_s^2}{2\gamma U_s}\frac{d}{x_s}\right] \tag{25}$$

The ratio $R \equiv (\rho_0)_s/\rho_1$ occurring in Eq. (25) can be computed from

$$R = ((\rho_0)_s/\rho_w)(\rho_w/\rho_1)$$
$$(\rho_0)_s/\rho_w = [(1 - U_s^2)/(1 - q_w^2)]^{1/(\gamma - 1)}$$

and

$$\frac{\rho_w}{\rho_1} = \frac{(\gamma + 1)M_1^2 \sin^2 \theta_w}{(\gamma - 1)M_1^2 \sin^2 \theta_w + 2}$$

Sauer's Method of Potential Flow

As already pointed out in the introduction, the method developed by R. Sauer differs from the one described above mainly in that the former is based on the hypothesis of irrotationality, and, hence, isentropy of the flow. Another distinctive feature of Sauer's approach consists in assuming the same shock surface for both axial and oblique flow and rotating the cone as a whole through a small angle in order to insure the vanishing of the normal velocity component of the oblique flow at the cone. The other assumptions made by Stone—namely, steadiness of the flow, its conical char-

acter, and smallness of the perturbations—are left unchanged.

Starting, then, from

$$\Phi(r, \theta, \omega) = \varphi(r, \theta) + H(r, \theta) \cos \omega \tag{26}$$

where Φ denotes the potential function of the oblique flow (again in spherical coordinates), φ the potential function of the axially symmetric flow, and H the small disturbance potential; noting that $\varphi = rU(\theta)$ and that H is of the form $H = rh(\theta)$, there result for the velocity components X, Y, Z the expressions

$$\begin{aligned} X &= \Phi_r = U + h \cos \omega \\ Y &= \Phi_\theta / r = V + h' \cos \omega \\ Z &= \Phi_\omega / r \sin \theta = -(\sin \omega / \sin \theta) h \end{aligned} \tag{27}$$

If these relationships are introduced in the continuity equation $\nabla \cdot (\rho q^*) = 0$, if use is made of the equation of state, and if terms of the order h^2 are neglected, the following equation is obtained:

$$Eh'' + A_1 h' + B_1 h = 0 \tag{28}$$

where E, A_1, B_1 were defined in Eqs. (19). It is thus seen that, with respect to form, Eqs. (20) and (28) differ only in the term C_1 containing the variation of entropy.

Now let β be the small angle of attack (see Fig. 2). As shown in reference 2 the Rankine-Hugoniot conditions specialize to

$$\begin{aligned} h/\beta &= U \tan \theta \\ (h/\beta)' &= [2(\gamma - 1)U/(\gamma + 1)] + V \cot \theta \end{aligned} \tag{29}$$

at $\theta = \theta_w$, to the order of accuracy considered here. Once Eq. (28) for the function $\zeta = h/\beta$ subject to the conditions (29) has been integrated, it becomes possible to compute the angle ν through which the cone must be turned until the normal component $d\Phi/dn$ of $q^* = \nabla \Phi$ vanishes. This requirement may be shown to lead to

$$\nu = h'/2U, \qquad \text{at } \theta = \theta_s \tag{30}$$

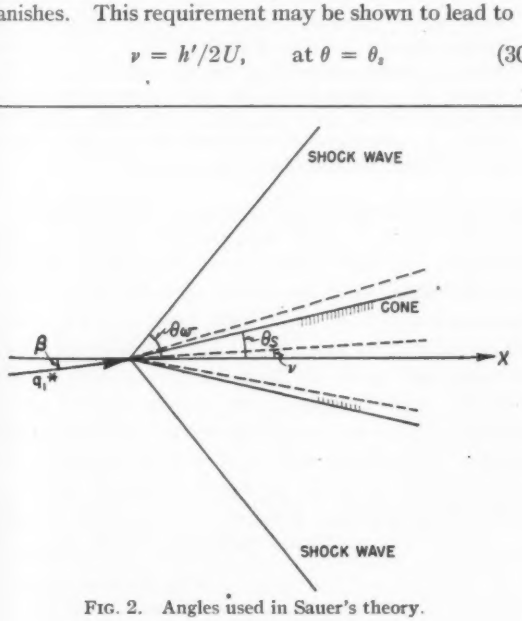

FIG. 2. Angles used in Sauer's theory.

Since β here represents the shock yaw and $\beta - \nu$ is the cone yaw, the ratio $\alpha^{(0)}$ corresponding to $\alpha = \alpha_1/\epsilon$ [see Eq. (12)] can be obtained from

$$\alpha^{(0)} = \frac{\beta}{\beta - \nu} = \frac{\beta/\nu}{(\beta/\nu) - 1} \tag{31}$$

where, by Eq. (30),

$$\beta/\nu = 2U_s/\zeta_s'$$

THE NORMAL FORCE COEFFICIENT $K_N^{(0)}$

Let us now calculate the normal force coefficient $K_N^{(0)}$ based on the pressure distribution resulting from Sauer's theory.

Since

$$\gamma p/\rho = (1/2)(\gamma - 1)(1 - q^2)$$

so that

$$p = (1/2\gamma)(\gamma - 1)\rho(1 - q^2)$$

and

$$\rho_s = F(1 - q_s^2)^{1/(\gamma - 1)}$$

with

$$F = (1 - q_w^2)^{-1/(\gamma - 1)} (\rho_w/\rho_1)\rho_1$$

it follows that

$$p_s = (1/2\gamma)(\gamma - 1)F(1 - q_s^2)^{\gamma/(\gamma - 1)}$$

But by Eqs. (27),

$$q_s^2 = X_s^2 + Y_s^2 + Z_s^2 = U_s^2 + 2U_s\beta\zeta_s \cos \omega$$

Therefore, using the binomial theorem, and, again, $\cos \omega = \cos \psi$,

$$p_s = (1/2\gamma)(\gamma - 1)F(1 - U_s^2)^{\gamma/(\gamma - 1)} - (\rho_0)_s U_s \beta \zeta_s \cos \psi$$

By definition [Eq. (22)], then,

$$N^{(0)} = -(1/8)\pi D^2 \cot \theta_s (\rho_0)_s U_s \beta \zeta_s$$

whence, by Eq. (31),

$$K_{N(0)} = (\pi/8)R(\cot \theta_s/q_1^2) U_s \zeta_s' \alpha^{(0)} \tag{32}$$

NUMERICAL RESULTS

Integrations of Eq. (28) were carried out for a number of cases, and the values of $\alpha^{(0)}$ and $K_N^{(0)}$ were determined. Some of the results are shown in Table 1. The values of α exhibited there are taken from the M.I.T. Table No. 3.

As may be deduced from the cases shown in this table, the values of α and $\alpha^{(0)}$ show good agreement, the error $\Delta\alpha = (\alpha - \alpha^{(0)})/\alpha$ being in no case larger than about 3 per cent.

In view of this result it is permissible, for the following considerations, to put

$$\alpha = \alpha^{(0)} \tag{33}$$

TABLE 1

θ_s	M_1	α	$\alpha^{(0)}$	$\Delta\alpha(\%)$
9°32′	1.678	0.112	0.111	0.9
10°	2.779	0.341	0.339	0.6
20°	2.839	0.729	0.715	1.9
20°	4.154	0.864	0.847	2.0
30°	1.820	0.800	0.775	3.1
1°	∞	1.055	1.041	1.3

Now a comparison of Eqs. (11.1) and (27.1) shows that $\epsilon x_s = -\beta\zeta_s$. Since the angle β corresponds to the shock yaw α_1, it follows that

$$x_s = -(\beta/\epsilon)\zeta_s = -(\alpha_1/\epsilon)\zeta_s = -\alpha\zeta_s = -\alpha^{(0)}\zeta_s$$

in view of Eq. (33). By virtue of this fact Eq. (32) becomes

$$K_N^{(0)} = -(\pi/8)R(\cot\theta_s/q_1^2)U_s x_s \tag{34}$$

$K_N^{(0)}$ is thus seen to be the main term in Eq. (25) for K_N. We may conclude, then, that

$$K_N - K_N^{(0)} = -\frac{\pi}{8}R\frac{\cot\theta_s}{q_1^2}\frac{1-U_s^2}{2\gamma}d \tag{35}$$

In case of irrotationality, and, hence, isentropy, $d = 0$ in the Eq. (11.6) of state, so that, by Eq. (35), the values of K_N and $K_N^{(0)}$ agree. For $d > 0$, it may be deduced from Eq. (35) that $K_N < K_N^{(0)}$. The error of K_N in that case is given by

$$\Delta K \equiv \frac{K_N - K_N^{(0)}}{K_N} = \left[\frac{2\gamma U_s}{1-U_s^2}\left(\frac{x_s}{d}\right)+1\right]^{-1} \tag{36}$$

As the M.I.T. table shows, the quantity $2\gamma U_s x_s/d(1-U_s^2)$ increases for increasing θ_s, as well as for increasing M_1 from large negative values to a value of about -1.4. The error ΔK may thus become large. This fact has also been illustrated in Fig. 3, where ΔK has been plotted against M_1, for some values of θ_s. If one were to take into account the actually existing small discrepancy in $\alpha - \alpha^{(0)}$, which, by Table 1, seems to be positive, then the values of ΔK would have to be multiplied by $1 - \Delta\alpha + (\Delta\alpha/\Delta K)$; since $\Delta\alpha > 0$, $\Delta K < 0$,

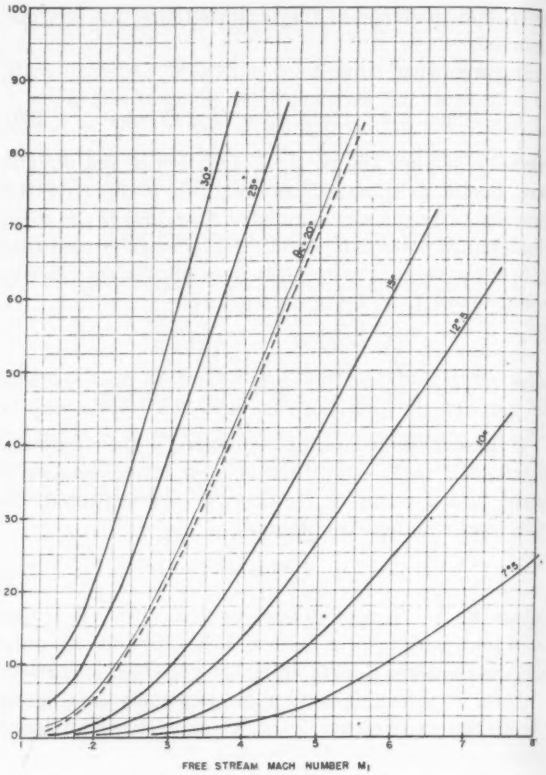

FIG. 3. Error of normal force coefficient due to neglect of vorticity.

one would thus obtain values of the error in $K_N^{(0)}$ somewhat below those depicted in Fig. 3. The dashed curve in Fig. 3 gives the corrected error for $\theta_s = 20°$, on the assumption of $\Delta\alpha = 2$ per cent.

REFERENCES

[1] Stone, A. H., *The Aerodynamics of a Slightly Yawing Supersonic Cone*, NDRC Report No. A-358, 1945.

[2] Sauer, R., Luftfahrtforschung, Vol. 19, 1942.

[3] Taylor, G. I., and Maccoll, J. W., *The Air Pressure on a Cone Moving at High Speeds*, Proc. Roy. Soc., A, Vol. 139, p. 278, 1933.

[4] Kopal, Z., *Supersonic Flow Around Yawing Cones*, M.I.T. Technical Report No. 3, 1947.

The Bending Modulus of Rupture of Round Magnesium Tubing

C. H. MORTENSON*
The Dow Chemical Company

SUMMARY

Bend tests were conducted on 28 round tubes of FS-1a and Ma magnesium alloy. Each alloy covered the d/t range from 20 to 75. The results are summarized empirically, and the following formula is established as representing a minimum value for the bending strength.

$$f_r \text{ (min.)} = 0.7F_{cy}(Et/F_{cy}d)^{0.25}$$

SYMBOLS

f_r = modulus of rupture stress
F_{cy} = compression yield stress
E = modulus of elasticity
t = wall thickness
d = mean diameter
σrs = fr/F_{cy}
$1/\delta_s$ = $Et/F_{cy}d$

INTRODUCTION

BECAUSE OF THE LACK of any previously published experimental data, these bending tests were conducted to establish preliminary design data for the bending modulus of rupture of round magnesium tubing. In order most effectively to simulate actual production applications and at the same time cover a large d/t range, these round tubes were fabricated by arc welding from flat magnesium sheet. The method of testing and evaluation of test results is similar to that of reference 1 for aluminum and steel. The selection of an empirical formula to fit magnesium data differed only slightly from that used in reference 1.

PREPARATION OF SPECIMENS

A total of 28 specimens was prepared for this test, three of which were extruded tubes, while the remaining 25 were fabricated by welding from flat magnesium sheet. The fabricated tubes were hot-rolled from flat Ma and FS-1a sheet alloy and closed by arc welding a longitudinal butt weld. The tubes were rolled so that the longitudinal direction of the tube was transverse to the rolling direction of the original sheet. All tubes were welded in a fixture that fitted the outside diameter. This resulted in the O.D. being reasonably constant over the thickness range of 0.040 to 0.125 in. All fabricated tubes were prepared with a nominal outside diameter of 3 in. and a length of 36 in.

Received April 12, 1948.

* Division of Tests, Magnesium Laboratories.

METHOD OF TESTING

The test setup is shown in Fig. 4. Variations were made in the distance between the load support points during the tests by increasing the length of the tubes. This was accomplished by the use of solid extension end plugs, which were used in all tubes with a $d/t \leq 36$. The exact distances are recorded with the test data in Table 1 and vary between $4.6D$ and $7.4D$. The smaller distance ($4.6D$) was suitable for the larger d/t ratios where the bending failure was local and occurred centrally between loading points. The greater distance ($7.4D$) was provided when it was observed that the specimens having the smaller values of d/t were failing by a gradual flattening of the tube between loading points in addition to extreme deflection. The greater span between loading points permitted the tubes to assume their natural shape without restraint from the semicircular formers at the loading points.

The extruded tubing was loaded through snug-fitting wooden formers in the loading hangers. The fabricated tubes were loaded through steel formers over the upper half of the diameter only. The width of both the wood and steel formers at the point where they contacted the specimens was $^3/_8$ in. Solid circular formers about 1 in. long and snugly fitting the inside of the tube were located under the loading formers in all tubes with a $d/t \geq 47$.

The end support formers rotated on knife edges, which were, in turn, mounted on small roller bearings not visible in the figure. This practically eliminated the possibility of any axial loads in the tubes. The extruded tubing was tested with the thinnest wall in compression. The fabricated tubing was tested with the weld seam adjacent to the neutral axis on the compression side.

RESULTS

Test results are given in Table 1. The design curves of the bending modulus of rupture as determined empirically from the test data, are plotted in Fig. 1 as a function of d/t for various values of F_{cy}.

In order to show the fit of various empirical curves to a nondimensional plot of the test data, Fig. 2 has been included. The relationship between two mean hyberbolic curves of the same type used in reference 1 for steel and aluminum, as well as a mean power function curve, is shown. A minimum value of the power

TABLE 1
Tubing Bend Test Results

Specimen, In.	d/t	S_1 (In.)	$S^{\circ}_{2max.}$ (In.)	L (In.)	Ult. Mach. Load (Lbs.)	Maximum Moment Supported (In.Lbs.)	$f_r = MC/I$ (Lbs. per Sq.In.)	$1/\delta_s = Et/F_{cy}d_m$	$\sigma rs = f_r/F_{cy}$	F_{cy}
						FS-1a Alloy				
0.041 × 3.05	74.4	14.15	9.81	33.77	1,235	6,930	23,800	4.66	1.253	19,000
0.042 × 3.06	72.8	14.05	10.57	35.00	1,085	6,680	22,150	4.82	1.175	18,850
0.052 × 3.04	58.5	14.06	10.74	35.18	1,540	9,230	25,300	5.31	1.188	21,300
0.052 × 3.08	59.2	14.10	10.64	35.34	1,615	9,540	25,600	5.18	1.186	21,600
0.067 × 3.07	45.8	14.09	10.74	35.45	2,050	11,980	25,470	6.75	1.186	21,500
0.081 × 3.06	37.8	14.04	16.25	46.42	1,540	13,980	25,350	8.31	1.190	21,300
0.103 × 3.04	29.5	13.97	16.21	46.40	2,050	18,080	26,900	10.80	1.275	21,100
0.100 × 3.02	30.2	14.07	16.47	46.92	2,065	18,450	28,080	11.10	1.396	20,100
0.100 × 3.05	30.5	13.99	16.37	46.70	1,940	17,330	26,000	11.25	1.326	19,600
0.128 × 3.02	23.6	20.15	15.79	51.65	2,925	24,500	30,400	13.33	1.408	21,600
0.128 × 3.06	23.9	20.10	15.74	51.40	3,025	25,200	30,400	12.56	1.345	22,600
FS-1 Ext. 0.125 × 2.5	20.0	18.84	15.72	48.83	2,250	19,100	36,300	15.08	1.512	
FS-1 Ext. 0.125 × 2.5	20.0	18.95	15.48	48.66	2,125	17,800	33,900	15.08	1.412	
						Ma Alloy				
0.040 × 3.05	76.2	14.09	9.98	34.06	770	4,730	16,840	7.85	1.531	11,000
0.054 × 3.03	56.2	14.09	10.70	35.42	935	5,950	16,050	11.00	1.493	10,750
0.052 × 3.04	58.5	14.09	10.68	35.40	1,110	6,870	19,350	7.20	1.232	15,700
0.053 × 3.05	57.6	14.12	10.62	35.28	985	6,170	16,910	9.93	1.458	11,600
0.065 × 3.02	46.5	14.07	10.74	35.49	1,175	7,270	16,700	12.67	1.480	11,300
0.065 × 3.05	46.9	14.24	10.68	35.53	1,225	7,480	16,680	12.53	1.477	11,300
0.082 × 3.01	36.7	14.03	16.37	56.73	1,035	9,930	18,800	15.43	1.595	11,800
0.082 × 3.03	37.0	14.07	10.74	35.51	1,700	10,100	18,730	15.45	1.600	11,700
0.081 × 3.01	37.2	14.05	18.45	50.78	900	9,940	18,410	14.80	1.513	12,190
0.102 × 3.00	29.4	14.08	16.35	46.75	1,350	12,500	19,300	21.00	1.772	10,900
0.100 × 3.07	30.7	14.13	16.42	46.93	1,300	12,140	18,050	20.35	1.680	10,750
0.100 × 3.07	30.7	14.11	16.40	46.87	1,200	11,300	16,680	19.90	1.516	11,000
0.123 × 3.03	24.6	14.05	16.43	46.78	1,850	16,680	21,200	20.80	1.606	13,200
0.123 × 3.06	24.9	20.05	15.62	52.39	1,925	16,440	20,600	20.50	1.550	13,300
M Ext. 0.125 × 2.5	20.0	18.90	15.59	48.41	1,700	14,630	27,800	27.00	2.320	

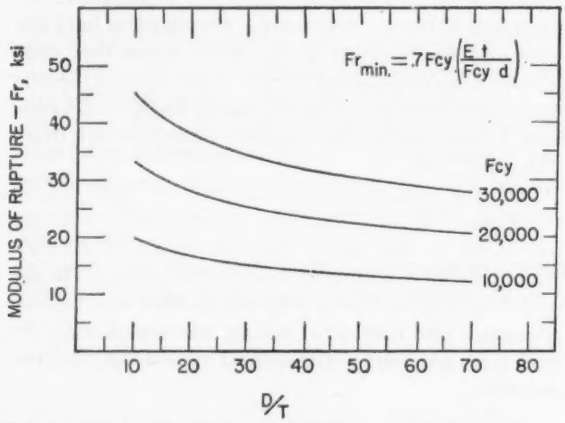

FIG. 1. The bending modulus of rupture of round magnesium alloy tubing.

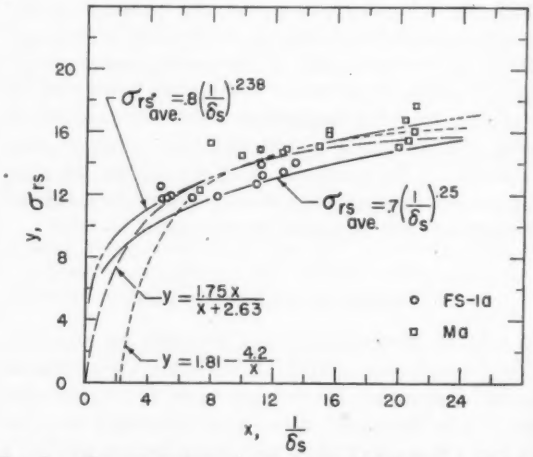

FIG. 2. The comparison of several empirical curves fitted to the nondimensional data for FS-1a and Ma alloy.

function curve is also plotted. The equation of this curve was used to establish the design curves of Fig. 1.

An illustration of typical load deflection curves for the FS-1a tubes with four values of d/t is shown in Fig. 3. The significance of these curves will be brought out in the section titled "Discussion."

In order to differentiate between the types of failure in the large and small d/t ranges, Fig. 5 has been included. The gradual bowing of the small d/t specimens is compared to the crippling type of failure in the walls of those tubes with a large d/t ratio.

DISCUSSION

In the analysis of the test data contained in Table 1, the modulus of rupture, f_r, has been computed from the flexure formula:

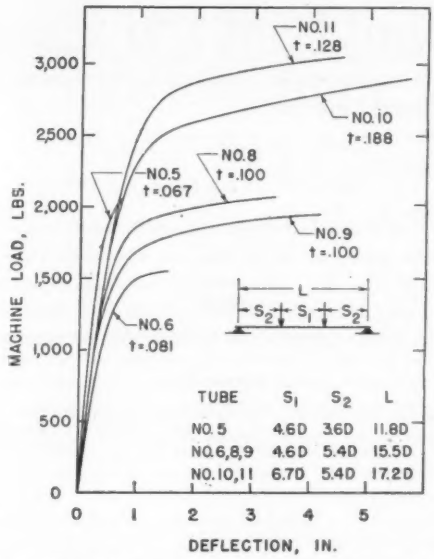

FIG. 3. Load deflection curves for FS-1a alloy tubing. O.D. = 3 in.

$$f_r = Mc/I$$

where M is the maximum moment supported by the specimen and I/C is the section modulus. The test results contained in Table 1 have been converted to nondimensional form and plotted in Fig. 2 in a manner similar to that of reference 1. The plot of the data in Fig. 2 makes use of the following parameters:

$$\sigma rs = fr/F_{cy}$$

and

$$1/\delta_s = Et/F_{cy}d_m$$

where

t = wall thickness
d_m = O.D. $- t$ (mean diameter)
E = modulus of elasticity (6.5×10^6 lbs. per sq.in.)
F_{cy} = compression yield strength

The compression yield strength shown in Table 1 was obtained from flattened specimens cut from unstressed portions of the tubes after static test. The properties were taken in the longitudinal direction of the tube, which is transverse to the rolling direction of the original sheet.

Three empirical curves have been fitted to the nondimensional plot of the data, as shown in Fig. 2. Two of these curves are hyperbolas of the form $y = ax/(x + b)$ and $y = a - (b/x)$. They were selected for fitting as a result of their use in the interpretation of the data for aluminum and steel tubing in reference 1. In addition a simple power function curve of the form $y = ax^b$ has been fitted to the data (Fig. 2) and has been selected to compute the design values of the modulus of rupture stress as plotted in Fig. 1. This formula has been fitted to the data twice, once as an average curve through the test points and again as a minimum curve representing the test data and suggested as a minimum design value.

The construction curves for the determination of the constants in hyperbolic and power function formulas will not be discussed here, since the method is simple and straightforward. It is apparent that the two hyperbolic curves fit the data about as well as the power function curve. The latter was selected to represent the data, because of its simplicity.

The use of the results in Figs. 1 and 2 should not be without careful consideration of the permissible amount of deflection. This is particularly true when designing in the range of $d/t \leq 35$. A study of the load deflection curves plotted for each tube indicated that, for a d/t ratio of less than about 35, the deflection will probably become critical before the tube actually

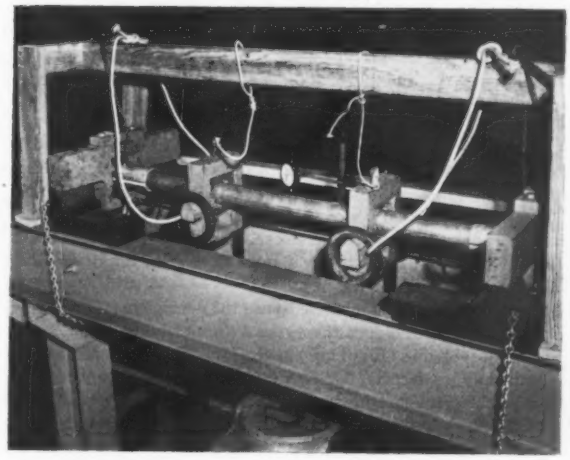

FIG. 4. Test setup for determining modulus of rupture.

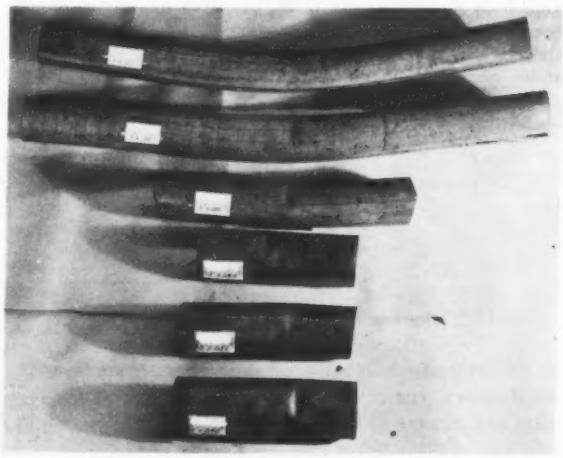

FIG. 5. Typical failures of FS-1a alloy tubing.

fails by bending. Fig. 3 has been included to show the load deflection curves for several values of d/t of the FS-1a tubes. It is apparent in these curves that, for a ratio of $d/t < 38$, the last 10 per cent of load is accompanied by approximately a 100 per cent increase in deflection. Obviously, these deflections are so excessive as to be intolerable in any structure. In general, those tubes with a $d/t \geq 38$ failed by sudden instability of the tube walls, which produced a sharp ended load deflection curve similar to tube No. 5, Fig. 3. The failures of those tubes with a $d/t \leq 38$ consisted of a general flattening of the tubes together with excessive deflection. Fig. 5 clearly illustrates the type of failures experienced in the FS-1a tubes over the entire d/t range.

Conclusions

The bending modulus of rupture of round magnesium FS-1a and Ma alloy tubing can be represented by the following formulas:

$$f_r(\text{min.}) = 0.7F_{cr}(Et/F_{cy}d_m)^{0.25}$$

$$f_r(\text{av.}) = 0.8F_{cy}(Et/F_{cy}d_m)^{0.238}$$

The first formula represents a minimum value of the test data and has been used to establish the design curves of Fig. 1. The second formula represents a mean curve through the test points and may also be used for design purposes if the designer so wishes.

Reference

[1] Osgood, William R., *The Crinkling Strength and the Bending Strength of Round Aircraft Tubing*, N.A.C.A. T.R. No. 632, 1938.

Letter to the Editor

Dear Sir:

In his "Letter to the Editor" (JOURNAL OF THE AERONAUTICAL SCIENCES, Vol. 15, No. 8, p. 502, August, 1948), F. R. Shanley has discussed some results in my paper "Inelastic Column Theories and an Analysis of Experimental Observations" (JOURNAL OF THE AERONAUTICAL SCIENCES, Vol. 15, No. 5, p. 283, May, 1948). However, I feel that the points raised in the discussion, need further clarification.

It would be indeed a mistake to use the coefficient of end fixity C in the inelastic column theory as a "multiplying factor." In Eqs. (16), (18), and (19) of my paper, C was, however, not used as a "multiplying factor." This misunderstanding can be attributed to the fact that in the well-known elastic case—i.e., in the case of Euler's formula—C can actually be used as a "multiplying factor." In the inelastic case, the Eq. (16)

$$P_{cr} = (C\pi^2\overline{EI})/L^2$$

is, in fact, not sufficient in determining the buckling load P_{cr}, since both P_{cr} and $\overline{EI}$ are variables. Actually, one additional equation is needed to give the relationship between P_{cr} and $\overline{EI}$, and this is usually tacitly given in the form of stress-strain curve of the material from which this relationship can be computed. P_{cr}, therefore, must be determined from two simultaneous equations, one of which is given in the form of a curve. If this fact is made clear, there is no danger of misinterpreting C as a "multiplying factor" as mentioned by Shanley. Shanley has also suggested the use of another factor $k_0 = L_0/L$; actually this amounts exactly to the same thing, for k_0 is equal to $\sqrt{C}$.

Mr. Shanley has pointed out that the use of two tangent moduli instead of a simple one in the writer's paper does not lead to simple computation. This is indeed so, since the two-moduli formula was never intended for actual computational use. The reason for introducing the two moduli is to *explain* some of the column behaviors that could not be explained by the tangent modulus theory. Mr. Shanley has contended that the deviation of test results from the tangent modulus formula can all be attributed to the initial imperfections of the column specimens. However, in the writer's paper, in using the two-moduli formula, one can go one step farther by proving that, even if perfect column specimens are possible, there would still be deviations from the tangent modulus formula.

CHI-TEH WANG
Associate Professor of Aeronautical Engineering
New York University

Unsteady One-Dimensional Flows with Heat Addition or Entropy Gradients*

A. KAHANE† AND LESTER LEES‡
Princeton University

SUMMARY

The present interest in aerodynamic propulsive devices, such as the pulse-jet and the ram-jet, has stimulated recent research in the field of combustion. One important aspect of the combustion problem considered herein is the unsteady gas dynamic effects associated with the burning process.

Nonlinear differential equations of the Riemann type are derived for the solution of problems involving the propagation of one-dimensional waves in flows in tubes of slowly varying cross section with heat addition or entropy variation. These equations can be solved graphically or numerically with the method of characteristics; the method is described in the Appendix. The transient flows arising when heat is added to a section (as in a combustion chamber) of an initially isentropic flow in a tube have been calculated. The results of this calculation afford an insight into the gas dynamic aspects of intermittent heat addition in a flowing gas, as well as to the apparently anomalous behavior at sonic velocity of steady gas flows with heat addition. The equations derived are well suited to the calculation of the nonlinear pulse-jet cycle with heat addition, once a suitable model of combustion has been selected.

INTRODUCTION

THE PROPAGATION OF PLANE WAVES due to combustion was theoretically investigated by MacDonald[1] and others with application to the pulse-jet cycle. The Lagrangian form of the equations of motion were used; analytic solutions were obtained by linearizing through the use of the small perturbation method. A disadvantage of the linearization, however, is that waves of finite amplitude are essentially nonlinear and, with linearization, phenomena such as the distortion of the wave form and the formation of shock waves are precluded. In the present report, nonlinear differential equations of the Riemann type are derived for the solution of problems involving the propagation of one-dimensional waves in flows in tubes of slowly varying cross-sectional area with heat addition or entropy gradients. These equations can be solved graphically or numerically with the method of characteristics; the method is described in the Appendix. The transient flows arising when heat is added to a section (as in a combustion chamber) of an initially isentropic flow in a tube have been calculated. The results of this calculation afford an insight into the gas dynamic aspects of intermittent heat addition in a flowing gas as well as to the mechanism of the readjustment of the steady flow in a ram-jet when the quantity of heat added to the flow is changed.

The most complete analysis of the pulse-jet cycle up to the present time has been made by Schultz-Grunow.[2] His analysis, however, does not consider the effect of heat input, the combustion process being simulated merely by an isentropic pressure rise taking place in the combustion chamber, with all the resulting wave propagation processes also considered as isentropic. Although these simplifying assumptions lead to a quick method of calculating the effect of various parameters on the pulse-jet cycle, the method obviously cannot give any insight into the effects of heat addition on the cycle, nor can values of thrust be calculated. The equations derived herein make it possible to calculate the nonlinear pulse-jet cycle with a full consideration of heat addition, and it should be possible to obtain values of thrust from such calculations.

SYMBOLS

a	= velocity of sound, ft. per sec.
A	= cross-sectional area of tube, sq.ft.
C_p	= specific heat at constant pressure, B.t.u. per slug per °F.
C_v	= specific heat at constant volume, B.t.u. per slug per °F.
L	= length of heating chamber, ft.
p	= static pressure, lbs. per sq.ft.
P	= Riemann variable, $P = u + [2/(\gamma - 1)]a$, ft. per sec.
Q	= Riemann variable, $Q = u - [2/(\gamma - 1)]a$, ft. per sec.
Q^*	= quantity of heat added per unit mass, B.t.u. per slug
R	= gas constant, B.t.u. per slug per °F.
S	= entropy, B.t.u. per slug per °F.
t	= time, sec.
T	= absolute temperature, °R.
u	= particle velocity, ft. per sec.
x	= distance along tube, ft.
γ	= ratio of specific heats, C_p/C_v
ρ	= mass density of fluid, slugs per cu.ft.

DERIVATION OF CHARACTERISTIC EQUATIONS

The characteristic equations for the propagation of waves in flows with heat addition or entropy variations will now be derived. The flows will be assumed to take place in tubes of slowly varying cross section and will therefore be assumed one-dimensional. It will further

Received December 12, 1947.

* This research was supported by Project Squid, which is a cooperative research project in jet propulsion under the sponsorship of the Office of Naval Research. Reproduction in whole or in part is permitted for any purpose of the United States Government.

† Research Associate.

‡ Associate Professor.

be assumed that the gas constant, R, and the specific heats, C_p and C_v, are constants.

The equations of motion are:

Dynamical equation

$$\frac{\partial u}{\partial t} + u\frac{\partial u}{\partial x} + \frac{1}{\rho}\frac{\partial p}{\partial x} = 0 \tag{1}$$

Continuity equation

$$\frac{\partial \rho}{\partial t} + \frac{1}{A}\frac{\partial(\rho u A)}{\partial x} = 0 \tag{2}$$

Energy equation

$$\frac{dQ^*}{dt} = T\frac{dS}{dt} = C_v\frac{dT}{dt} - \frac{p}{\rho^2}\frac{d\rho}{dt} \tag{3}$$

Equation of state

$$p = \rho RT \tag{4}$$

From Eqs. (3) and (4) the relation between the pressure and density can be found to be

$$p = \text{constant} \times \rho^{\gamma} e^{S/C_v} \tag{5}$$

and by defining†

$$a = \sqrt{\gamma p/\rho}$$

Eqs. (1) and (2) can be transformed to

$$\frac{\partial u}{\partial t} + u\frac{\partial u}{\partial x} + \frac{2}{\gamma - 1}a\frac{\partial a}{\partial x} - \frac{a^2}{(\gamma - 1)C_p}\frac{\partial S}{\partial x} = 0 \tag{1a}$$

$$\frac{2}{\gamma - 1}\frac{\partial a}{\partial t} + \frac{2}{\gamma - 1}u\frac{\partial a}{\partial x} + a\frac{\partial u}{\partial x} - \frac{\gamma}{\gamma - 1}\frac{a}{C_p}\frac{dS}{dt} + \frac{ua}{A}\frac{dA}{dx} = 0 \tag{2a}$$

where

$$dS/dt = (\partial S/\partial t) + u(\partial S/\partial x)$$

is the rate of change of entropy following a fluid particle. Addition and subtraction of the above equations give:

$$\frac{\partial}{\partial t}\left(u \pm \frac{2a}{\gamma - 1}\right) + (u \pm a)\frac{\partial}{\partial x}\left(u \pm \frac{2}{\gamma - 1}a\right) - \frac{a^2}{(\gamma - 1)C_p}\frac{\partial S}{\partial x} \mp \frac{\gamma}{\gamma - 1}\frac{a}{C_p}\frac{dS}{dt} \pm \frac{ua}{A}\frac{dA}{dx} = 0 \tag{6}$$

The above equations are essentially wave equations and indicate that disturbances are propagated downstream and upstream at the velocity a relative to the stream velocity (the upper and lower signs denote downstream and upstream wave motions, respectively).

It will be noted that for isentropic waves in constant cross-section tubes, the equations reduce to that of Riemann;[4, 5] because of heat addition and area change, therefore, a single progressive wave will be continually transmitted and reflected as it passes down the tube, and, of course, its reflections will in turn be transmitted and reflected. For steady flow, the equations can be reduced to those of Chambré and Lin.[6]

Since in most cases analytic solution of Eq. (6) is extremely difficult, the numerical or graphical calculation procedures of the well-known characteristic method must be used. Such calculations are carried out on the time-distance or t-x plane. The equations of the characteristic lines are

$$(dx/dt)_1 = u + a$$
$$(dx/dt)_2 = u - a$$

If the variables P and Q are introduced (Riemann and others used the symbols "r" and "s"), such that‡

$$P \equiv u + [2/(\gamma - 1)]a$$
$$Q \equiv u - [2/(\gamma - 1)]a$$

then the total change of these variables with time as one proceeds along characteristic lines is

$$\frac{\delta P}{dt} = \frac{\partial P}{\partial t} + \frac{\partial P}{\partial x}\left(\frac{dx}{dt}\right)_1$$

$$\frac{\delta Q}{dt} = \frac{\partial Q}{\partial t} + \frac{\partial Q}{\partial x}\left(\frac{dx}{dt}\right)_2$$

and from Eq. (6)

$$\frac{\delta P}{dt} = \frac{a^2}{(\gamma - 1)C_p}\frac{\partial S}{\partial x} + \frac{\gamma}{\gamma - 1}\frac{a}{C_p}\frac{dS}{dt} - \frac{ua}{A}\frac{dA}{dx} \tag{7a}$$

$$\frac{\delta Q}{dt} = \frac{a^2}{(\gamma - 1)C_p}\frac{\partial S}{\partial x} - \frac{\gamma}{\gamma - 1}\frac{a}{C_p}\frac{dS}{dt} + \frac{ua}{A}\frac{dA}{dx} \tag{7b}$$

Thus for a given tube the characteristic network may be constructed as long as the entropy variations are known. A method that may be used in constructing the network is described in the Appendix. The method of characteristics is also described in the Shock Wave Manual[7] and by Sauer.[8]

Applications

The equations derived in the preceding section have many interesting applications in the field of gas dynamics. Some possible applications include the calculation of the pulse-jet cycle, once a suitable model of combustion has been assumed, and studies of the stability of the flow pattern in the ram-jet. A study of the stability of the ram-jet operation might include the gas-dynamic effect of a wave disturbance upon the initial steady-flow combustion pattern or the effect of disturbances generated by "rough burning" (simulated by small variations of the quantity of heat input) on the motion of the diffuser shock wave in a supersonic ram-jet.

† The quantity a is equal to the value of the velocity of sound if the compression and expansion processes occurring in the sound wave are isentropic. If the passage of the sound wave in itself causes heat addition, so that the compressions and expansions of the sound wave are nonadiabatic, then a is not exactly the velocity of sound.[3]

‡ δ/dt indicates the total derivative along a characteristic line.

A problem that is treated in this report is the effect of addition of heat to an initially isentropic flow in a tube. The processes occurring in such a configuration are similar to those that occur during intermittent combustion in a flowing gas, as well as being similar to those that occur during steady-flow combustion when the quantity of heat addition is suddenly changed.

The Addition of Heat to an Initially Isentropic Flow

Of interest is the transient phenomena occurring when heat is suddenly added to an initially isentropic flow in a constant area tube of infinite length. Consider a tube in which the flow initially is at a Mach Number of 0.80. Heat will be assumed to be added between stations A and B, at a rate such that

$$(dQ^*/dt)/T = dS/dt = \text{constant} = K$$

within the heating chamber. The value of dS/dt was chosen as a constant to simplify the calculations.

The transients can now be calculated with the characteristic method utilizing Eqs. (7a) and (7b). The entropy may be determined in the following manner: a plot of the actual particle paths can be constructed along with the characteristic calculation on an x-t plane (the equation of a particle path line is $dx/dt = u$). The entropy at any point is found by performing the following integration along the particle path

$$S - S_1 = \int_1^t [(dQ^*/dt)/T]dt$$

Once the entropy distribution is known, values of $\partial S/\partial t$ and $\partial S/\partial x$ at a given point can be estimated.

A great simplification in the present calculation can be made by the following observations. If the characteristic x-t plane is divided up into regions bounded by the lines $x = A$ and $x = B$ (the entrance and exit of the heat chamber) and the particle path lines of the particles that are initially at $x = A$ and $x = B$ at the time $t = 0$ (see Fig. 1), then, for the prescribed heat addition $(dQ^*/dt)/T = K$, it can be ascertained that the entropy variations in the various regions are approximately

$$\begin{aligned}
&\text{I} && \begin{cases} \partial S/\partial t = 0 \\ \partial S/\partial x = 0 \end{cases} \\
&\text{II} && \begin{cases} \partial S/\partial t = K \\ \partial S/\partial x = 0 \end{cases} \\
&\text{III} && \begin{cases} \partial S/\partial t = 0 \\ \partial S/\partial x = K/u \end{cases} \\
&\text{IV} && \begin{cases} dS/dt = 0 \\ \partial S/\partial x = -K/u \end{cases}
\end{aligned} \qquad (8)$$

The above formulas were obtained by assuming that all the particle path lines in the x-t plane deviate only slightly from straight lines all parallel to each other. As an example, consider the region numbered II. Since the heat is first added at $t = 0$, at any given constant value of t within region II, each particle has increased its entropy by the same amount under the assumptions made. Thus, clearly, $\partial S/\partial x = 0$. Then, since

$$dS/dt = (\partial S/\partial t) + u(\partial S/\partial x) = K$$

it follows that

$$\partial S/\partial t = K$$

A similar reasoning applied to the other regions will give the remaining equations.

These approximations to the entropy variations were used in calculation of the transient flow. Use of the approximation may also be regarded as equivalent to slightly varying the addition of heat during the transient phase so that the expressions (8) are satisfied.

The characteristic x-t plane for this calculation is shown in Fig. 2; the main results are illustrated in Fig.

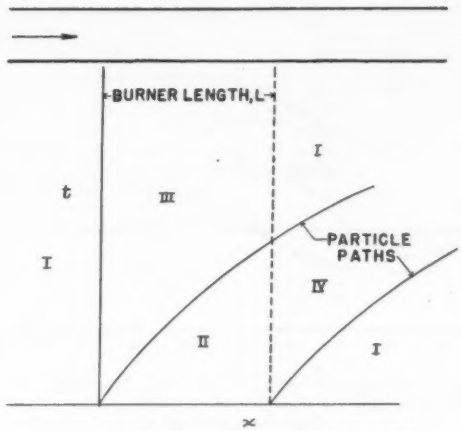

Fig. 1. Regions of the characteristic plane for which approximate entropy derivatives are determined.

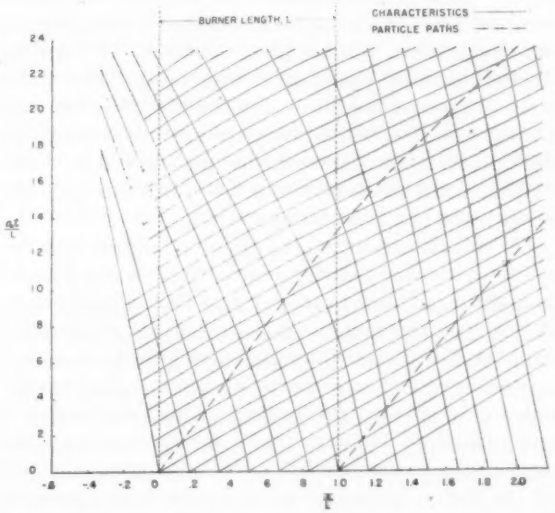

Fig. 2. Characteristic diagram for the addition of heat in a tube to an initially isentropic flow of $M_0 = 0.8$, $KL/a_0C_p = 0.36$.

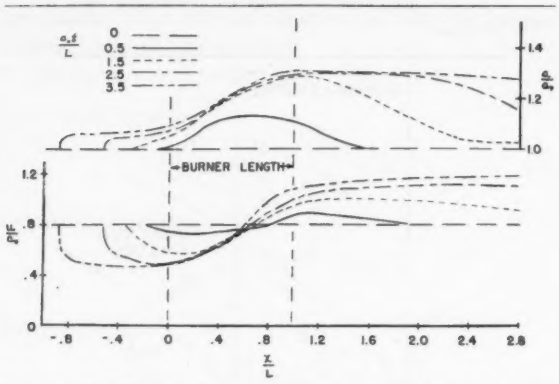

FIG. 3. Distribution of u/a_0 and a/a_0 for several values of the time parameter a_0t/L.

3, in which distributions of u/a_0 and a/a_0 are plotted against x/L for several values of the time parameter a_0t/L. These graphs indicate that, with the addition of heat, compression waves are propagated both upstream and downstream of the heat chamber. It may be observed that the upstream moving compression wave is rapidly steepening into a shock wave. For the infinite tube the flow would always be unsteady because of the upstream and downstream moving waves. The transition to a steady flow in a tube of finite length will be discussed in a later paragraph.

The calculation carried out affords an insight into the processes occurring during intermittent combustion in an initial steady flow. It is evident that in combustion of this type the pressure is raised in the combustion chamber, this pressure increase causing the propagation in both directions of compression waves. The magnitude of the pressure rise in the combustion chamber is proportional to the rapidity of combustion—i.e., the rate of release of energy Q^*. Thus, for large values of Q^* the thermodynamic combustion process approaches the constant-volume process (ρ = constant) obtained in the Otto-cycle; whereas for small values of Q^* the burning process approaches the so-called constant pressure process obtained with steady-flow combustion as in the ram-jet and turbojet.

The Transition to the Steady-Flow State

As pointed out earlier in this paper, no steady state flow will ever occur in an infinitely long tube when heat is being added to an initially isentropic flow. Consider now that the tube is of finite length, such as a ram-jet moving at a flight Mach Number of $M = 0.8$. (See Fig. 4.) When the heat is added to the flow, the compression waves that are propagated upstream and downstream will be reflected at the entry and exit of the tube and will continually reflect and refract until a new steady flow is established. The new steady flow will depend only on the ram stagnation pressure, the quantity of heat added by the burner, and the exit pressure (assuming frictionless flow) and can easily be calculated by the equations presented by Chambré and Lin[6] or Hicks.[9] Since the exit pressure is atmospheric and since the steady addition of heat causes a pressure drop across the burner, it is evident that the pressure upstream of the burner is higher than that occurring in the completely adiabatic flow. Thus, the velocity ahead of the burner and, therefore, the mass flow through the system are reduced. Also, it may be observed that, since the stagnation pressure of the flow is reduced in passing through the combustion chamber, the exit Mach Number is less than that of the completely adiabatic flow. A plot of flow parameters for steady state flows with several values of the quantity of heat added is presented in Fig. 4. It is evident that increasing the quantity of heat added will cause a readjustment of the flow with a further reduction of mass flow through the system.

Consider now a ram-jet propelled at supersonic speed with a supersonic diffuser at the inlet (Fig. 5). In this configuration the mass flow is fixed once the supersonic flow is established in the inlet of the diffuser, and a normal shock wave will be present in the diverging portion of the diffuser. If the quantity of heat added is increased, a new steady flow will be established with the shock moved to a more forward position.

The reason for this can easily be seen by considering the diverging part of the diffuser as analogous to the diverging part of a Laval nozzle. Since the mass flow through the system is fixed, as long as sonic velocity exists at the throat of the exhaust nozzle, it follows that the Mach Number at the burner exit must remain constant. Thus, increasing the quantity of heat added will reduce the Mach Number M_A at the entry of the

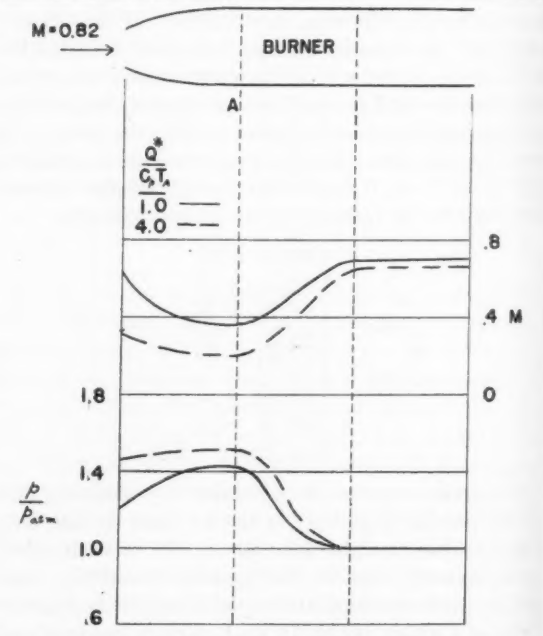

FIG. 4. The steady flow obtained in an initially subsonic flow for several values of the quantity of heat added.

burner. Since the flow is adiabatic upstream of the burner, the mass flow per unit area depends only on the stagnation density behind the shock; the stagnation temperature, which is constant; and the Mach Number at the burner entry—i.e., $m = \rho_S \sqrt{T_S} f(M_A)$. Therefore, a reduction in M_A must be accompanied by an increase in ρ_S behind the shock, and the shock wave is weaker and occurs farther upstream. Additional increase in the quantity of heat added will finally move the shock to a more forward position, until eventually it will reach the converging portion of the diffuser where it is unstable[6] and it will move out in front of the ramjet tube as a detached shock. Now the internal flow is subsonic, and the effect of further addition of heat will be the same as that of the subsonic jet.

The conclusions of the present study also give an insight into the apparently anomalous behavior at sonic velocity of a steady gas flow in a straight tube with a steady rate of heat addition. From the equations of motion for steady flow it is concluded that the gas cannot absorb heat at sonic velocity. Chambré and Lin[6] conclude that a "sharp front" will result if heat is added to the gas at or beyond the point at which sonic velocity is attained. From the present study it appears that when a quantity of heat, greater than the "critical" amount that would bring the gas to sonic velocity, is added, compression waves traveling in both directions are generated initially, and a new equilibrium flow is established.

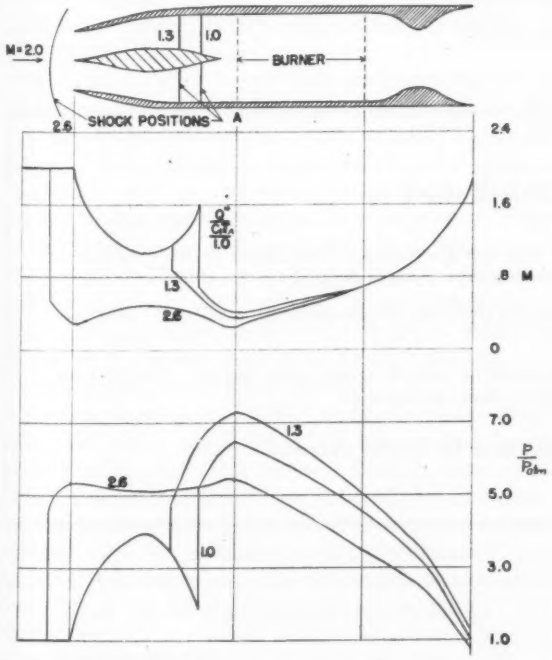

FIG. 5. The steady flow obtained in an initially supersonic flow for several values of quantity of heat added.

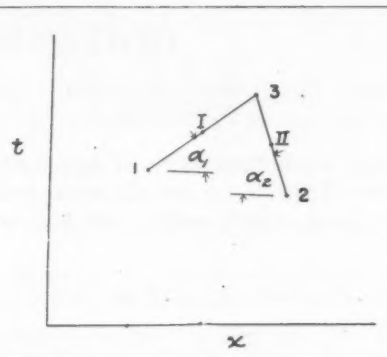

FIG. 6. Graphical method of constructing characteristics.

Appendix

A Graphical Calculation Procedure

The method of characteristics is a graphical or numerical procedure for integrating partial differential equations of the hyperbolic type. It is assumed here that all quantities including u, a, and S are known at the points 1 and 2 in the x-t plane and that the values of these quantities are to be found at a third point designated 3. The rate of heat release is also assumed known throughout the x-t plane, or

$$\dot{Q}^* = \dot{Q}^*(x,t)$$

To calculate the point 3, the characteristic differential Eqs. (7a) and (7b) are written as difference equations and are solved by substitution in them of mean values of the quantities between 1 and 3 and 2 and 3, which are referred to as the quantities at I and II, respectively. Inasmuch as the quantities at 3 are unknown as yet, the computation is of necessity an iterative procedure, the first approximation of which is as follows (see Fig. 6):

(1) The characteristic lines are drawn through points 1 and 2 at angles

$$\alpha_1 = \cot^{-1}(u_1 + a_1)$$
$$\alpha_2 = \cot^{-1}(a_2 - u_2)$$

The intersection of these segments will be considered the first approximation to the point 3.

(2) The values of dS/dt and $\partial S/\partial x$ are to be found at the points I and II which bisect the characteristic segments 1–3 and 2–3, respectively. The value of dS/dt may be found from

$$\frac{dS}{dt} = (dQ^*/dt)/T = \frac{(\gamma - 1)C_p(dQ^*/dt)}{a^2}$$

Since the value of a at I and II is not yet known, the values at 1 and 2 may be used. The value of $\partial S/\partial x$ may be estimated from the definition of a partial derivative, which for the point I is

$$\left(\frac{\partial S}{\partial x}\right)_I = \lim_{\Delta_x \to 0} \frac{S[x_I + (\Delta x/2), t_I] - S[x_I - (\Delta x/2), t_I]}{\Delta x}$$

In estimating $\partial S/\partial x$ finite values of Δx must be used. The values of S used in the formula are determined by integrating along suitable particle path lines using the equation

$$S - S_0 = \int_{t_0}^{t} [(dQ^*/dt)/T]dt$$

(3) Eqs. (7a) and (7b) are utilized to determine P_3 and Q_3. They may be written as follows:

$$P_3 - P_1 = \left[\frac{a_I^2}{(\gamma-1)C_p}\left(\frac{\partial S}{\partial x}\right)_I + \frac{\gamma}{\gamma-1}\frac{a_I}{C_p}\left(\frac{dS}{dt}\right)_I - u_I a_I \left(\frac{d\log A}{dx}\right)_I\right](t_3 - t_1)$$

$$Q_3 - Q_2 = \left[\frac{a_{II}^2}{(\gamma-1)C_p}\left(\frac{\partial S}{\partial x}\right)_{II} - \frac{\gamma}{\gamma-1}\frac{a_{II}}{C_p}\left(\frac{dS}{dt}\right)_{II} + u_{II} a_{II} \left(\frac{d\log A}{dx}\right)_{II}\right](t_3 - t_2)$$

where

$$u_I = (u_1 + u_3)/2$$
$$u_{II} = (u_2 + u_3)/2$$

etc. Since u_3 and a_3 are unknown as yet, in the first approximation the values of u and a at 1 and 2 are substituted for their values at I and II, respectively. Values of u_3 and a_3 are then found from

$$u_3 = (P_3 + Q_3)/2$$
$$a_3 = [(\gamma - 1)/4](P_3 - Q_3)$$

The second approximation consists of constructing new characteristic segments using mean values of u and a between 1 and 3 and 2 and 3, finding a better approximation to the entropy derivatives, and recalculating P_3 and Q_3 using the mean values of u and a along the segments as well as the more accurate time change. The method usually converges rapidly, and for most applications the first approximation is sufficiently accurate.

References

[1] *A Gas Dynamical Formulation for Waves and Combustion in Pulse-Jets*, A.M.G.-N.Y.U. No. 151, June, 1946.

[2] Schultz-Grunow, F., *Gas Dynamic Investigations of the Pulse-Jet Tube, Parts I and II*, N.A.C.A. T.M. No. 1131, February, 1947.

[3] Richards, W. T., *Supersonic Phenomena*, Phys. Rev., Vol. 11, p. 36, 1939.

[4] Riemann, B., *Über die Fortpflanzung ebener Luftwellen von endlicher Schwingungsweite*, Göttingen Abhandlungen, Vol. 8, 1860.

[5] Kantrowitz, Arthur, *The Formation and Stability of Normal Shock Waves in Channel Flows*, N.A.C.A. T.N. No. 1225, 1947.

[6] Chambré, Paul, and Lin, Chia-Chiao, *On the Steady Flow of a Gas Through a Tube with Heat Exchange or Chemical Reaction*, Journal of the Aeronautical Sciences, Vol. 13, No. 10, pp. 537–542, October, 1946.

[7] *Supersonic Flow and Shock Waves*, NDRC, AMP Report 38.2R (A.M.G.-N.Y.U. No. 62), August, 1944.

[8] Sauer, R., *Theory of Non-Stationary Gas Flow I Laminar Steady Gas Waves*. A.A.F. Translation Rep. No. F-TS-763-RE, July 31, 1946.

[9] Hicks, Bruce L., *Addition of Heat to a Compressible Fluid in Motion*, N.A.C.A. Wartime Report ACR No. E5A29, February, 1945.

Notice to Contributors

Manuscripts submitted for publication *must be* double- or triple-spaced originals. There should be wide margins on both sides of the sheets and triple spacing around formulas to allow for the marking of directions for the printer.

Original drawings (jet black India ink on white paper or tracing cloth) should accompany the manuscript. *(Blueprints are not acceptable.)* Photographs *must be* on glossy white paper.

Only the simplest formulas should be typewritten; all others should be carefully written in pen and ink. The difference between capital and lower-case letters and Greek symbols should be clearly distinguished.

See the Inside Back Cover of this issue for further details.

Transonic Separation

VERNON OUTMAN* AND ARTHUR A. LAMBERT†
McDonnell Aircraft Corporation

SUMMARY

The problems of avoiding airflow separation, air-frame shaking, and control surface buffeting at transonic flight speeds are discussed. A design parameter, identified as the angle between the aft surface of a body and the line of flight is proposed as a useful tool for avoiding these difficulties and is correlated with flight and wind-tunnel test data. The correlation showed that, for preliminary design purposes, the proposed parameter represents a satisfactory index of the Mach Number at which separation phenomena will occur on bodies and lifting surfaces. For wing-body junctures and tail intersections it is suggested that separation Mach Numbers be considered greater than the critical Mach Numbers by 0.10.

INTRODUCTION

ON HIGH-SPEED AIRCRAFT many new aerodynamic phenomena have occurred. Disturbances have been encountered by airplanes diving to speeds that have never before been reached. In reviewing the nature of the disturbances encountered at these high speeds, we see that they have taken various forms. At first it was usually a longitudinal disturbance as evidenced by a change in trim, elevator control position, or elevator force, and these phenomena are at present reasonably well understood. Such changes in stability and control usually resulted from changes in the lift curve, pitching moment curve, and down-wash. A summary of information on this phase of the problem is presented in reference 1.

More recently, difficulty has been experienced in directional stability and lateral control at high speeds. The directional difficulty is a type of dynamic instability which is sometimes caused by a combination of pressure distribution changes and separation on the vertical tail which influence the hinge moments of the rudder. The lateral control difficulty experienced is a type of control surface oscillation, or one-degree flutter, sometimes called "buzz," a phenomena that has been discussed in various papers. These problems are being investigated by research organizations, the military services, and manufacturers of high-speed aircraft.

Another problem, which may be related to the above difficulties but in some respects is independent, is beginning to appear. This problem is the occurrence of airflow separation and buffeting at high Mach Numbers, causing shake of the air frame or buffeting of a control surface. It is this problem that is to be discussed, and an attempt will be made to provide a means of avoiding this type of difficulty on high-speed aircraft.

Received June 28, 1948.

* Chief Technical Engineer.

† Project Aerodynamicist.

THEORETICAL CONSIDERATIONS

From the practical point of view a design parameter is needed which, when correlated with test data, will serve as a criterion for avoiding separation and, hence, buffeting at transonic speeds. Before discussing a design parameter, however, it may be well to examine the conditions that may lead to separation at high Mach Numbers. An adverse pressure gradient permits separation, and thus the magnitude of such gradients that exist on a body will be of cardinal importance in establishing a design parameter with which to correlate the Mach Number of separation. In this regard, the difference in the effect of stream filament contraction on the pressure gradients for subsonic and supersonic flows must be considered, since both types of flow are encountered locally on an airfoil traveling at high transonic speeds, and these effects will have a direct bearing on the magnitude of separation that may develop. In subsonic flow, a tendency for the stream filaments to contract, due to a wedge-shaped boundary-layer growth, will result in a tendency to decrease the local adverse pressure gradients and thus allay further thickening of the boundary layer. In supersonic flow, however, the opposite is true. Stream filament contraction due to a wedge-shaped boundary-layer growth results in increased adverse pressure gradients and, therefore, in a greater tendency for the boundary layer to thicken or separate. Hence, when a region of supersonic flow exists on an airfoil or similar aerodynamic body, disturbances in the boundary layer resulting from the occurrence of shock waves, combined with a large adverse pressure gradient, will result in a considerable boundary-layer growth, possible airflow separation, and, in general, a high degree of turbulence.

As the Mach Number of the principal flow approaches unity, the main shock waves move to the trailing edge and the unstable tendency of the boundary layer disappears, as is shown by high-speed schlieren photographs. Thus, severe buffeting may be expected to begin at free stream Mach Numbers somewhat above the critical value for the airfoil and disappear at approximately sonic speed.

High-speed wind-tunnel tests offer a good means of indicating regions of transonic separation when the model is properly tufted. Usually, however, several months are required to build a high-speed model, since in most cases they must be made of steel. Therefore in the interests of expediency, it is usually necessary to settle the design before the wind-tunnel test results are available. Because of this the designer needs a tool

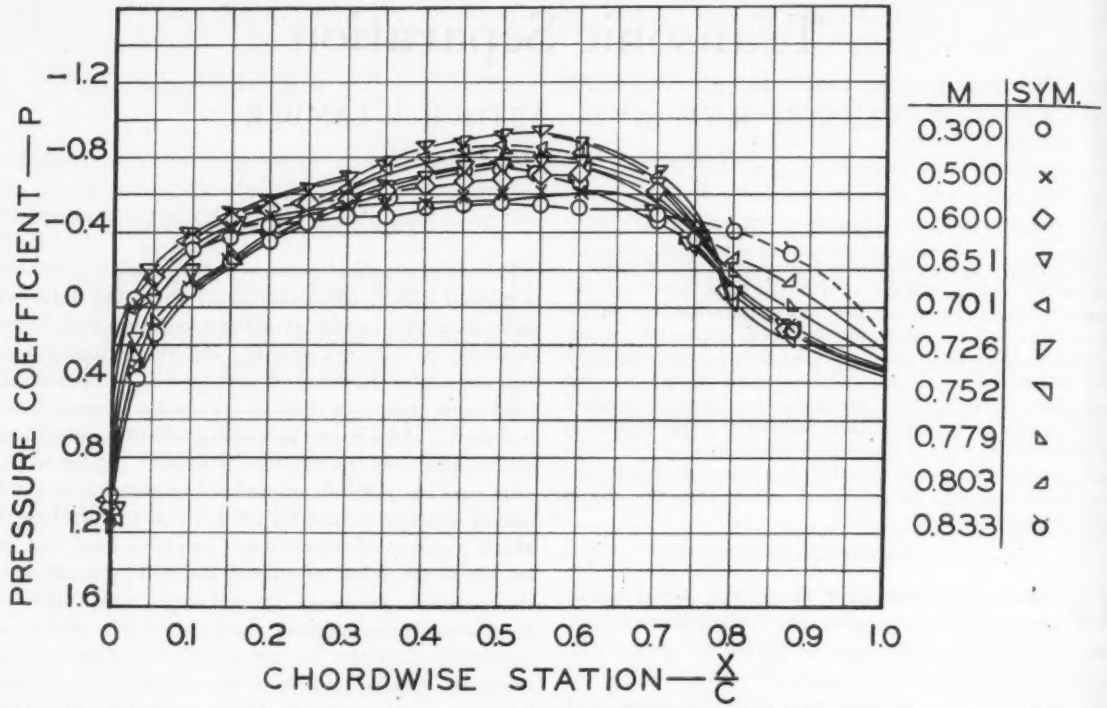

FIG. 1. Upper surface pressure distribution versus Mach Number for the NACA 66,2-215 airfoil at zero degrees angle of attack.

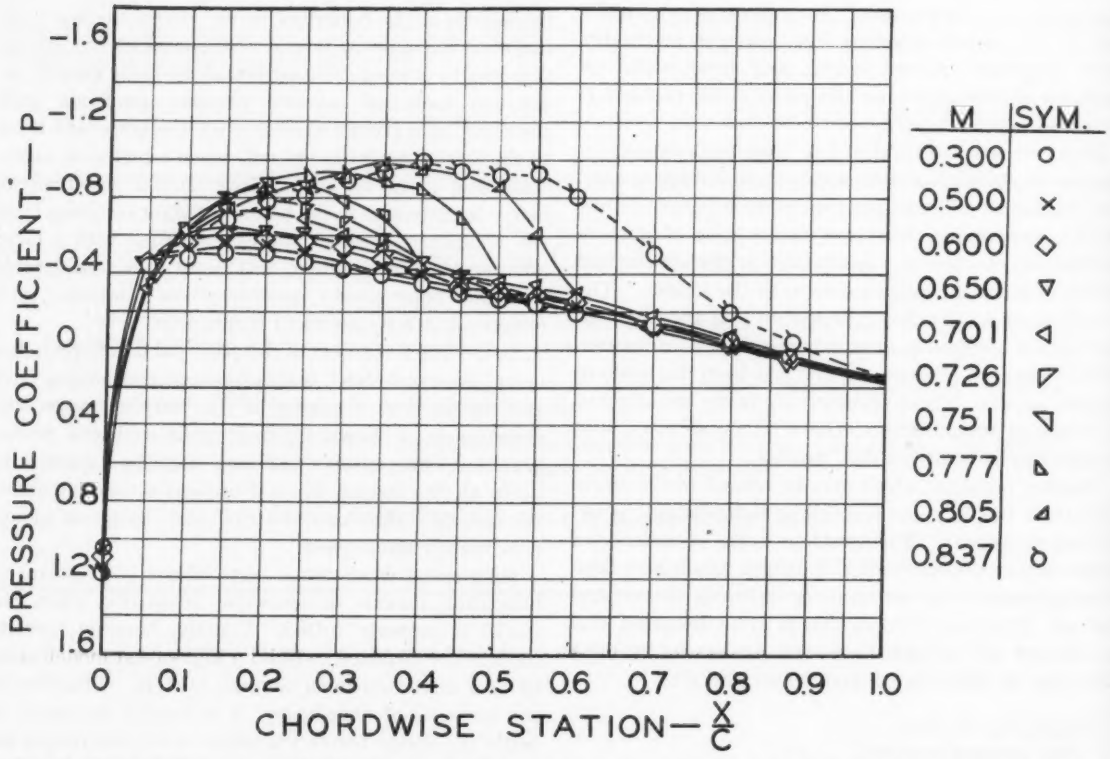

FIG. 2. Upper surface pressure distribution versus Mach Number for the NACA 0015 airfoil at zero degrees angle of attack.

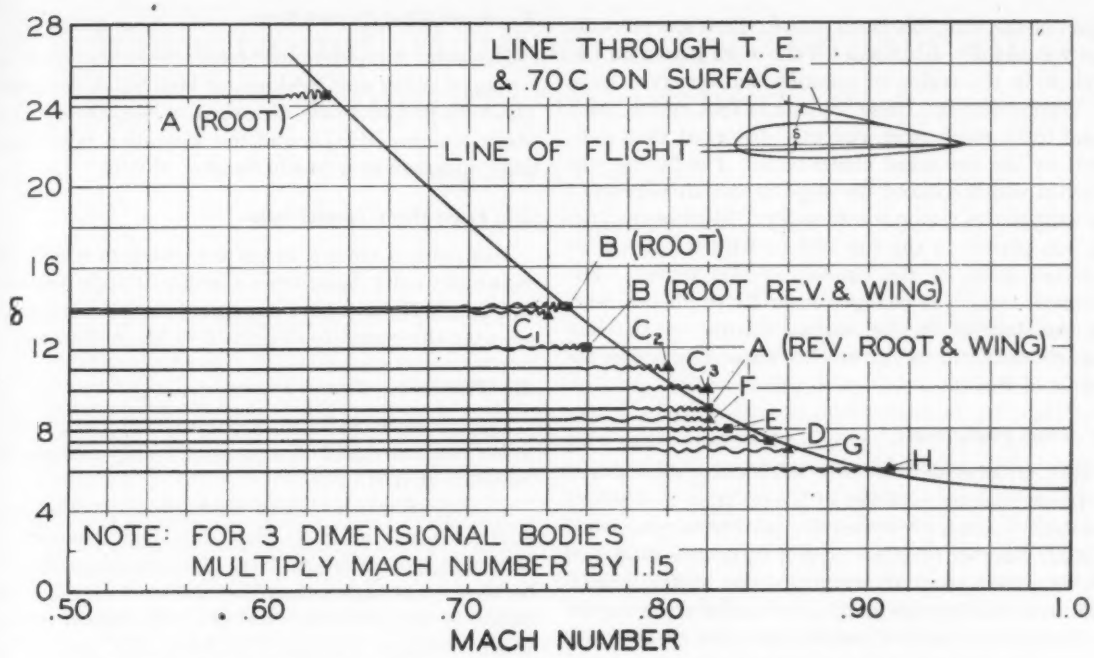

FIG. 3. Transonic separation criterion—angle of airfoil surface to line of flight versus Mach Number.

to lay out the airplane to avoid transonic separation. Such a rough tool is indicated by the above rudimentary considerations.

PROPOSED DESIGN PARAMETER

The single design parameter that offers the best index of the adverse pressure gradient existing on a body in potential flow is the slope of the surfaces aft of the position of maximum thickness. For a given type of body, this afterbody angle can also serve as an index of the body's critical Mach Number. Because of this interrelation, a design parameter identified as the angle between the surface of the aft portion of a body and the line of flight is suggested.

The relation between the suggested design parameter and boundary-layer conditions at high Mach numbers is illustrated by the pressure distribution diagrams presented in Figs. 1 and 2. Fig. 1 presents the variation of surface pressure coefficient with Mach Number and chordwise position for the 66,2-215 ($a = 0.6$) airfoil which has an afterbody angle at zero lift (θ) of 10.7° as measured on the upper surface between the 70 per cent chord point and the trailing edge. Referring to the figure, it is found that the upper surface pressures over the aft 30 per cent of the chord are essentially constant up to and including a Mach Number of 0.752. At $M = 0.779$ and above, drastic changes in the pressure distribution over the afterbody occur which are not explained by potential flow theory and, hence, can be attributed to boundary-layer conditions. Therefore, the possibility of considerable turbulence of the airflow over the upper surface and airflow separation at these Mach Numbers is indicated. The experimental critical Mach Number for the airfoil at this angle of attack is $M = 0.67$.

Fig. 2 presents similar data for the 0015 airfoil where $\theta = 8.8°$. For this airfoil, the upper surface pressures over the aft 30 per cent of the chord are essentially constant up to and including $M = 0.805$. At $M = 0.837$ the aft pressures undergo a considerable change. The critical Mach Number for this condition is $M = 0.70$.

Buffeting and airflow separation is related to these pressure distribution changes as will be shown by a correlation with the angle θ of the Mach Number for airflow separation as determined from flight and wind-tunnel test data.

FLIGHT AND WIND-TUNNEL EXPERIENCE WITH TRANSONIC SEPARATION

Various examples of transonic separation have been accumulated and the data correlated in Fig. 3. The phenomena, as observed on several airplanes in flight and some wind-tunnel models, are discussed below.

(A) *From Flight Tests*

This airplane has a local section which had a rather high thickness ratio and the aft portion of the wing was steep. At a Mach Number of 0.63 the airplane experienced severe buffeting, which restricted the pilot from going to a higher Mach Number. Examination of low-speed wind-tunnel data showed that, in the

region of the wing described above, there was one tuft that was slightly disturbed. Tufts were placed on the airplane in the region in question and observed from an accompanying "hase" plane. The region was found to be much more violently disturbed than indicated by the low-speed model tests. The fairing was installed which reduced the slope of the aft portion of the wing in this region considerably. Most of the fairing was placed on the top surface with the intent to take out some of the camber in this region. The thickness ratio was changed from 22 to 20 per cent, but the slope of the top surface relative to the wing was reduced from $24^1/_2°$ to 9°. These two points are located in Fig. 3.

(*B*) *From Flight Tests*

This airplane, with a fairly thick wing, experienced air-frame shaking, changes in lateral trim, and rolling instability, which prevented the pilot from going over a Mach Number of 0.75. Again, tufts were placed on the wing to discover the critical region of flow separation, and a fairing was installed to improve this region. In this case it was not possible to make an extensive change without rebuilding the wing, and only a slight gain was realized as indicated on Fig. 3.

(*C*) *From Flight and Wind-Tunnel Tests*

This airplane began to experience buffeting at a Mach Number of 0.70, and the pilot was not able to go beyond a Mach Number of 0.75. Tests were made in the wind tunnel to determine the critical region, and two modifications were made. The first consisted of extending the chord in the critical region, reducing the thickness ratio, and reducing the trailing edge angle from 21° to 15°. Another modification consisted of adding a fairing mostly to the top surface of the wing, giving the section a reflex. This modification also reduced the thickness ratio somewhat and reduced the trailing-edge angle from 21° to 20°. This point is marked C-3. These two modifications show remarkable agreement with the curve as drawn in Fig. 3. If these data were to be correlated on a thickness ratio basis or based on the total trailing-edge angle, the gain in critical Mach Number would not be consistent.

(*D*) *From Flight Data*

This airplane was prevented from going to higher Mach Numbers because of buffeting reported by the pilot.

(*E*) *From Flight Data*

This airplane encountered buffeting, buzz, and general instability at this Mach Number. It has been flown to a higher Mach Number, but more serious difficulties have been encountered.

(*F*) *From Wind-Tunnel Data*

This point was determined from tuft studies made on a wing of 12 per cent thickness at high Mach Numbers. The tufts began to be disturbed at slightly above a Mach Number of 0.75, and the separation is substantially complete at a Mach Number of 0.82.

(*G*) *From Wind-Tunnel Data*

This point is from a 10 per cent wing in which tuft tests indicated a disturbance starting at approximately 0.80 Mach Number and increasing until separation is substantially complete at point 0.86 Mach Number.

(*H*) *From Wind-Tunnel Data*

Tuft studies indicate separation starting above Mach Number 0.85 and separation being substantially complete at 0.91.

A study of tuft action on wind-tunnel models tested at high speeds indicates that the Mach Number for transonic separation on three-dimensional bodies will be 15 per cent higher than that shown in Fig. 3. This factor is in agreement with the theoretical critical Mach Number difference between two- and three-dimensional ellipsoids.

A comparison of the values of the separation Mach Numbers given in Fig. 3 with general data on the critical Mach Numbers of airfoils shows that transonic separation in general occurs at approximately $0.10M$ above the wing section critical Mach Number. This rough rule may be applied to predict separation Mach Numbers for wing-body intersections and tail junctures. Under certain conditions, however, the results may be slightly conservative, particularly for airfoils of the more conventional type where the position of maximum thickness is located well forward. For unfilleted junctures, using the assumption that the local velocities are additive, reasonable estimates of critical Mach Numbers can be obtained. When extensive filleting is used, low-speed wind-tunnel tests are necessary to determine the critical Mach Number and, hence, the approximate separation Mach Number.

Conclusion

It is concluded that for preliminary design purposes the afterbody angle of a lifting surface or body represents a satisfactory index of the Mach Number at which airflow separation and buffeting will occur.

For wing-body junctures and tail intersections it is suggested Mach Numbers be considered greater than the critical Mach Numbers by 0.10.

Reference

[1] Hood, M. J., and Allen, J. H., *The Problem of Longitudinal Stability and Control at High Mach Numbers*, N.A.C.A. Report No. TR767.

Variational Method in the Theory of Compressible Fluid*

CHI-TEH WANG†
New York University

SUMMARY

The variational principle in hydrodynamics was first studied by Hargreaves,[1] who has shown that, when the hydrodynamic equations are satisfied, the integrand in the variational principle is a linear function of the pressure. For steady, irrotational flows, Bateman[2,3] has shown that the integrand is the pressure only, which can be written as a function of the velocity potential ϕ. A direct method to obtain approximate solution in the case of subsonic flow of a compressible fluid can therefore be formulated following the Rayleigh-Ritz method instead of solving the original nonlinear differential equations. In applying this method to the case of a compressible fluid passing an arbitrary airfoil, however, there are two difficulties: first, since the fluid region is infinite, Bateman's integral is not directly applicable; second, it is not easy to assume the potential function satisfying the boundary conditions. The nonlinear problem of compressible flow passing an arbitrary airfoil has been formulated in this paper. It is proved that, by conformal transformation, the velocity potential can be set up to satisfy the boundary conditions in the general case, and, hence, the Rayleigh-Ritz method can be applied. It is also shown that, by using the Theory of Residues in the integration and a modified Crout[10] method in solving the resulting simultaneous equations, the computational labor can be materially reduced. Since the variational principle is valid for subsonic, sonic, and supersonic flows, the possibility of applying it to the study of mixed flow is indicated. A numerical example of the nonlinear problem of the compressible flow around a circular cylinder is carried out, and the results compare favorably with those found by the existing methods.

INTRODUCTION‡

IN THE THEORETICAL STUDY of subsonic flow of a compressible fluid, there are at least three different analytical methods for the approximate solutions of the complicated nonlinear differential equations. The methods are: the development of the velocity potential ϕ into power series in the Mach Number, the development of ϕ in powers of a thickness parameter, and the hodograph method. The method of developing ϕ into power series in the Mach Number is generally known as the Rayleigh-Janzen Method. Its modifications and extensions bear the name of Poggi, Imai and Aihara, and others. By this method solutions of first approximation have been carried out in the case of flow passing a circular cylinder, elliptic cylinder, Joukowsky airfoil, and a sphere. Second approximation solutions have been carried out in the case of a circular cylinder and a sphere; third approximation, in the case of a circular cylinder.[12] Computation beyond the third approximation is practically unmanageable. In the case of flow passing a given arbitrary airfoil, the method is so tedious that it is almost impossible to carry out the computation beyond the first approximation. Since the solution is expressed in terms of power series of Mach Number, obviously for high-speed airflow, the method does not give good approximate results.

The method of developing ϕ in powers of a thickness parameter gives the so-called Prandtl-Glauert rule as its first approximation. An iteration process for computing higher order approximations has been developed by Ackeret. Kaplan has carried out the calculations up to the third approximation in the case of flow past a bump. The computation proves to be laborious.

The hodograph method transforms the exact nonlinear equations of motion into exact linear equations, thus greatly simplifying the differential equations. However, in doing so, the boundary conditions are made more difficult to fulfill. The present-day application of the method is essentially based on two simplifying assumptions. First, γ, the ratio of specific heat at constant pressure to that at constant volume, is assumed to be -1. Second, in the application of the well-known rule of Kármán-Tsien, a distortion of the shape of the airfoil is assumed to be only slight and is disregarded. In explaining the assumption of $\gamma = -1$, the isentropic pressure-density relation is usually plotted with pressure and volume as the coordinate axes. In this case, the relation appears to be a straight line with $\gamma = -1$. However, if they are plotted with pressure and density as coordinate axes, the discrepancy is much more amplified—i.e., the isentropic curve and the curve with $\gamma = -1$ will have the second derivative in different signs (Fig. 4). On the other hand, the distortion of the airfoil shape can now be calculated by the recent methods developed by Lin[7] and Gelbart.[13] It can be shown that the distortion increases with the Mach Number and is actually large at large Mach Numbers. If an arbitrary airfoil is given, it is almost impossible to compute, by the hodograph method, the

Received February 17, 1948. Revised and received September 10, 1948.

* The author is indebted to Prof. Th. von Kármán, K. O. Friedrichs, and C. C. Lin for their many inspiring discussions. To Profs. R. von Mises and H. S. Tsien, the author is indebted for their valuable criticisms.

† Associate Professor of Aeronautical Engineering, Daniel Guggenheim School of Aeronautics, College of Engineering.

‡ For a more detailed discussion of the many methods mentioned, the reader may refer to reference 5.

flow past the same airfoil in the compressible plane at various Mach Numbers.

In view of these drawbacks of the existing methods, it does not seem to be useless to make a study of another method based on an entirely different approach—namely, the variational method. The variational method has the advantage of being a direct method—i.e., by means of which one may be able to calculate the compressible flow passing a *given* airfoil at different Mach Numbers. Computation can also be made to obtain a solution of higher accuracy without additional mathematical difficulty. In the variational method, instead of solving the nonlinear differential equations of motion, a variational integral is formulated and approximate solutions are calculated by the Rayleigh-Ritz procedure. Braun,[4] in his dissertation at Göttingen under Prandtl, used the variational principle to study a linearized problem, but unfortunately the method was erroneously carried out. The nonlinear problem of a compressible flow past a given arbitrary airfoil has been formulated in the present paper. A numerical example is carried out for the case of flow past a circular cylinder, and methods for simplifying the computational work are indicated. The results compare favorably with Taylor's[6] experimental results and the third approximation by the Rayleigh-Janzen method computed by Imai.[12] Since the variational integral is valid for subsonic, sonic, as well as supersonic flows so long as the flow is irrotational, it is believed that the method can be used to investigate the mixed subsonic and supersonic flows before the appearance of a compression shock. This case is now being studied, and the result will be reported in a subsequent paper.

The Variational Principle

It was first shown by Hargreaves[1] that, when the hydrodynamical equations are satisfied, the integrand in the variational principle is a linear function of the pressure. A variational principle for an inviscid compressible fluid was derived by Bateman.[2] For steady, irrotational flows, Bateman has shown that the integrand is just the pressure, and he has further proved that the "pressure energy" is a maximum and the variational problem is regular when the velocity everywhere is below the local velocity of sound.

Bateman's work, in a simplified form, can be proved as follows. By denoting the velocity vector by $\vec{q}$, the Cartesian coordinates by x_1, x_2, x_3, and the corresponding velocity components by v_1, v_2, and v_3, the continuity equation for a steady flow is

$$\operatorname{div}(\rho\vec{q}) = 0$$

or

$$\sum_{i=1}^{3} (\partial/\partial x_i)(\rho v_i) = 0 \tag{1}$$

where ρ is the density. The condition of irrational flow is

$$\operatorname{rot}\vec{q} = 0$$

or

$$\left.\begin{aligned} (\partial v_3/\partial x_2) - (\partial v_2/\partial x_3) &= 0 \\ (\partial v_1/\partial x_3) - (\partial v_3/\partial x_1) &= 0 \\ (\partial v_2/\partial x_1) - (\partial v_1/\partial x_2) &= 0 \end{aligned}\right\} \tag{2}$$

With Eq. (2), the Euler equations of motion can be written as

$$(\rho/2)(\partial q^2/\partial x_i) = -\partial p/\partial x_i \quad (i = 1, 2, 3) \tag{3}$$

where $q^2 = v_1^2 + v_2^2 + v_3^2$ and p is the pressure. For ideal gases, the pressure-density relation is of the following form:

$$p = A + B\rho^{\gamma} \tag{4}$$

where A, B, and γ are constants. Eqs. (1), (2), (3), and (4) describe the steady irrotational motions of a compressible fluid. Bateman's problem is to prove that the first variation of the integral

$$\int_V p\, d\tau = \text{max.} \tag{5}$$

is equivalent to Eq. (1) when Eqs. (2), (3), and (4) are satisfied, where $d\tau$ is the elementary volumes of the fluid and the integration is to be extended to the whole volume of the fluid.

Eqs. (2) are satisfied if we introduce the velocity potential ϕ so that $v_i = \partial\phi/\partial x_i$. Since $dp/d\rho = a^2$, where a is the velocity of sound, Eq. (3) can be integrated to give

$$a^2 + [(\gamma - 1)/2]\, q^2 = a_0^2 + [(\gamma - 1)/2]\, q_0^2 \tag{6}$$

where the subscript 0 refers to the quantities at infinity. From Eq. (4), we have

$$dp/d\rho = B\gamma\rho^{\gamma-1} \tag{7}$$

Again noting $dp/d\rho = a^2$, we obtain, from Eq. (6),

$$B\gamma\rho^{\gamma-1} = a_0^2 + [(\gamma - 1)/2]\,(q_0^2 - q^2) \tag{8}$$

Combining Eqs. (4) and (8) gives

$$p = A + B^{-1/(\gamma-1)}\,\gamma^{-1/(\gamma-1)}\{a_0^2 + [(\gamma - 1)/2] \times (q_0^2 - q^2)\}^{\gamma/(\gamma-1)}$$

Since the constants are irrelevant to the variational problem, the variational integral (5) can be written as

$$\int \{a_0^2 + [(\gamma - 1)/2]\,(q_0^2 - q^2)\}^{\gamma/(\gamma-1)}\, d\tau = \text{max.} \tag{9}$$

To simplify the integral, write

$$q_m^2 = [2/(\gamma - 1)]a_0^2 + q_0^2$$

and the variational integral becomes

$$\int_V (q_m^2 - q^2)^{\gamma/(\gamma-1)}\, d\tau = \text{max.} \tag{10a}$$

or

$$\delta \int_V (q_m^2 - q^2)^{\gamma/(\gamma-1)}\, d\tau = 0 \tag{10b}$$

Since

$$q^2 = \sum_{j=1}^{3} (\partial\phi/\partial x_j)(\partial\phi/\partial x_j)$$

following the usual tensor notation that a repetition of the subscripts indicates the summation, Eq. (10b) can be written into the following form:

$$\delta \int_V [q_m{}^2 - (\partial\phi/\partial x_j)(\partial\phi/\partial x_j)]^{\gamma/(\gamma-1)}\, d\tau = 0 \quad (10c)$$

Carrying out the first variation and dropping out the constant, it is obtained that

$$\int_V [q_m{}^2 - (\partial\phi/\partial x_j)(\partial\phi/\partial x_j)]^{1/(\gamma-1)}(\partial\phi/\partial x_j)\delta \times (\partial\phi/\partial x_j)\, d\tau = 0 \quad (11)$$

Combining with Eq. (8) and neglecting the constant coefficient, Eq. (11) is then

$$\int_V \rho(\partial\phi/\partial x_j)(\partial/\partial x_j)(\delta\phi) d\tau = 0 \quad (12)$$

It is obvious that

$$\frac{\partial}{\partial x_j}\left(\rho\delta\phi\,\frac{\partial\phi}{\partial x_j}\right) = \rho\,\frac{\partial\phi}{\partial x_j}\,\frac{\partial}{\partial x_j}(\delta\phi) + \delta\phi\,\frac{\partial}{\partial x_j}\left(\rho\,\frac{\partial\phi}{\partial x_j}\right)$$

and, therefore, Eq. (12) can be written as

$$\int_V \left[\frac{\partial}{\partial x_j}\left(\rho\delta\phi\,\frac{\partial\phi}{\partial x_j}\right) - \delta\phi\,\frac{\partial}{\partial x_j}\left(\rho\,\frac{\partial\phi}{\partial x_j}\right)\right] d\tau = 0$$

or

$$\int_V \frac{\partial}{\partial x_j}\left(\rho\delta\phi\,\frac{\partial\phi}{\partial x_j}\right) d\tau - \int_V \delta\phi\,\frac{\partial}{\partial x_j}\left(\rho\,\frac{\partial\phi}{\partial x_j}\right) d\tau = 0 \quad (13)$$

Applying Gauss's theorem to the first integral, we have

$$\int_V \frac{\partial}{\partial x_j}\left(\rho\delta\phi\,\frac{\partial\phi}{\partial x_j}\right) d\tau = -\int_S \rho\delta\phi\,\frac{\partial\phi}{\partial n}\, dS \quad (14)$$

where $\partial\phi/\partial n$ is derivative in the inner normal direction and S is the surface that encloses the volume V, and the integration is taken over the surface S. With the relation (14) established, Eq. (13) becomes

$$-\int_S \rho\delta\phi\,\frac{\partial\phi}{\partial n}\, dS - \int_V \delta\phi\,\frac{\partial}{\partial x_j}\left(\rho\,\frac{\partial\phi}{\partial x_j}\right) d\tau = 0 \quad (15)$$

In fluid dynamics, the boundary conditions are of the following two types: (1) if the boundaries are stream surfaces, $\partial\phi/\partial n = 0$ on the boundary; (2) if the boundary is not a stream surface, the value of ϕ is prescribed and $\delta\phi = 0$. As a result, $\rho\delta\phi(\partial\phi/\partial n) = 0$ on the boundary, and, if the domain is finite, the first integral of Eq. (15) vanishes. Since V is arbitrary, the second integral then gives us the continuity equation

$$(\partial/\partial x_j)\,[\rho(\partial\phi/\partial x_j)] = 0$$

and it thus completes the proof. It is to be noted that the variational principle is valid no matter whether the flow is subsonic, sonic, or supersonic; however, the integral can be proved to be maximum only in the case of subsonic flow.

Approximate Solutions by Rayleigh-Ritz Method

A great advantage in transforming differential equations into variational integral is that one can then use the Rayleigh-Ritz Method to obtain expressions closely approximating the solution of the boundary value problem. The Rayleigh-Ritz Method consists, essentially, of choosing a sequence of functions that all satisfy the boundary conditions but with undetermined constants, such as $a_i, b_i, c_i \ldots$ and $i = 1, 2, \ldots, N$ in the functions. Let I be the variational integral. Then, by substituting these functions into I and setting the first variation of I to be zero, we obtain a set of simultaneous algebraic equations as follows:

$$\frac{\partial I}{\partial a_i} = 0; \quad \frac{\partial I}{\partial b_i} = 0; \quad \frac{\partial I}{\partial c_i} = 0; \quad \ldots \text{etc.} \qquad (i = 1, 2, \ldots, N)$$

Solving these simultaneous equations, the constants can thus be determined.

If the sequence of functions chosen is complete and the integral has a minimum or maximum, it can be proved that the solution so obtained is a minimizing or maximizing sequence to the original variational problem. An enumerable sequence of functions contained in the class $\mathcal{R}$ is said to be complete if every function in R can be approximated by a finite linear combination of the functions with preassigned accuracy. Although the method was originally applied by Ritz to a linear problem, the proof is also valid for nonlinear problems.

The Rayleigh-Ritz Method has been widely used in the field of Theory of Elasticity because the boundary conditions in these cases are relatively simple and functions that satisfy these conditions are not too difficult to choose. In fluid dynamics, the situation is different; the boundary conditions—e.g., flow around an arbitrary airfoil—are difficult to prescribe in simple analytical form. This is perhaps one of the reasons why the variational method has not been used very much in fluid dynamics. It will be shown in this paper that such difficulty can be overcome by using the idea of conformal mapping.

The Variational Integral in Infinite Domain

In applying the variational integral (5) to the case where the fluid extends to infinity, two difficulties arise. First, the integral becomes infinity, and it may be argued that a maximum or minimum is meaningless in this case. Secondly, the integral (14) may not be zero, although the integrand may approach zero at infinity, since S now is an infinite surface. Let us begin with the first difficulty. In the case of incompressible flow, it can be easily seen that Bateman's variational principle is equivalent to Kelvin's well-known theorem by minimizing the kinetic energy. In applying Kelvin's theorem to the infinite domain, it is a usual practice[6] to

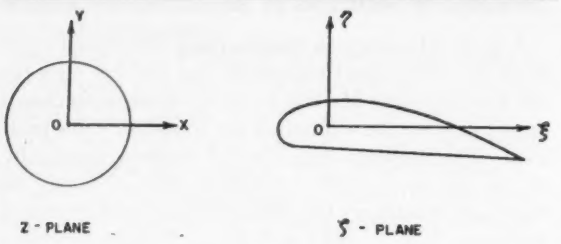

FIG. 1.

find the velocity potential of a corresponding flow that is at rest at infinity, and the actual velocity potential of the fluid is the sum of the velocity potential so obtained and that due to the uniform motion. In such a way, the variational integral becomes finite. This method, however, cannot be applied to the compressible flow, since the principle of superposition is now no longer applicable.

It can be noted that the addition or subtraction of an invariant function—i.e., a function whose variation is zero—is irrelevant to the variational principle. In other words, after carrying out the integration of the integral (5), all terms that do not contain the undermined constants may be subtracted from the integral without affecting the variational principle. The resulting integral may then be finite. In the subsonic flow, it is convenient, as will be shown later, to assume the velocity potential as consisting of two parts, ϕ_1 and ϕ_2, ϕ_1 being the velocity potential of the corresponding incompressible flow and ϕ_2 the correction part due to the compressibility effect. The terms in $p(\phi)$ which do not contain the undetermined constants are equal to $p(\phi_1)$, since ϕ_1 is a definite function,

$$\delta \int_V p(\phi_1)\, d\tau = 0$$

and the variational integral (5) can be replaced by

$$\int_V [p(\phi) - p(\phi_1)] d\tau = \max. \qquad (16)$$

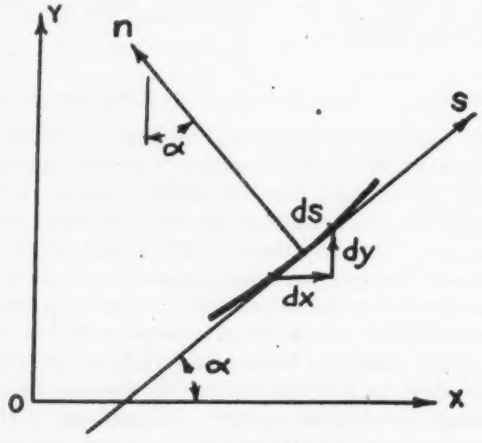

FIG. 2.

With ϕ_1 and ϕ_2 as assumed in the next section, the variational integral (16) is actually finite, provided that the integration is first carried out with respect to θ. This latter restriction is due to the fact that the integral is improper, and one may arbitrarily choose the order of integration in such cases.

So far as the second difficulty is concerned, let us again take the case with ϕ_1 and ϕ_2 as assumed in the next section. Without dropping the constants, the first variation of Eq. (16) is equal to the expression (15) multiplied by $-\left[\frac{2\gamma}{(\gamma-1)}\right]^{\gamma/(\gamma-1)}$. We have then

$$\rho = \left(\frac{\gamma-1}{2\gamma}\right)^{1/(\gamma-1)} \left[q_m^2 - \left(\frac{\partial\phi}{\partial r}\right)^2 - \left(\frac{1}{r}\frac{\partial\phi}{\partial\theta}\right)^2\right]^{1/(\gamma-1)}$$

$$= \left(\frac{\gamma-1}{2\gamma}\right)^{1/(\gamma-1)} \left[q_m^2 - U^2 + 0\left(\frac{1}{r^2}\right)\right]^{1/(\gamma-1)}$$

$$\delta\phi = \frac{1}{r}\sum_{n=1}^{N} (\delta A_{1n} \cos n\theta + \delta B_{1n} \sin n\theta) + 0\left(\frac{1}{r^2}\right)$$

In treating the problem where the fluid extends to infinity, we may first consider the fluid enclosed in a circular boundary and then extend the boundary to infinity. We therefore have:

$$\frac{\partial\phi}{\partial n} = -\frac{\partial\phi}{\partial r} = -U\cos\theta + 0\left(\frac{1}{r^2}\right)$$

where $0(1/r^2)$ represents terms of the order $1/r^2$ or higher. Substituting into the integral (14), taking $\gamma = 2$, and integrating, we have

$$\left(\frac{2\gamma}{\gamma-1}\right)^{\gamma/(\gamma-1)} \int_{\theta=0}^{\theta=2\pi} \rho\delta\phi \frac{\partial\phi}{\partial n} r\, d\theta \Big]_{r=\infty} =$$

$$-4(q_m^2 - U^2) U\pi\delta A_{11} \qquad (17)$$

Similar results can be obtained by taking $\gamma = 1.5$ and 1.33; the significances of taking γ to be these values will be discussed later. It is obvious that the expression (17) is not zero unless A_{11} is a known constant. But there is no reason why, in the general case of fluid dynamics, one should expect A_{11} to be any given value. If integral (14) is not zero, then the first variation of Eq. (16) is not equivalent to the original differential Eq. (1). It is clear that Bateman's principle must be modified when it is applied to the fluid extending to infinite region. The necessary modification can be obtained by subtracting from the integral (16) a term that is equal to Eq. (17), if ϕ_1 and ϕ_2 are so assumed. Then the final corrected variational integral in this case is as follows:

$$I = \int_S [p(\phi) - p(\phi_1)] dS + 4(q_m^2 - U^2) U\pi A_{11} =$$

$$\text{maximum} \qquad (18)$$

Note that the first variation of Eq. (18) is now exactly equivalent to the differential Eq. (1). If ϕ_1 and ϕ_2 are assumed in other forms, similar terms can be worked out and should be subtracted from Eq. (16).

Braun, in his analysis of the linearized problem of compressible flow passing a circular cylinder, used Bateman's integral without such corrections. His results are therefore erroneous. However, because of the mistake that he made subsequently in his calculations, his final results turned out to be reasonable. The present writer has checked Braun's work and found that the coefficient A_{11} is a large value with an opposite sign as given by Braun if using Bateman's original integral. The results do not check at all with those found by Taylor and Imai.

Compressible Flow Passing a Circular Cylinder

The boundary conditions for the two-dimensional potential flow about a body of arbitrary shape, in terms of polar coordinates, are as follows: (1) At $r = \infty$, $q = U$ or $\partial\phi/\partial r = U\cos\theta$ and $(1/r)(\partial\phi/\partial\theta) = -U\sin\theta$; (2) on the surface of the body, $\partial\phi/\partial n = 0$, where n is the normal. To satisfy the boundary conditions, it is convenient to consider ϕ as consisting of two parts, ϕ_1 and ϕ_2, where ϕ_1 satisfies the above-mentioned conditions (1) and (2) and ϕ_2 satisfies the condition (2) but at $r = \infty$, $\partial\phi_2/\partial r = (1/r)(\partial\phi_2/\partial\theta) = 0$. It is obvious that $\phi = \phi_1 + \phi_2$ satisfies the given boundary conditions.

Let us consider first the case of a compressible flow passing a circular cylindrical body. We can assume ϕ_1 and ϕ_2 as follows:

$$\phi_1 = U[r + (b^2/r)]\cos\theta - (\kappa/2\pi)\theta \tag{19}$$

$$\phi_2 = \sum_{m=1}^{M}\sum_{n=1}^{N}[A_{mn}R_m(r)\cos n\theta + B_{mn}R_m(r)\sin n\theta] \tag{20}$$

where

$$R_m(r) = (b^{m+1}/mr^m) - [b^{m+3}/(m+2)r^{m+2}]$$

in which b is the radius of the circular cylinder and κ is the strength of circulation, A_{mn} and B_{mn} are undetermined constants. The boundary conditions are seen to be satisfied.

Two-Dimensional Compressible Flow Passing a Body of Arbitrary Shape*

For cylindrical bodies of arbitrary shapes, the circle can be mapped into any desirable shape by conformal mapping. If the mapping is conformal, even though the function ϕ is not harmonic, it can be proved that the boundary conditions are preserved—i.e.,

$$\partial\phi/\partial r = U\cos\theta$$

and

$$(1/r)(\partial\phi/\partial\theta) = U\sin\theta, \qquad \text{at } r = \infty$$

and $\partial\phi/\partial n = 0$ on the surface of the body.

* The author is indebted to Professor Lin who helped in formulating this section.

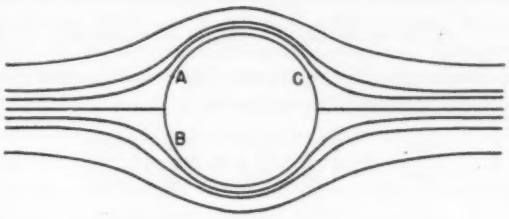

Fig. 3.

The proof can be established as follows: Referring to Fig. 1, let $x = x(\xi, \eta)$ and $y = y(\xi, \eta)$. Then

$$\frac{\partial\phi}{\partial n} = \left(\frac{\partial\phi}{\partial x}\right)\left(\frac{\partial x}{\partial n}\right) + \left(\frac{\partial\phi}{\partial y}\right)\left(\frac{\partial y}{\partial n}\right) \tag{21}$$

$$\frac{\partial\phi}{\partial n'} = \left(\frac{\partial\phi}{\partial\xi}\right)\left(\frac{\partial\xi}{\partial n'}\right) + \left(\frac{\partial\phi}{\partial\eta}\right)\left(\frac{\partial\eta}{\partial n'}\right) \tag{22}$$

where n is the normal in the z-plane and n' is the normal in the ζ-plane. Let s be the direction of tangent in z-plane and σ be the direction of tangent in ζ-plane.

From Fig. 2, it is seen that

$$dx = ds\cos\alpha$$

$$dx/ds = \cos\alpha$$

also

$$dy = dn\cos\alpha$$

$$dy/dn = \cos\alpha$$

Therefore,

$$dx/ds = dy/dn \tag{23a}$$

Similarly,

$$\frac{dy}{ds} = \sin\alpha, \qquad \frac{dx}{dn} = -\sin\alpha, \qquad \frac{dy}{ds} = -\frac{dx}{dn} \tag{23b}$$

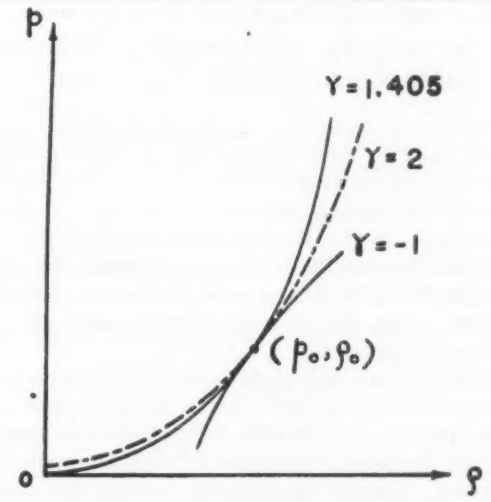

Fig. 4.

In the ζ-plane, we can establish the relations

$$d\xi/d\sigma = d\eta/dn', \qquad d\eta/d\sigma = -d\xi/dn' \tag{24}$$

Substituting the relations (23a), (23b), and (24) into Eqs. (21) and (22), we obtain

$$\frac{\partial\phi}{\partial n} = -\left(\frac{\partial\phi}{\partial x}\right)\left(\frac{\partial y}{\partial s}\right) + \left(\frac{\partial\phi}{\partial y}\right)\left(\frac{\partial x}{\partial s}\right) \tag{25}$$

$$\frac{\partial\phi}{\partial n'} = -\left(\frac{\partial\phi}{\partial\xi}\right)\left(\frac{\partial\eta}{\partial\sigma}\right) + \left(\frac{\partial\phi}{\partial\eta}\right)\left(\frac{\partial\xi}{\partial\sigma}\right) \tag{26}$$

Since

$$\frac{\partial\phi}{\partial x} = \left(\frac{\partial\phi}{\partial\xi}\right)\left(\frac{\partial\xi}{\partial x}\right) + \left(\frac{\partial\varphi}{\partial\eta}\right)\left(\frac{\partial\eta}{\partial x}\right) \tag{27}$$

$$\frac{\partial\phi}{\partial y} = \left(\frac{\partial\phi}{\partial\xi}\right)\left(\frac{\partial\xi}{\partial y}\right) + \left(\frac{\partial\phi}{\partial\eta}\right)\left(\frac{\partial\eta}{\partial y}\right) \tag{28}$$

by combining Eqs. (27) and (28) with Eq. (25), we have,

$$\frac{\partial\phi}{\partial n} = \frac{\partial\phi}{\partial\xi}\left(-\frac{\partial y}{\partial s}\frac{\partial\xi}{\partial x} + \frac{\partial x}{\partial s}\frac{\partial\xi}{\partial y}\right) + \frac{\partial\phi}{\partial\eta}\left(-\frac{\partial y}{\partial s}\frac{\partial\eta}{\partial x} + \frac{\partial\eta}{\partial y}\frac{\partial x}{\partial s}\right) \tag{29}$$

If the mapping is conformal, (x, y) and (ξ, η) must satisfy the following Cauchy-Riemann conditions.

$$\partial\xi/\partial x = \partial\eta/\partial y, \qquad \partial\eta/\partial x = -\partial\xi/\partial y \tag{30}$$

Substituting Eqs. (30) into Eq. (29) and noting that

$$\frac{\partial\eta}{\partial s} = \left(\frac{\partial\eta}{\partial y}\right)\left(\frac{\partial y}{\partial s}\right) + \left(\frac{\partial\eta}{\partial x}\right)\left(\frac{\partial x}{\partial s}\right) \tag{31}$$

$$\frac{\partial\xi}{\partial s} = \left(\frac{\partial\xi}{\partial x}\right)\left(\frac{\partial x}{\partial s}\right) + \left(\frac{\partial\xi}{\partial y}\right)\left(\frac{\partial y}{\partial s}\right) \tag{32}$$

it is obtained

$$\frac{\partial\phi}{\partial n} = -\left(\frac{\partial\phi}{\partial\xi}\right)\left(\frac{\partial\eta}{\partial s}\right) + \left(\frac{\partial\phi}{\partial\eta}\right)\left(\frac{\partial\xi}{\partial s}\right) = -\left(\frac{\partial\phi}{\partial\xi}\right)\left(\frac{\partial\eta}{\partial\sigma}\right)\left(\frac{d\sigma}{ds}\right) + \left(\frac{\partial\phi}{\partial\eta}\right)\left(\frac{\partial\xi}{\partial\sigma}\right)\left(\frac{d\sigma}{ds}\right) = \left(\frac{\partial\phi}{\partial n'}\right)\left(\frac{d\sigma}{ds}\right)$$

The differential quotient $d\sigma/ds$ in the above relation is in the form of total differentials because, for any mapping, σ is a function of s only.

Denote the mapping function by $\zeta = f(z)$. Then we have $d\sigma/ds = f'(z)$. For conformal mappings, $f'(z) \neq 0$. Therefore, if $\partial\phi/\partial n$ in the z-plane is zero along the circle, $\partial\phi/\partial n'$ in the ζ-plane must also be zero along the arbitrary shape that is mapped from z-plane by the conformal mapping.

We have shown that, if the assumed potential ϕ for a compressible flow around a circle in the z-plane can be mapped conformally onto the ζ-plane, even though ϕ is not harmonic, the boundary conditions are still preserved. Thus, if the mapping function that transforms a circle into an airfoil in an incompressible flow is known, the expression for ϕ satisfying the boundary conditions in compressible flow around the same airfoil can be easily assumed.

With ϕ thus assumed, we can substitute the expression into the variational integral, differentiate the integral with respect to the unknown constants, and set the final expression equal to zero. Thus, we have as many equations as unknown constants, and these constants can be determined by solving the equations simultaneously.

In the actual computation, however, instead of substituting the mapping function into ϕ directly, some simplification can be worked out. Let the velocity and potential function in z-plane and ζ-plane be denoted by $q(z)$, $\phi(z)$, and $q(\zeta)$, $\phi(\zeta)$, respectively. Then, according to the Theory of Complex Variables,

$$q(\zeta)^2 = \left[\frac{\partial\phi(\zeta)}{\partial\xi}\right]^2 + \left[\frac{\partial\phi(\zeta)}{\partial\eta}\right]^2 = \left\{\left[\frac{\partial\phi(z)}{\partial x}\right]^2 + \left[\frac{\partial\phi(z)}{\partial y}\right]^2\right\}\left\{\left[\frac{\partial x}{\partial\xi}\right]^2 + \left[\frac{\partial x}{\partial\eta}\right]^2\right\} = q(z)^2\left|\frac{dz}{d\zeta}\right|^2$$

If we denote the polar coordinates in the z-plane as r and θ and those in the ζ-plane as R and Θ, we have

$$\iint_{\zeta\text{-plane}} [q_m{}^2 - q(\zeta)^2]^{\gamma/(\gamma-1)}\, R\, dR\, d\Theta = \iint_{z\text{-plane}}\left[q_m{}^2 - \left[\frac{q(z)^2}{|d\zeta/dz|^2}\right]^{\gamma/(\gamma-1)}\left|\frac{d\zeta}{dz}\right|^2 r\, dr\, d\theta \tag{33}$$

where

$$q(z)^2 = \left[\frac{\partial\phi(z)}{\partial x}\right]^2 + \left[\frac{\partial\phi(z)}{\partial y}\right]^2$$

Application to the Mixed Flow Problems

In establishing Ritz's proof, the integral must have either a maximum or minimum, and it has long been regarded that the Rayleigh-Ritz Method cannot be applied if the boundary value problem does not lead to an equivalent extremum problem. However, Courant and Friedrichs[9] have recently pointed out that the Rayleigh-Ritz Method can still be applied in such a case. The mathematical significance in this case lies in the fact that we are seeking to satisfy the differential equation, as well as the boundary condition, not completely but in the mean.

Therefore, even though the variational integral (5) does not have an extreme value when the flow is not entirely subsonic, as long as the flow is irrotational or before the occurrence of a compression shock, a good approximation can be obtained by means of the variational method if there exists a solution in the mixed flow region at all.

Numerical Example

To illustrate the method, a numerical example has been carried out for the case of a compressible flow

passing a circular cylinder with unit radius without circulation. Referring to Fig. 3, since there is no circulation, the flow must be symmetrical with respect to θ or the horizontal axis, and, therefore, $B_{mn} = 0$. The horizontal velocity components must also be equal at points symmetrically situated with respect to the vertical, as well as the horizontal, axes such as points A, B, C. As a result A_{mn} must be zero when m, n are even integers.

The potential function φ can now be written as follows:

$$\phi = U\left(r + \frac{1}{r}\right)\cos\theta + A_{11}\left(\frac{1}{r} - \frac{1}{3r^3}\right)\cos\theta + A_{13}\left(\frac{1}{r} - \frac{1}{3r^3}\right)\cos 3\theta + A_{31}\left(\frac{1}{3r^3} - \frac{1}{5r^5}\right)\cos\theta + A_{33}\left(\frac{1}{3r^3} - \frac{1}{5r^5}\right)\cos 3\theta + A_{15}\left(\frac{1}{r} - \frac{1}{3r^3}\right)\cos 5\theta + A_{51}\left(\frac{1}{5r^5} - \frac{1}{7r^7}\right)\cos\theta \quad (34)$$

The variational integral in polar coordinates for two-dimensional flow is as follows:

$$\delta\left\{\int_{r=1}^{r=\infty}\int_{\theta=0}^{\theta=2\pi}\left[q_m^2 - \left(\frac{\partial\phi}{\partial r}\right)^2 - \left(\frac{1}{r}\frac{\partial\phi}{\partial\theta}\right)^2\right]^{\gamma/(\gamma-1)} \times r\,dr\,d\theta + 4(q_m^2 - U^2)U\pi A_{11}\right\} = 0 \quad (35)$$

The integral can be integrated analytically when $\gamma/(\gamma-1)$ is an integer. For different values of $\gamma/(\gamma-1)$, the corresponding values of γ are as follows:

$\gamma/(\gamma-1)$	γ
$1/2$	-1
2	2
3	1.5
4	1.333

The value of γ for air is 1.405, which is between the values of 1.5 and 1.333. If the calculation is carried out at $\gamma = 1.333$, a good approximate solution can be obtained. In the hodograph method used by Chaplygin and von Kármán-Tsien, the value of γ is taken to be equal to -1. The variational integral in this case then becomes the familiar problem of determining the minimum surface in the Calculus of Variations. As pointed out by von Kármán and Tsien, the velocity in the flow field would not differ too much from the undisturbed velocity in the infinity—i.e., only a small portion of the p vs. ρ curve will be used. If one makes the curve with $\gamma = -1$ tangent to the curve with $\gamma = 1.405$ at the point that represents the conditions at infinity and uses the curve with $\gamma = -1$, the error probably would not be too great. In our case, we may follow the same method and use $\gamma = 2$. The advantage of using $\gamma = 2$ instead of $\gamma = -1$ can be easily seen in Fig. 4. Although the curve with $\gamma = -1$ and $\gamma = 1.405$ may be made tangent to each other at (p_0, ρ_0), their second derivatives have opposite signs. Whereas by making the curves with $\gamma = 2$ and $\gamma = 1.405$ tangent to each other at (p_0, ρ_0), there are small portions of the curves more or less close together, and therefore the curve $\gamma = 2$ provides a much better approximation. By using $\gamma = 3$ or $\gamma = 4$, a still better approximation can be obtained; however, the amount of labor in carrying out the integration and solving the simultaneous equations would also be materially increased.

Substituting ϕ as given by Eq. (34) into Eq. (35) taking four constants A_{31}, A_{51}, A_{33}, A_{53}, and differentiating the resulting integral with respect to the constants, we have

$$\left.\begin{aligned} \partial I/\partial A_{11} = 0, \quad \partial I/\partial A_{13} = 0, \quad \partial I/\partial A_{31} = 0 \\ \partial I/\partial A_{33} = 0, \quad \partial I/\partial A_{15} = 0, \quad \partial I/\partial A_{51} = 0 \end{aligned}\right\} \quad (36)$$

Integrating these equations, we obtain, finally,*

$$\left.\begin{aligned}
&(2.07407q_m^2 - 7.31852U^2)A_{11} + 7.06667U^2A_{13} + (0.325926q_m^2 - 1.03704U^2)A_{31} + 0.915555U^2A_{33} + (0.144286q_m^2 - 0.340136U^2)A_{51} = K_1 \\
&7.06667U^2A_{11} + (13.3333q_m^2 - 44.2667U^2)A_{13} + 1.20000U^2A_{31} + (1.60000q_m^2 - 5.97334U^2)A_{33} + 32.4444U^2A_{15} + 0.440816U^2A_{51} = K_2 \\
&(0.325926q_m^2 - 1.03704U^2)A_{11} + 1.20000U^2A_{13} + (0.0900741q_m^2 - 0.207407U^2)A_{31} + 0.192254U^2A_{33} + (0.0411428q_m^2 - 0.0810885U^2)A_{51} = K_3 \\
&0.915555U^2A_{11} + (1.60000q_m^2 - 5.97334U^2)A_{13} + 0.192254U^2A_{31} + (0.277333q_m^2 - 1.01181U^2)A_{33} + 4.92444U^2A_{15} + 0.0813062U^2A_{51} = K_4 \\
&32.4444U^2A_{13} + 4.92444U^2A_{33} + (35.4444q_m^2 - 120.948U^2)A_{15} = K_5 \\
&(0.114286q_m^2 - 0.340136U^2)A_{11} + 0.440816U^2A_{13} + (0.0411428q_m^2 - 0.0810885U^2)A_{31} + 0.0813062U^2A_{33} + (0.0218309q_m^2 - 0.0360739U^2)A_{51} = K_6
\end{aligned}\right\}$$

where $K_1, K_2, K_3, K_4, K_5, K_6$ are sums of nonlinear terms in A_{11}, A_{13}, A_{31}, A_{33}, A_{15}, and A_{51} and their complete expressions are given in Appendix I. Denote $A_{ij}' = A_{ij}/a_0$ and $K_i' = K_i/a_0^3$, for $M = 0.4$, we have

$$\left.\begin{aligned}
&3.30904A_{11}' + 1.13067A_{13}' + 0.538074A_{31}' + 0.146489A_{33}' + (0)A_{15}' + 0.192435A_{51}' = K_1' \\
&1.13067A_{11}' + 21.7173A_{13}' + 0.192000A_{31}' + 2.50027A_{33}' + 5.19111A_{15}' + 0.0705306A_{51}' = K_2' \\
&0.538074A_{11}' + 0.192000A_{13}' + 0.161375A_{31}' + 0.0307606A_{33}' + (0)A_{15}' + 0.0758944A_{51}' = K_3' \\
&0.146489A_{11}' + 2.50027A_{13}' + 0.0307606A_{31}' + 0.437150A_{33}' + 0.787911A_{15}' + 0.0130090A_{51}' = K_4' \\
&(0)A_{11}' + 5.19111A_{13}' + (0)A_{31}' + 0.787911A_{33}' + 58.0883A_{15}' + (0)A_{51}' = K_5'
\end{aligned}\right\} \quad (37)$$

* The numerical example was carried out by Messrs. Harry H. Hilton and G. V. R. Rao.

TABLE 1
Velocity Distribution at $\theta = \pi/2$ from Various Methods

r/b \ q/U	Variational Method: One term	Two terms	Three terms	Four terms	Five terms	Six terms	Rayleigh-Janzen Method—3rd Approx. $\gamma = 2$	$\gamma = 1.4$	Taylor's Experimental Results, $\gamma = 1.407$
1.0	2.138	2.286	2.284	2.298	2.333	2.334	2.303	2.284	...
1.04	2.057	2.199	2.198	2.210	2.244	2.244	2.215	2.197	2.13
1.2	1.805	1.874	1.924	1.931	1.959	1.959	1.934	1.920	1.89
1.5	1.523	1.607	1.609	1.610	1.629	1.629	1.611	1.603	1.60
2.0	1.298	1.348	1.351	1.349	1.360	1.360	1.347	1.345	1.35
3.0	1.133	1.157	1.159	1.157	1.162	1.162	1.156	1.155	1.18

$$\left.\begin{aligned} 0.192435A_{11}' + 0.0705306A_{13}' + 0.0758944A_{31}' \\ + 0.0130090A_{33}' + (0)A_{15}' + \\ 0.0413830A_{51}' = K_6' \end{aligned}\right\} \quad (37\ cont.)$$

With Eqs. (37) so arranged, it is seen that the Crout method[10] for solving a system of linear simultaneous equations can be used, and the constants A_{ij}' may be written in terms of K_1', K_2', K_3', K_4', K_5' and K_6' as follows:

$$\left.\begin{aligned} A_{11}' &= 1.15571K_1' - 0.0185510K_2' - 9.60031K_3' + 0.0273402K_4' + 0.00128699K_5' + 12.2554K_6' \\ A_{13}' &= -0.0185512K_1' + 0.135726K_2' + 0.0111499K_3' - 0.770094K_4' - 0.00168374K_5' + 0.0765767K_6' \\ A_{31}' &= -9.60031K_1' + 0.0111473K_2' + 125.199K_3' - 0.155007K_4' + 0.00110634K_5' - 184.936K_6' \\ A_{33}' &= 0.0273412K_1' - 0.770094K_2' - 0.155021K_3' + 6.75435K_4' - 0.0227960K_5' - 0.653607K_6' \\ A_{15}' &= 0.00128700K_1' - 0.00168373K_2' + 0.00110620K_3' - 0.0227960K_4' + 0.0176748K_5' + 0.00202234K_6' \\ A_{51}' &= 12.2554K_1' + 0.0765810K_2' - 184.936K_3' - 0.653631K_4' + 0.00202211K_5' + 306.415K_6' \end{aligned}\right\} \quad (38)$$

where it may be mentioned again that K_1', K_2', K_3', K_4', K_5', K_6' contain nonlinear terms in A_{11}', A_{13}', A_{31}', A_{33}', A_{15}', and A_{51}'. To solve for these constants, a method of successive approximations may be used. First, assume the value of A's to be zero in the K's; then A_{11}', A_{13}', A_{31}', A_{33}', A_{15}' and A_{51}' can be obtained from Eq. (38). This is actually the solution for the linearized problem. Use the values of A's so determined to compute K's, and solve for these constants again. This then gives us a second approximation. Repeat the cycle until the desired accuracy is obtained. To make the convergence more rapid, after the third approximation, instead of following the method of successive approximation rigidly, one may extrapolate the results and use the values of A's so obtained to repeat the process.

For $M = 0.4$, Eqs. (38) are solved by the method of successive approximation and the constants, accurate to four significant figures after decimal point, have the following values:

$$A_{11}' = 0.1038, \quad A_{13}' = -0.02264 \quad A_{31}' = -0.06156$$

$$A_{33}' = -0.03727, \quad A_{15}' = 0.003156, \quad A_{51}' = 0.03036$$

and the potential function is, therefore, equal to

$$\frac{\phi}{a_0} = 0.4\left(r + \frac{1}{r}\right)\cos\theta + 0.1038\left(r + \frac{1}{r}\right)\cos\theta - 0.02264\left(r + \frac{1}{r}\right)\cos 3\theta - 0.06157\left(\frac{1}{3r^3} - \frac{1}{5r^5}\right)\cos\theta - 0.03727\left(\frac{1}{3r^3} - \frac{1}{5r^5}\right)\cos 3\theta - 0.003156 \times \left(r + \frac{1}{r}\right)\cos 5\theta + 0.03036\left(\frac{1}{5r^5} - \frac{1}{7r^7}\right)\cos\theta$$

To compare with Taylor's[6] experimental results and the third approximation of the Rayleigh-Janzen Method by Imai,[12] the velocities at $\theta = \pi/2$ are computed and are tabulated in Table 1. The velocity at $\theta = \pi/2$ can be computed from the following equation:

$$\frac{q}{U} = -\frac{1}{r}\frac{\partial}{\partial\theta}\left(\frac{\phi}{a_0 b}\right)\Big/M = \left(1 + \frac{1}{r^2}\right) + 3.8986\left(\frac{1}{3r^4} - \frac{1}{5r^6}\right) - 4.8998\left(\frac{1}{5r^6} - \frac{1}{7r^8}\right)$$

To get an idea of the convergence of the results, the velocities at these points are also computed by taking the series with only one term—i.e., term containing A_{11}—two terms—i.e., A_{11}, A_{13}—and so forth until six terms are taken. It is seen from the results that the convergence of the series is satisfactory. It may perhaps be mentioned that if only A_{11} is used, the first equation in the system of Eqs. (37), which is actually $\partial I/\partial A_{11} = 0$, must be used in solving for A_{11}. If two constants are to be used, say A_{11} and A_{13}, then the equations $\partial I/\partial A_{11} = 0$ and $\partial I/\partial A_{13} = 0$ must be used in solving for these constants. The values of A_{11} are different when they are obtained from different calculations.

The values of A's so computed are as follows:

(1) With term containing A_{11} only, we have $A_{11}' = 0.8307$. At $\theta = \pi/2$, the velocity is equal to

$$\frac{q}{U} = \left(1 + \frac{1}{r^2}\right) + 0.2077\left(\frac{1}{r^2} - \frac{1}{3r^4}\right)$$

(2) With terms containing A_{11} and A_{13}, we obtain $A_{11}' = 0.09430$ and $A_{13}' = -0.02580$. The velocity at $\theta = \pi/2$ is equal to

$$\frac{q}{U} = \left(1 + \frac{1}{r^2}\right) + 1.741\left(\frac{1}{r^2} - \frac{1}{3r^4}\right)$$

(3) With terms containing A_{11}, A_{13}, and A_{31}, we have $A_{11}' = 0.1026$, $A_{13}' = -0.02581$, and $A_{31}' = -0.04693$. The velocity at $\theta = \pi/2$ is equal to

$$\frac{q}{U} = \left(1 + \frac{1}{r^2}\right) + 0.4502\left(\frac{1}{r^2} - \frac{1}{3r^4}\right) - 0.1173\left(\frac{1}{3r^4} - \frac{1}{5r^6}\right)$$

(4) With terms containing only A_{11}, A_{13}, A_{31}, and A_{33}, we obtain $A_{11}' = 0.1018$, $A_{13}' = -0.02225$, $A_{31}' = -0.04381$, and $A_{33}' = -0.03156$. The velocity at $\theta = \pi/2$ then equals

$$\frac{q}{U} = \left(1 + \frac{1}{r^2}\right) + 0.4214\left(\frac{1}{r_2} - \frac{1}{3r^4}\right) + 0.1271\left(\frac{1}{3r^4} - \frac{1}{5r^6}\right)$$

(5) With terms containing only A_{11}, A_{13}, A_{31}, A_{33}, and A_{15}, we have $A_{11}' = 0.1025$, $A_{13}' = -0.02265$, $A_{31}' = -0.04297$, $A_{33}' = -0.03722$, and $A_{15}' = 0.0033155$. The velocity at $\theta = \pi/2$ is equal to

$$\frac{q}{U} = \left(1 + \frac{1}{r^2}\right) + 0.4654\left(\frac{1}{r^2} - \frac{1}{3r^4}\right) + 0.1717\left(\frac{1}{3r^4} - \frac{1}{5r^6}\right)$$

Discussion of the Accuracy of the Results

If one can take infinitely many terms of a complete set to represent ϕ, it can be proved that Ritz's procedure will give an exact solution. When finite number of terms are taken, the result is only approximate. Comparing our results with those of Imai (also by taking $\gamma = 2$), the variational method yields higher values of the velocity. However, it is to be seen (Table 2) that, in the Rayleigh-Janzen method, the values of the velocities increase with the increase of the number of approximations. This suggests that probably the results given by the third approximation in the Rayleigh-Janzen method are still too small in comparison with the exact values. In this respect, the higher values given by the present method is toward the correct side.

On the other hand, the magnitude of the velocities given by the present method also increases with the number of terms taken. This again indicates that our results are probably smaller than the exact values. The effect of using $\gamma = 2$ instead of $\gamma = 1.4$ is, however, to make the velocities larger. This can be seen from the results of Rayleigh-Janzen in using $\gamma = 2$ and $\gamma = 1.4$ as tabulated in Table 1. It seems to suggest that these two effects may compensate each other to some extent on the final results.

Table 2
Velocity Distribution at $\theta = \pi/2$ from Various Approximations of Rayleigh-Janzen Method ($M = 0.4$, $\gamma = 2.0$)

$\frac{r}{b}$ \ $\frac{q}{U}$	Zero Approx.	First Approx.	Second Approx.	Third Approx.
1.0	2.000	2.187	2.262	2.303
1.04	1.925	2.104	2.176	2.215
1.2	1.694	1.845	1.903	1.934
1.5	1.444	1.552	1.592	1.611
2.0	1.250	1.315	1.337	1.347
3.0	1.111	1.142	1.152	1.156

Notes on Computations

In carrying out the integration of Eq. (36), much labor required in the computation can be reduced by using the following simplifications: First, for the integration with respect to θ, the integral is of the type

$$\int_0^{2\pi} F(\cos\theta, \sin\theta)d\theta$$

where the integrand is a rational function of $\cos\theta$ and $\sin\theta$ finite on the range of integration. The integral can be evaluated by writing $e^{i\theta} = z$, where z is a complex variable. Since

$$\cos\theta = \frac{1}{2}(z + z^{-1}), \qquad \sin\theta = \frac{1}{2i}(z - z^{-1})$$

the integral takes the form $\int_C S(z)dz$, where $S(z)$ is a rational function of z finite on the path of integration C, the circle of radius unity whose center is the origin. By the Theorem of Residues,[11] the integral is equal to $2\pi i$ times the sum of the residues of $S(z)$ at those of its pole which are inside that circle. Because the integration of Eq. (36) involves many trigometric functions, much time can be saved and also confusion can be avoided by using this theorem.

In the integration with respect to r, the same integral may occur many times in different equations. It would be convenient to list all the different integrals on another sheet, and each integral is evaluated only once. Since the limits of integration are from $r = 1$ to $r = \infty$ and since the integrand consists of terms of the type $\int_1^\infty (dr/r^n)$, $n > 1$, which is simply $1/(n-1)$ after integration, the result can be written down without thinking.

References

[1] Hargreaves, R., *A Pressure-Integral as Kinetic Potential*, Phil. Mag., pp. 436–444, September, 1908.

[2] Bateman, H., *Notes on a Differential Equation Which Occurs in the Two-Dimensional Motion of a Compressible Fluid and the Associated Variational Problems*, Proc. Royal Society, London, A 125, pp. 598–618, November, 1929.

[3] Bateman, H., *Irrotational Motion of a Compressible Inviscid Fluid*, Proceedings of National Academy of Sciences, Vol. 16, No. 12, pp. 816–825, December, 1930.

[4] Braun, G., *Die ebene kompressible Potentialstromung als Variations- und Eigenwertproblem*, Ann. d. Phys., Vol. 15, No. 6, pp. 645–676, December, 1932.

[5] von Kármán, Th., *Compressibility Effects in Aerodynamics*, Journal of the Aeronautical Sciences, Vol. 8, No. 9, pp. 337–356, July, 1941.

[6] Taylor, G. I., and Sharman, C. F., *A Mechanical Method for Solving Problems of Flow in Compressible Fluids*, Proc. Royal Society, Series A, Vol. 121, p. 194, 1928.

[7] Lin, C. C., *On the Extension of the von Kármán-Tsien Method to Two-Dimensional Subsonic Flows with Circulation Around Closed Profiles*, Quart. Appl. Math., Vol. 4, No. 3, October, 1946.

[8] Lamb, H., *Hydrodynamics*, 6th Ed., pp. 56–57; Cambridge Univ. Press, 1932.

[9] Courant, R., and Friedrichs, K. O., *Methods of Mathematical Physics*, Institute of Math. and Mech., New York University, N.Y., Part II, p. 24, 1943.

[10] Crout, P. D., *A Short Method for Evaluating Determinants and Solving Systems of Linear Equations with Real or Complex Coefficients*, Transactions of the A.I.E.E., Vol. 60, 1941.

[11] Whittaker, E. T., and Watson, G. N., *A Course of Modern Analysis*, 4th ed., p. 112; Cambridge University Press, reprinted 1940.

[12] Imai, I., *On the Flow of a Compressible Fluid Past a Circular Cylinder, II*, Proc. of the Physico-Math. Society of Japan, Third Series, Vol. 23, No. 3, pp. 180–193, March, 1941.

[13] Gelbart, A., *On Subsonic Compressible Flows by a Method of Correspondence, I—Methods for Obtaining Subsonic Circulatory Compressible Flows about Two-dimensional Bodies*, N.A.C.A. T.N. No. 1170, 1947.

Appendix I

Expressions of K_1, K_2, K_3, K_4, K_5, K_6

$$K_1 = 8.22222U^3 + 1.64444UA_{11}^2 + 9.86667UA_{13}^2 + 0.0421164UA_{31}^2 + 0.275556UA_{33}^2 + 27.4074UA_{15}^2 + 0.00698418UA_{51}^2 - 3.7926UA_{11}A_{13} + 0.512169UA_{11}A_{31} - 0.633228UA_{11}A_{33} + 0.186243UA_{11}A_{51} - 0.580741UA_{13}A_{31} + 3.14921UA_{13}A_{33} - 18.4593UA_{13}A_{15} - 0.195374UA_{13}A_{51} - 0.119789UA_{31}A_{33} + 0.0331367UA_{31}A_{51} - 2.79450UA_{33}A_{15} - 0.0467426UA_{33}A_{51} - 0.412699A_{11}^2A_{13} + 0.118731A_{11}^2A_{31} + 0.0793648A_{11}^2A_{33} + 0.0466519A_{11}^2A_{51} + 3.24233A_{13}^2A_{11} + 0.602752A_{13}^2A_{31} + 7.72275A_{13}^2A_{15} + 0.235043A_{13}^2A_{51} + 0.0276543A_{31}^2A_{11} + 0.000211740A_{31}^2A_{13} - 0.000251150A_{31}^2A_{33} + 0.00380477A_{31}^2A_{51} + 0.0993296A_{33}^2A_{11} + 0.0206111A_{33}^2A_{31} + 0.225960A_{33}^2A_{15} + 0.00869874A_{33}^2A_{51} + 8.91429A_{15}^2A_{11} + 1.64995A_{15}^2A_{31} + 0.642938A_{15}^2A_{51} + 0.00574819A_{51}^2A_{11} + 0.00276237A_{51}^2A_{13} + 0.00197180A_{51}^2A_{31} + 0.000545640A_{51}^2A_{33} + 0.203175A_{11}^3 + 0.00261873A_{31}^3 + 0.000361590A_{51}^3 - 0.0948150A_{11}A_{13}A_{31} + 1.07768A_{11}A_{13}A_{33} - 4.52064A_{11}A_{13}A_{15} - 0.0228974A_{11}A_{13}A_{51} - 0.0218696A_{11}A_{31}A_{33} + 0.0242076A_{11}A_{31}A_{51} - 0.680635A_{11}A_{33}A_{15} - 0.00669122A_{11}A_{33}A_{51} + 0.210793A_{13}A_{31}A_{33} - 0.616721A_{13}A_{31}A_{15} + 0.00548246A_{13}A_{31}A_{51} + 2.63154A_{13}A_{33}A_{15} + 0.0853833A_{13}A_{33}A_{51} - 0.184894A_{13}A_{15}A_{51} - 0.0823982A_{31}A_{33}A_{15} + 0.000880140A_{31}A_{33}A_{51} - 0.0190871A_{33}A_{15}A_{51}$$

$$K_2 = -7.06667U^3 - 1.89630UA_{11}^2 - 0.0334396UA_{31}^2 + 0.00163270UA_{51}^2 + 19.7333UA_{11}A_{13} - 0.580741UA_{11}A_{31} + 3.14921UA_{11}A_{33} - 18.4593UA_{11}A_{15} - 0.195374UA_{11}A_{51} + 2.78857UA_{13}A_{31} + 50.8444UA_{13}A_{15} + 0.912108UA_{13}A_{51} + 0.481269UA_{31}A_{33} - 3.02138UA_{31}A_{15} - 0.0132427UA_{31}A_{51} + 7.63937UA_{33}A_{15} + 0.163629UA_{33}A_{51} - 1.07719UA_{15}A_{51} + 3.24233A_{11}^2A_{13} - 0.0474075A_{11}^2A_{31} + 0.538838A_{11}^2A_{33} - 2.26032A_{11}^2A_{15} - 0.0114487A_{11}^2A_{51} + 6.82287A_{13}^2A_{33} + 0.000211740A_{31}^2A_{11} + 0.143916A_{31}^2A_{13} + 0.0261427A_{31}^2A_{33} + 0.0203168A_{31}^2A_{15} + 0.00178155A_{31}^2A_{51} + 1.20889A_{33}^2A_{13} + 75.3439A_{15}^2A_{13} + 12.5681A_{15}^2A_{33} + 0.00276237A_{51}^2A_{11} + 0.0343677A_{51}^2A_{13} + 0.0115756A_{51}^2A_{31} + 0.00657200A_{51}^2A_{33} + 0.00883425A_{51}^2A_{15} - 0.137566A_{11}^3 + 13.6381A_{13}^3 + 0.000838230A_{31}^3 + 0.0744644A_{33}^3 + 0.000233450A_{51}^3 + 1.20550A_{11}A_{13}A_{31} + 15.4455A_{11}A_{13}A_{15} + 0.470087A_{11}A_{13}A_{51} + 0.210793A_{11}A_{31}A_{33} - 0.616721A_{11}A_{31}A_{15} + 0.00548246A_{11}A_{31}A_{51} + 2.63154A_{11}A_{33}A_{15} + 0.0853833A_{11}A_{33}A_{51} + 0.184894A_{11}A_{15}A_{51} + 2.69545A_{13}A_{31}A_{15} + 0.132909A_{13}A_{31}A_{51} + 1.00887A_{13}A_{15}A_{51} + 0.526137A_{31}A_{33}A_{15} + 0.0248924A_{31}A_{33}A_{51} + 0.00699350A_{31}A_{15}A_{51} + 0.218654A_{33}A_{15}A_{51}$$

$$K_3 = 0.631111U^3 + 0.256085UA_{11}^2 + 1.39429UA_{13}^2 + 0.00495237UA_{31}^2 + 0.0424126UA_{33}^2 + 3.90349UA_{15}^2 + 0.00407200UA_{51}^2 - 0.580741UA_{11}A_{13} + 0.0842327UA_{11}A_{31} - 0.119789UA_{11}A_{33} + 0.0331367UA_{11}A_{51} - 0.0668791UA_{13}A_{31} + 0.481269UA_{13}A_{33} - 3.02138UA_{13}A_{15} - 0.0132427UA_{13}A_{51} - 0.0196402UA_{31}A_{33} + 0.00326554UA_{31}A_{51} - 0.439791UA_{33}A_{15} - 0.00644570UA_{33}A_{51} - 0.0474075A_{11}^2A_{13} + 0.0276543A_{11}^2A_{31} - 0.0109348A_{11}^2A_{33} + 0.0121038A_{11}^2A_{51} + 0.602752A_{13}^2A_{11} + 0.143916A_{13}^2A_{31} + 1.34773A_{13}^2A_{15} + 0.0664544A_{13}^2A_{51} + 0.00785619A_{31}^2A_{11} + 0.00251469A_{31}^2A_{13} + 0.000646110A_{31}^2A_{33} + 0.00153984A_{31}^2A_{51} + 0.0206111A_{33}^2A_{11} + 0.00556006A_{33}^2A_{31} + 0.0502731A_{33}^2A_{15} + 0.00276736A_{33}^2A_{51} + 1.64950A_{11}^2A_{15} + 0.390548A_{15}^2A_{31} + 0.180134A_{15}^2A_{51} + 0.00197180A_{51}^2A_{11} + 0.00115756A_{51}^2A_{13} + 0.000882780A_{51}^2A_{31} + 0.000329100A_{51}^2A_{33} + 0.0395768A_{11}^3 + 0.000953470A_{31}^3 + 0.000177840A_{51}^3 + 0.000423480A_{11}A_{13}A_{31} + 0.210793A_{11}A_{13}A_{33} - 0.616721A_{11}A_{13}A_{15} + 0.00548246A_{11}A_{13}A_{51} - 0.000502300A_{11}A_{31}A_{33} + 0.00760954A_{11}A_{31}A_{51} - 0.0823982A_{11}A_{33}A_{15} + 0.000880140A_{11}A_{33}A_{51} + 0.0522855A_{11}A_{31}A_{33} - 0.0406336A_{13}A_{31}A_{15} + 0.00356310A_{13}A_{31}A_{51} + 0.526137A_{13}A_{33}A_{15} + 0.0248924 \times A_{13}A_{33}A_{51} + 0.00699350A_{13}A_{15}A_{51} - 0.00112654A_{31}A_{33}A_{15} + 0.000955200A_{31}A_{33}A_{51} + 0.00438570A_{33}A_{15}A_{51}$$

$$K_4 = -0.800000U^3 - 0.316614UA_{11}^2 - 0.00982009UA_{31}^2 - 0.000742200UA_{51}^2 + 3.14921UA_{11}A_{13} - 0.119789UA_{11}A_{31} + 0.551112UA_{11}A_{33} - 2.79450UA_{11}A_{15} - 0.0467426UA_{11}A_{51} + 0.481269UA_{13}A_{31} + 7.63967UA_{13}A_{15} + 0.163629UA_{13}A_{51} + 0.0848252UA_{31}A_{33} - 0.439791UA_{31}A_{15} - 0.0064570UA_{31}A_{51} + 1.19873UA_{33}A_{15} + 0.0287347UA_{33}A_{51} - 0.147785UA_{15}A_{51} + 0.538838A_{11}^2A_{13} - 0.0109348A_{11}^2A_{31} + 0.0993296A_{11}^2A_{33} - 0.340318A_{11}^2A_{15} - 0.00334561A_{11}^2A_{51} + 1.20889A_{13}^2A_{33} - 0.000251150A_{31}^2A_{11} + 0.0261427A_{31}^2A_{13} + 0.00556006A_{31}^2A_{33} - 0.000563270A_{31}^2A_{15} + 0.000477600A_{31}^2A_{51} + 0.223393A_{33}^2A_{13} + 12.5681A_{15}^2A_{13} + 2.27753A_{15}^2A_{33} + 0.000545640A_{51}^2A_{11} + 0.00657200A_{51}^2A_{13} + 0.000329100A_{51}^2A_{31} + 0.00152112A_{51}^2A_{33} + 0.00238452A_{51}^2A_{15} - 0.0264549A_{11}^3 + 2.27429A_{13}^3 + 0.000215370A_{31}^3 + 0.0143717A_{33}^3 + 0.0000720001A_{51}^3 + 0.210793A_{11}A_{13}A_{31} + 2.63154A_{11}A_{13}A_{15} + 0.0853833A_{11}A_{13}A_{51} + 0.0412221A_{11}A_{31}A_{33} - 0.0823982A_{11}A_{31}A_{15} + 0.000880140A_{11}A_{31}A_{51} + 0.451920A_{11}A_{33}A_{15} + 0.0173975A_{11}A_{33}A_{51} - 0.0190871A_{11}A_{15}A_{51} + 0.526137A_{13}A_{31}A_{15} + 0.0248924A_{13}A_{31}A_{51} + 0.218654A_{13}A_{15}A_{51} + 0.100546A_{31}A_{33}A_{15} + 0.00553472A_{31}A_{33}A_{51} + 0.00438570A_{31}A_{15}A_{51} + 0.0453130A_{33}A_{15}A_{51}$$

$$K_5 = 25.4222UA_{13}^2 + 0.599365UA_{33}^2 - 18.4593UA_{11}A_{13} - 2.79450UA_{11}A_{33} + 54.8148UA_{11}A_{15} - 3.02138UA_{13}A_{31} + 7.63937UA_{13}A_{33} - 1.07719UA_{13}A_{51} - 0.439791UA_{31}A_{33} + 7.80699UA_{31}A_{15} - 0.147785UA_{33}A_{51} + 2.56097UA_{15}A_{51} - 2.26032A_{11}^2A_{13} - 0.340318A_{11}^2A_{33} + 8.91429A_{11}^2A_{15} + 7.72275A_{13}^2A_{11} + 1.34773A_{13}^2A_{31} + 75.3439A_{13}^2A_{15} + 0.504433A_{13}^2A_{51} - 0.0203168A_{31}^2A_{13} - 0.000563270A_{31}^2A_{33} + 0.390548A_{31}^2A_{15} + 0.225960A_{33}^2A_{11} + 0.0502731A_{33}^2A_{31} + 2.27753A_{33}^2A_{15} + 0.0026565A_{33}^2A_{51} + 0.00883425A_{51}^2A_{13} + 0.00238452A_{51}^2A_{33} + 0.0930836A_{51}^2A_{15} + 104.102A_{15}^3 - 0.616721A_{11}A_{13}A_{31} + 2.63154A_{11}A_{13}A_{33} - 0.184894A_{11}A_{13}A_{51} - 0.0823982A_{11}A_{31}A_{33} + 3.29990A_{11}A_{31}A_{15} - 0.0190871A_{11}A_{33}A_{51} + 1.28586A_{11}A_{15}A_{51} + 0.526137A_{13}A_{31}A_{33} + 0.00699350A_{13}A_{31}A_{51} + 25.1361A_{13}A_{33}A_{15} + 0.218654A_{13}A_{33}A_{51} + 0.00438570A_{31}A_{33}A_{51} + 0.360269A_{31}A_{15}A_{51}$$

$$K_6 = 0.213333U^3 + 0.0931215UA_{11}^2 + 0.456054UA_{13}^2 + 0.00163277UA_{31}^2 + 0.0143673UA_{33}^2 + 1.28048UA_{15}^2 - 0.0000465000UA_{51}^2 - 0.195374UA_{11}A_{13} + 0.0331367UA_{11}A_{31} - 0.0467426UA_{11}A_{33} + 0.0139684UA_{11}A_{51} - 0.0132427UA_{13}A_{31} + 0.163629UA_{13}A_{33} - 1.07719UA_{13}A_{15} + 0.00326540UA_{13}A_{51} - 0.00644570UA_{31}A_{33} + 0.000814400UA_{31}A_{51} - 0.147785UA_{33}A_{15} - 0.00148440UA_{33}A_{51} - 0.0114487A_{11}^2A_{13} + 0.0121038A_{11}^2A_{31} - 0.00334561A_{11}^2A_{33} + 0.00574819A_{11}^2A_{51} + 0.235043A_{13}^2A_{11} + 0.0664544A_{13}^2A_{31} + 0.504433A_{13}^2A_{15} + 0.0343677A_{13}^2A_{51} + 0.00380477A_{31}^2A_{11} + 0.00178155A_{31}^2A_{13} + 0.000477600A_{31}^2A_{33} + 0.000882780A_{31}^2A_{51} + 0.00869874A_{33}^2A_{11} + 0.00276736A_{33}^2A_{31} + 0.0226565A_{33}^2A_{15} + 0.00152112A_{33}^2A_{51} + 0.642928A_{15}^2A_{11} + 0.180134A_{15}^2A_{31} + 0.0930835A_{15}^2A_{51} + 0.00108477A_{51}^2A_{11} + 0.000700350A_{51}^2A_{13} + 0.000533520A_{51}^2A_{31} + 0.000216000A_{51}^2A_{33} + 0.0155506A_{11}^3 + 0.000513280A_{31}^3 + 0.000112860A_{51}^3 + 0.00548246A_{11}A_{13}A_{31} + 0.0853833A_{11}A_{13}A_{33} - 0.184894A_{11}A_{13}A_{15} + 0.00552474A_{11}A_{13}A_{51} + 0.000880140A_{11}A_{31}A_{33} + 0.00394360A_{11}A_{31}A_{51} - 0.0190871A_{11}A_{33}A_{15} + 0.00109128A_{11}A_{33}A_{51} + 0.0248924A_{13}A_{31}A_{33} + 0.00699350A_{13}A_{31}A_{15} + 0.00231512A_{13}A_{31}A_{51} + 0.218654A_{13}A_{33}A_{15} + 0.0131440A_{13}A_{33}A_{51} + 0.0176685A_{13}A_{15}A_{51} + 0.00438570A_{31}A_{33}A_{15} + 0.000658200A_{31}A_{33}A_{51} + 0.00476904A_{33}A_{15}A_{51}$$

Changes of Address

Since the Post Office Department does not as a rule forward magazines to forwarding addresses, it is important that the Institute be notified of changes in address 30 days in advance of publishing date to ensure receipt of every issue of the *Journal* and *Review*.

Notices should be sent directly to the Institute of the Aeronautical Sciences, 2 East 64th Street, New York 21, N.Y.

The Theoretical Induced Deflection Angle in Cascades Having Wall Boundary Layers

GEORGE F. HAUSMANN*

United Aircraft Corporation

ABSTRACT

A theoretical analysis is presented which employs a lifting-line theory assuming incompressible, nonviscous flow to determine the induced deflection angle in two-dimensional cascades having wall boundary layers. Two correction factors are derived for the deflection angle of the idealized infinite cascade: one that accounts for the induced deflection due to the trailing vortex system in the wall boundary layer, and the other that accounts for the decrease in total circulation of the bound vortex system.

Plots are included which show the effect of blade length, boundary-layer thickness, and the number of blades in cascade on the deflection angle of several typical cascade configurations.

SYMBOLS

$0, 0'$	= arbitrary coplanar points equidistant upstream and downstream from the lifting line
h	= normal distance from 0 and 0′ to the lifting line
r	= distance from lifting-line element to 0 and 0′
ds	= lifting-line length element
$\theta, \xi, \gamma, \phi$	= angles associated with points 0 and 0′ and the lifting line (see Fig. 2)
l	= lifting-line length or cascade blade length, in.
Γ	= circulation
Γ_0	= free-stream circulation of a finite cascade blade or lifting line
y	= distance from tunnel wall to trailing vortex origin, in.
q	= induced downwash of bound vortex system
w	= induced downwash of trailing vortex system
C_L	= cascade lift coefficient
L	= cascade lift, lbs.
τ	= blade spacing, in.
b	= blade chord, in.
β	= air angle, deg., referred to cascade line
V	= velocity, ft. per sec.
ρ	= density, slugs per cu.ft.
C_x	= axial velocity component, ft. per sec.
C_u	= velocity component parallel to cascade, ft. per sec.
δ	= boundary-layer total thickness, in.
δ^*	= boundary-layer displacement thickness, in.
K	= circulation correction factor
n	= number of half-span lengths along lifting line, or cascade blade, image system
S	= blade relation within tunnel referred to tunnel centerline
P	= blade or image number referred to tunnel centerline
B	= number of lifting lines (odd), or blades, in cascade
R	= $(P - S)/B$

Subscripts

1 = conditions at cascade inlet
2 = conditions at cascade outlet
m = mean conditions where $\cot \beta m = (\cot \beta_1 + \cot \beta_2)/2$

Superscripts

′ = finite cascade characteristics corrected for induced downwash of trailing vortex system
″ = finite cascade characteristics corrected for induced downwash of trailing vortex system and modified downwash of bound vortex system

Received September 24, 1947. Revised and received June 28, 1948.

* Aeronautical Research Engineer, Research Department.

INTRODUCTION

THE LACK OF CORRELATION of deflection angle data from various cascade tunnels is primarily attributed to variations in the ratio of blade length to wall boundary-layer thickness, assuming that Reynolds Number and other such effects are equivalent. As a means of comparing cascade data from different tunnels on a common basis, it has been proposed to correct these data to "infinite" conditions by consideration of the induced velocities of the modified vortex system that is inherent with cascades having wall boundary layers. In theory, such corrected data could then be adapted to axial-flow compressor design by applying the induced effects that are to be expected in the elements of a rotating blade row.

Although a theoretical analysis of this nature does not contemplate the complicated secondary flows that are associated with retarding cascades, it is felt that the form of the variables in the derived equations will be helpful in compiling more accurate empirical relationships for axial-flow compressor design.

THEORETICAL ANALYSIS

The vortex system of an arbitrary two-dimensional cascade with side-wall boundary layers is shown in Fig. 1. The cascade vanes are replaced by lifting lines that induce components upstream and downstream and parallel to the cascade plane. As a means of simplifying the analysis, the end walls are assumed to be curved to match the streamlines that would be associated with a cascade having a prescribed circulation and an infinite number of lifting lines. By this expedient, the images of the bound vortex system have no reversal of sign, and the downwash expression may be readily derived.

The trailing vortex system shown in Figs. 1a and 1b is formed by the gradient of circulation in the low velocity, side-wall boundary layer at the blade extremities. At any arbitrary downstream station where the exit streamlines are straight, these vortices have images in the two dimensions of a plane that is normal to the exit air-stream direction. In order to satisfy the boundary

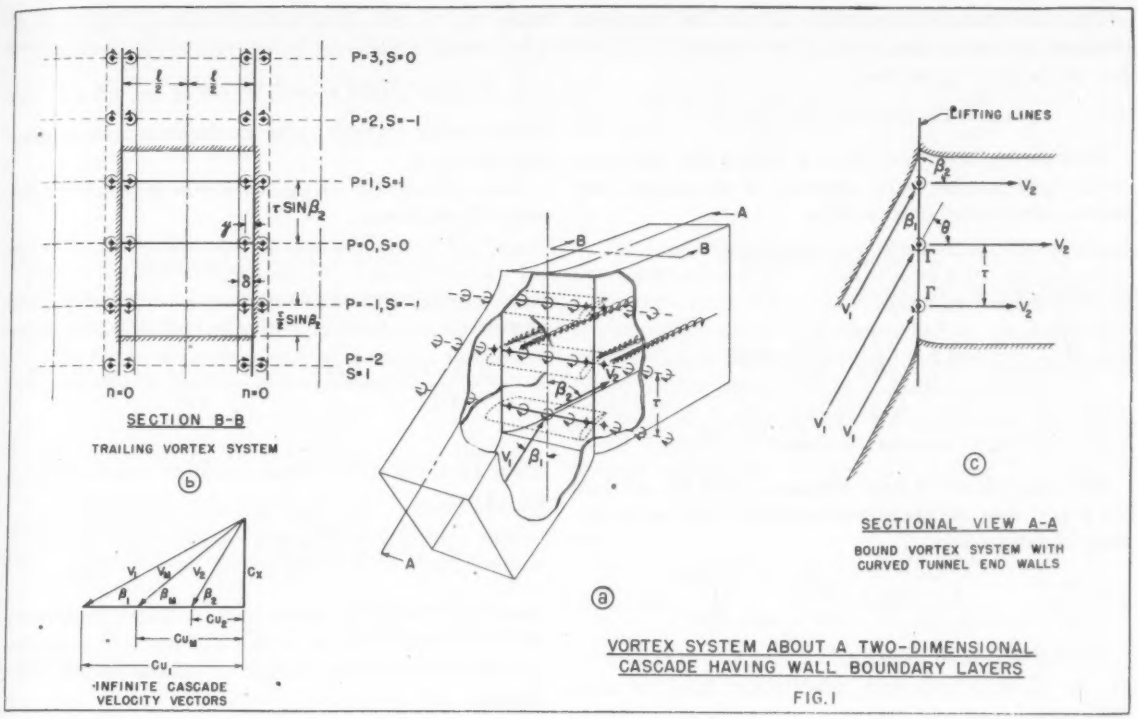

VORTEX SYSTEM ABOUT A TWO-DIMENSIONAL CASCADE HAVING WALL BOUNDARY LAYERS

FIG. 1

conditions, the vortex images that extend in the cascade direction have a cyclic variation of sign that depends on the number of blades in the cascade configuration. The side-wall images of the trailing vortex system are positive in sign as are the side-wall images of the bound vortex system.

Bound Vortex Correction

The presence of the side-wall boundary layers results in a decrease in circulation at the blade extremities which is reflected in the infinite number of images along the lifting line. In a cascade this cyclic pattern of the circulation produces a downwash angle that differs somewhat from the downwash resulting from a cascade having infinite lifting lines with constant circulation. The magnitude of this correction is evaluated from the following analysis.

Consider the line vortex diagram for an airfoil of length, l, in a tunnel bounded by end walls having boundary layers of thickness, δ, as shown in Fig. 2. The circulation around this line has a cyclic variation that repeats from $+\infty$ to $-\infty$. 0 and 0′ are arbitrary points equidistant upstream and downstream from the cascade, h is the normal distance from 0 to the line vortex system, and r is the distance from 0 to any element, ds, on the line.

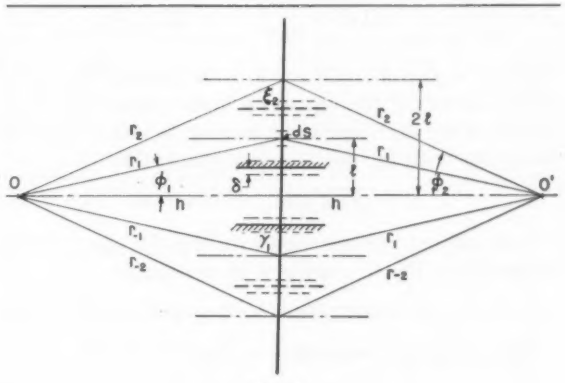

FIG. 2.

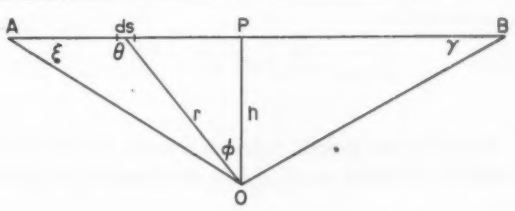

FIG. 3.

Now, referring to the vector diagram in Fig. 3, the general equation for the induced downwash at any point, 0, resulting from an element, ds, of a straight line vortex of length, AB, is

$$dq = \frac{\Gamma ds}{4\pi r^2} \sin\theta = \frac{\Gamma}{4\pi h} \cos\phi d\phi \qquad (1)$$

The total induced downwash of the line vortex is obtained by integrating from $\phi = -[(\pi/2) - \xi]$ to $\phi = +[(\pi/2) - \gamma]$ so that

$$q = (\Gamma/4\pi h)(\cos \xi + \cos \gamma) \tag{2}$$

Considering, now, each cascade lifting line and each of the wall images to be elements of an infinite line vortex, the induced downwash is

$$q = \int_{-\infty}^{+\infty} (\Gamma ds/4\pi r^2) \sin \theta$$

or, with reference to Fig. 2,

$$q = \int_{-l/2}^{l/2} \frac{\Gamma ds}{4\pi r^2} \sin \theta + \int_{l/2}^{3l/2} \frac{\Gamma ds}{4\pi r^2} \sin \theta + \int_{-3l/2}^{-l/2} \frac{\Gamma ds}{4\pi r^2} \sin \theta + \ldots \tag{3}$$

Assuming that h is large compared with $l/2$, so that $\sin \theta/4\pi r^2$ may be considered constant over each element of integration,

$$q = \frac{\sin \theta}{4\pi r^2}\bigg|_{s=l/2} \int_{-l/2}^{l/2} \Gamma ds + \frac{\sin \theta}{4\pi r^2}\bigg|_{s=3l/2} \int_{l/2}^{3l/2} \Gamma ds \tag{4}$$

Noting that each integration extends over the limits of one blade length and substituting $K\Gamma_0 l$ for each integrand,

$$q = \frac{\sin \theta}{4\pi r^2}\bigg|_{s=l/2} K\Gamma_0 l + \frac{\sin \theta}{4\pi r^2}\bigg|_{s=3l/2} K\Gamma_0 l + \ldots \tag{5}$$

where $K = \int_{-l/2}^{l/2} \Gamma ds/\Gamma_0 l$ and Γ_0 is the value of the circulation outside of the boundary layer. Since the summation of the $\sin \theta/4\pi r^2$ terms extends to infinity in both directions from the measurement plane, then

$$q = \int_{-\infty}^{+\infty} (K\Gamma_0 \sin \theta/4\pi r^2) ds \tag{6}$$

Comparing this expression with Eqs. (1) and (2), it is evident that Eq. (2) may now be written as

$$q = (K\Gamma_0/4\pi h)(\cos \xi + \cos \gamma) \tag{7}$$

Now, since $\xi = -\pi$ and $\gamma = +\pi$,

$$q = K\Gamma_0/2\pi h \tag{8}$$

From the law of Kutta-Joukowsky, the circulation may be expressed as

$$L = \rho V_m \Gamma l \tag{9}$$

where V_m is the mean velocity through the cascade. The cascade lift is given by the familiar expression

$$L = {}^1/_2 \rho V_m^2 C_L b l = \rho \tau C_x V_m (\cot \beta_1 - \cot \beta_2) \tag{10}$$

where τ is the blade gap and the angles are self-explanatory in Fig. 1.

Now, solving for the circulation in terms of the cascade lift coefficient,

$$\Gamma = L/\rho V_m l = V_m C_L b/2 \tag{11}$$

By assuming a turbulent boundary-layer velocity profile where $V/V_m = (y/\delta)^{1/7}$, K may be evaluated as follows:

$$K = \frac{\int_{-l/2}^{l/2} \Gamma ds}{\Gamma_0 l} = \frac{\Gamma_0(l - 2\delta) + V_m C_L b \int_0^{\delta} (y/\delta)^{1/7} dy}{\Gamma_0 l} \tag{12}$$

where δ is the boundary-layer thickness and $V_m C_L b/2 = \Gamma_0$. Then,

$$K = \frac{\Gamma_0 l - 2\Gamma_0 \delta + ({}^{11}/_8)\delta\Gamma_0}{\Gamma_0 l} = 1 - \frac{\delta}{4l} \tag{13}$$

From the downwash derivation of Kutta-Joukowsky, the total downwash, or vector difference of velocities, parallel to an infinite cascade of infinite length lifting lines is

$$\Delta C_u = \Gamma_0/\tau = C_x(\cot \beta_1 - \cot \beta_2) \tag{14}$$

From the preceding analysis on the cyclic variation of circulation along the infinite lifting line, it is evident that the corrected downwash resulting from the bound vortex system of a two-dimensional cascade having wall boundary layers is

$$\Delta C_u = \Gamma_0/K\tau = C_x(\cot \beta_1 - \cot \beta_2)/[1 - (\delta/4l)] \tag{15}$$

Trailing Vortex Correction

The induced downwash parallel to the cascade which results from the trailing vortex system shown in Figs. 1a and 1b is derived on the basis of Eq. (2), where

$$q = (\Gamma/4\pi h)(\cos \xi + \cos \gamma)$$

Since the induced downwash due to trailing vorticity is considered at an infinite distance downstream from the cascade $\xi = -\pi$ and $\gamma = \pi$ so that

$$q = \Gamma/2\pi h \tag{16}$$

Applying this general expression to the cascade of lifting lines having wall boundary layers such that the strength of trailing vorticity is $(d\Gamma/dy)dy$, the induced downwash, w, resulting from the complete image system is

$$w = \frac{1}{2\pi} \int_0^{\delta} \frac{d\Gamma}{dy} dy \left(\frac{2}{(l/2) - y} - \frac{2}{(l/2) + y} + 4\left\{ \frac{(l/2) - y}{[(l/2) - y]^2 + \tau^2 \sin^2 \beta_2} - \frac{(l/2) + y}{[(l/2) + y]^2 + \tau^2 \sin^2 \beta_2} \right\} + \ldots \right) \tag{17}$$

On expansion, this becomes

$$w = \frac{1}{2\pi} \int_0^{\delta} \frac{d\Gamma}{dy} y dy \left(\frac{4}{(l^2/4) - y^2} + \left\{ \frac{8[(l^2/4) - y^2 - \tau^2 \sin^2 \beta_2]}{2l^2[(l^2/8) - y^2 - \tau^2 \sin^2 \beta_2] + 4(y^2 + \tau^2 \sin^2 \beta_2)^2} \right\} + \ldots \right) \tag{18}$$

At the blade center-span where $0 < y^2 < \delta^2$ is small compared with $l^2/4$, the y^2 terms may be omitted, and the downwash resulting from the complete trailing vortex system may be expressed as a sum in the following manner:

$$w = \frac{1}{\pi} \sum_{n=-\infty}^{n=+\infty} \sum_{R=-\infty}^{R=\infty} \sum_{S=-(B-1)/2}^{S=(B-1)/2} \frac{(2n+1)^2(l^2/4) - (BR+S)^2\tau^2 \sin^2\beta_2}{[(2n+1)^2(l^2/4) + (BR+S)^2\tau^2 \sin^2\beta_2]^2} (-1)^R \int_0^\delta \frac{d\Gamma}{dy}\, y dy \qquad (19)$$

where the n limits refer to the number of half span lengths in the lateral direction, the S limits refer to the relation of blades in the tunnel, and the R limits refer to the images in the longitudinal, or cascade, direction. If P is the blade, or image, number referred to the tunnel centerline, R is related by the expression

$$R = (P - S)/B$$

where B is the number (odd) of lifting lines in the finite cascade.

No simple solution for this triple summation has been found, nor has its convergence been definitely established. The form of this equation is, however, similar to the expression derived by Glauert[1] for the induced downwash of a single airfoil bounded by tunnel walls. Glauert's equation has been empirically correlated and is generally accepted as authoritative. A numerical substitution of values in Eq. (19) indicates convergence, although this test cannot be considered decisive.

The value of the integral in Eq. (19) may be established by again assuming a turbulent boundary-layer velocity distribution where $V/V_m = (y/\delta)^{1/7}$. Then

$$\Gamma = {}^1/_2 V_m C_L b (y/\delta)^{1/7}$$

and

$$y(d\Gamma/dy) = ({}^1/_7) V_m C_L b y^{1/7} \delta^{-1/7}$$

Therefore,

$$\int_0^\delta (d\Gamma/dy) y dy = (V_m C_L b/2)({}^1/_8\,\delta) \qquad (20)$$

and since the displacement thickness, δ^*, of a seventh root boundary-layer velocity distribution is equal to ${}^1/_8\delta$,

$$w = (V_m C_L b \delta^*/2\pi) \sum_{n=-\infty}^{n=\infty} \sum_{R=-\infty}^{R=\infty} \sum_{S=-(B-1)/2}^{S=(B-1)/2} \cdots \qquad (21)$$

Substituting Eq. (10) for $(V_m C_L b/2)$,

$$\frac{w}{c_x} = \frac{\tau\delta^*(\cot\beta_1 - \cot\beta_2)}{\pi} \sum_{n=-\infty}^{n=\infty} \sum_{R=-\infty}^{R=\infty} \sum_{S=(B-1)/2}^{S=(B-1)/2} \frac{(2n+1)^2(l^2/4) - (BR+s)^2\tau^2 \sin^2\beta_2}{(2n+1)^2(l^2/4) + (BR+s)^2\tau^2 \sin^2\beta_2]^2} (-1)^R \qquad (22)$$

Application of Corrections

The induced velocity vectors that are evaluated from the equations derived in the preceding analysis are applied to the finite cascade velocity vector diagram to determine the equivalent infinite cascade performance.

Referring to the vector diagram in Fig. 4, V_1 and β_1 are the inlet velocity and direction to the actual cascade and also to the corrected infinite cascade. V_2 and β_2 refer to the velocity vector at the exit of the arbitrary cascade having wall boundary layers. V_2' and β_2' describe the exit velocity vector that has been modified by the application of the tangential component of the induced downwash, w, resulting from the trailing vortex system. V_2'' and β_2'' describe the velocity vector that also includes the change of the downwash, ΔC_u, resulting from the nonuniformity of circulation around the lifting lines. V_2'' and β_2'' thus define the outlet velocity of the arbitrary cascade having wall boundary layers but corrected to infinite conditions.

From the vector diagram and the preceding analysis,

$$\cot\beta_1 = C_{u1}/C_x, \qquad \cot\beta_2 = C_{u2}/C_x$$

$$\cot\beta_2' = C_{u2}'/C_x, \qquad \cot\beta_2'' = C_{u2}''/C_x$$

$$\sin\beta_2 = (C_{u2}' - C_{u2})/w$$

Substituting,

$$\cot\beta_2' = (w\sin\beta_2 + C_{u2})/C_x \qquad (23)$$

and

$$\Delta C_u = (C_{u1} - C_{u2}')/K = C_{u1} - C_{u2}''$$

Substituting for ΔC_u from Eq. (15),

$$\cot\beta_2'' = \cot\beta_1 - \frac{\cot\beta_1 - \cot\beta_2 - (w/C_x)\sin\beta_2}{1 - (\delta/4l)} \qquad (24)$$

Discussion

The induced deflection angles of several typical cascade configurations have been calculated and are plotted in Figs. 5 and 6. For the example, a cascade inlet angle,

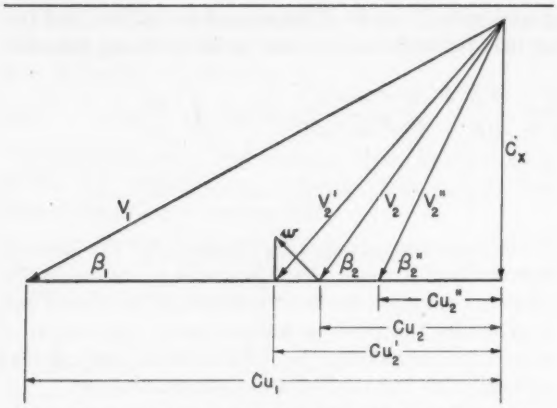

FIG. 4. Vector diagram of induced cascade deflection angles.

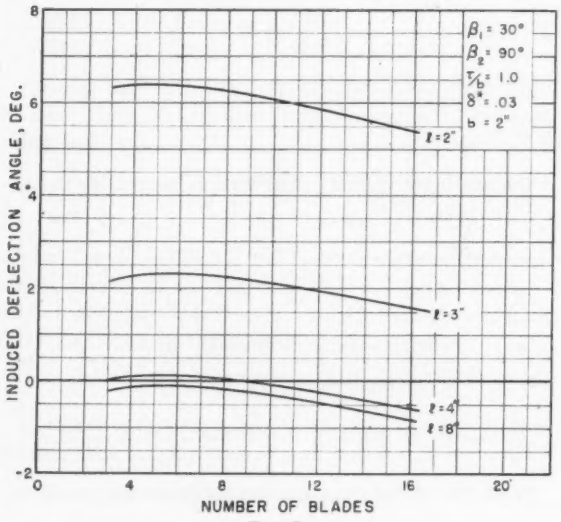

FIG. 5.

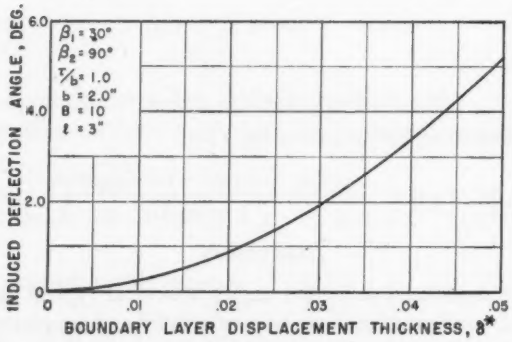

FIG. 6.

β_1, of 30°, outlet angle, β_2, of 90°, and a gap-chord ratio equal to 2 have been chosen. The circulation required to produce the 60° turning is independent of vane camber or cascade stagger angle.

The form of the linear cascade variables in Eq. (22) excludes the use of nondimensional parameters so that the examples have been calculated in terms of absolute cascade dimensions. The summation of terms from Eq. (22) has been carried out in symmetrical order and includes all downwash terms that are greater than 1 per cent of the induced downwash resulting from the vane at the tunnel centerline.

Referring to Fig. 5, it is seen that the number of vanes in the finite cascade has little effect on the induced deflection angle of the arbitrary configuration. It should be realized, however, that the inlet walls to the cascade are assumed to be curved to match the inlet streamlines so that the upstream potential flow field is inherently independent of the number of vanes in the cascade row.

The curves in Fig. 5 also show the effect of blade length on the induced deflection angle of a cascade that has a given blade spacing (2 in.), chord (2 in.), and boundary-layer total thickness (0.24 in.). It is interesting to note that an increase in blade length results in a reversal in the sign of the induced deflection angle so that a particular combination of blade length and number of blades actually results in a zero correction for the induced deflection angle of the specific finite cascade. An aspect ratio parameter has not been applied to the curves in Fig. 5, since the blade length and spacing in Eqs. (22) and (24) are independent variables for a given aspect ratio and gap-chord ratio.

The effect of wall boundary-layer thickness on the induced deflection angle of an arbitrary cascade is shown in Fig. 6. The curve is not extended beyond a value of δ^* equal to 0.10, since the simplifying assumption used in obtaining Eq. (18) limits the analysis to small values of boundary-layer thickness.

The principal limitation of the application of the theoretical correction to the induced deflection angle appears to be in the use of a realistic value of wall boundary-layer thickness and velocity distribution. Although the theory assumes a lifting line in place of the cascade vane, the boundary layer through an actual cascade changes shape and thickness along the vane chord, so that true representative boundary-layer conditions are difficult to establish. It is also probable that the complex, secondary flow vortices within the blade passages have considerable influence on the induced downwash. In spite of these shortcomings, it is felt that the theory presented in this paper could be useful in establishing a first approximation to the induced effects in cascades.

REFERENCE

[1] Glauert, *The Elements of Aerofoil and Airscrew Theory*, Cambridge University Press, London, 1937.

Surface-Pressure Gradient and Shock-Front Curvature at the Edge of a Plane Ogive with Attached Shock Front

M. M. MUNK* AND R. C. PRIM*
Naval Ordnance Laboratory

SUMMARY

The flow of air at high Mach Numbers past a sufficiently sharp plane ogive is characterized by the presence of a curved shock front attached to the edge of the ogive. This paper presents and carries out a simple method for computing the exact surface-pressure gradient and shock-front curvature at the edge of the ogive.

A comparison is made between the exact edge-pressure gradient and that given by two approximate methods of computing the pressure distribution along an ogive.

The numerical results, presented graphically, cover all ogives with attached shock fronts for Mach Numbers up to 13.

INTRODUCTION

THE FLOW OF A PERFECT GAS at high Mach Numbers past a sufficiently sharp plane ogive is characterized by the presence of a curved shock front attached to the edge of the ogive. Even when the vorticity and non-uniformity of entropy resulting from the curvature of the shock front are negligible, the detailed computation of the flow field behind the shock front requires a laborious step-by-step calculation for each special case. Hence, the application of simpler approximate methods to the computation of pressure distributions on bodies of this type is highly desirable. The degree of accuracy to be expected from the application of any of these methods to a specific case is, however, difficult to ascertain.

This paper presents and carries out a simple method for computing the *exact* surface-pressure gradient at the edge of the ogive. This information is useful both in its own right and as a means of appraising the reliability of results obtained by approximate methods.

The curvature of the attached shock near the edge is also computed. This information is of assistance in the initial steps of detailed computations of flows of this type by characteristic methods and for interpretation of experimental results.

THE "WEDGE + PRANDTL-MEYER" AND "TANGENT-WEDGE" APPROXIMATIONS

An obvious and reasonable approximation to the pressure distribution on plane-ogival bodies can be obtained from the well-known wedge and Prandtl-Meyer solutions. The shock front is taken as that for a flow at the given Mach Number impinging on a wedge of the same included angle as the edge angle of the ogive. The flow along the curved wall is then computed as a simple Prandtl-Meyer flow, with initial conditions determined by the straight shock front established as above.

A second plausible approximation procedure is to assign as the pressure at each point on the ogival surface the surface pressure in a flow at the given Mach Number against a wedge tangent to the ogive at the point in question.

CORRECTION OF THE "WEDGE + PRANDTL-MEYER" APPROXIMATION AT THE OGIVE EDGE

The approximation involved in the "Wedge + Prandtl-Meyer" method lies in the neglect of the interaction between the shock front and the successive disturbance lines originating along the ogive surface. Actually, this interaction gives rise to reflected families of disturbance lines which progressively weaken the shock front so that its inclination decreases with distance along the shock, approaching asymptotically the Mach angle of the undisturbed flow. (At points remote from the body, the difference between the shock angle and the Mach angle decreases more rapidly than the inverse of the distance. Otherwise, the wave drag can be shown to be infinite.)

By limiting consideration to a region sufficiently near the ogive edge that the pressure, Mach angle, shock angle, and streamline inclination and the first derivatives of these quantities do not differ appreciably from their initial values, the initial rates of change of these quantities will be evaluated. This amounts to performing a linearization that approaches exactness as the régime considered shrinks to the edge itself.

Fig. 1 represents the flow régime near the ogive edge. The ogive wall OBC is inclined at the angle δ to the oncoming flow. The rate of change of the inclination δ with distance along the wall is determined by the given wall curvature. The shock front OAD is inclined at the angle α to the oncoming flow. Its curvature must be determined so as to be consistent with the shock relations and with the strengths of the basic and reflected disturbances arising from the curvature of the wall.

Received March 10, 1948.
* Mechanics Division.

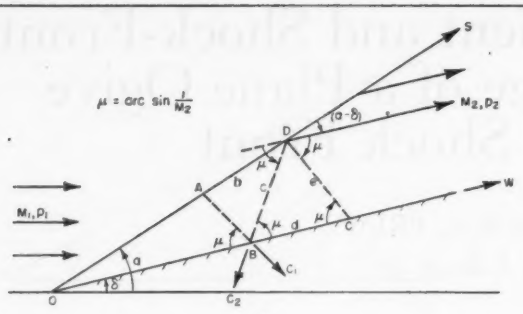

FIG. 1.

BD is a member of the basic family of disturbance lines originating at the wall; AB and DC are members of the family of disturbance lines reflected from the shock front. The "strength" of these disturbance lines may be defined in terms of the rates of change of pressure along members of each family. That is, a measure of the intensity of the basic family of disturbance lines originating at the wall (e.g., BD) is the rate of change of pressure along a disturbance line of the reflected family —i.e., $\partial p_2/\partial C_1$. Similarly, the rate of change of pressure along a basic disturbance line ($\partial p_2/\partial C_2$) is a measure of the intensity of the reflected family of disturbance lines. These rates of change of pressure along the two families of disturbance lines and the curvature of the shock front may be considered as the three basic unknown quantities. The conditions necessary for their evaluation are furnished by the two characteristic equations relating the changes in pressure and changes in flow direction along disturbance lines of the same family and by the shock relations, which relate the changes in pressure and changes in direction along the shock front.

The procedure will be to impose the conditions that (1) the pressure difference between points A and D immediately behind the shock front must be the same when computed from the shock relations along AD or from the characteristic relations along ABD and (2) that the change in flow direction computed along BDC be the same as that given by the prescribed curvature along BC.

Letting $P \equiv p_2/p_1$ and applying the first condition, we obtain

$$P_D - P_A = \left(\frac{dP}{d\delta}\right)_s (\delta_D - \delta_A) = \frac{\partial P}{\partial C_1} a + \frac{\partial P}{\partial C_2} c \quad (1)$$

But,

$$\delta_D - \delta_A = (\partial\delta/\partial C_1)a + (\partial\delta/\partial C_2)c \quad (2)$$

and from the characteristic equations

$$\partial\delta/\partial C_1 = (\partial P/\partial C_1)(d\delta/dP)_{C_1} \quad (3)$$

$$\frac{\partial\delta}{\partial C_2} = \frac{\partial P}{\partial C_2}\left(\frac{d\delta}{dP}\right)_{C_1} = -\frac{\partial P}{\partial C_2}\left(\frac{d\delta}{dP}\right)_{C_1} \quad (4)$$

From Eqs. (1)–(4),

$$\frac{\dfrac{\partial P}{\partial C_1}}{\dfrac{\partial P}{\partial C_2}} = \frac{\left(\dfrac{dP}{d\delta}\right)_s \left(\dfrac{d\delta}{dP}\right)_{C_1} + 1}{\left(\dfrac{dP}{d\delta}\right)_s \left(\dfrac{d\delta}{dP}\right)_{C_1} - 1} \left(\frac{c}{a}\right) \quad (5)$$

but from Fig. 1,

$$c/a = \sin(\mu + \alpha - \delta)/\sin(\mu - \alpha + \delta) \quad (6)$$

where μ is the Mach angle behind the shock front. Hence,

$$\frac{\dfrac{\partial P}{\partial C_1}}{\dfrac{\partial P}{\partial C_2}} = \frac{\left(\dfrac{dP}{d\delta}\right)_s \left(\dfrac{d\delta}{dP}\right)_{C_1} + 1}{\left(\dfrac{dP}{d\delta}\right)_s \left(\dfrac{d\delta}{dP}\right)_{C_1} - 1} \frac{\sin(\mu + \alpha - \delta)}{\sin(\mu - \alpha + \delta)} \quad (7)$$

Now applying the second condition and proceeding as in Eqs. (2)–(4), we obtain

$$\delta_c - \delta_D = -K_w d = \left(\frac{d\delta}{dP}\right)_{C_1}\left(\frac{\partial P}{\partial C_1} e - \frac{\partial P}{\partial C_2} C\right) \quad (8)$$

where K_w is the curvature of the wall. But from Fig. 1,

$$e/d = c/d = 1/2 \cos\mu \quad (9)$$

Hence

$$\frac{\partial P}{\partial C_1} - \frac{\partial P}{\partial C_2} = -\frac{2K_w \cos\mu}{(d\delta/dP)_{C_1}} \quad (10)$$

and

$$\begin{aligned} \frac{dP}{dw} d &= \frac{\partial P}{\partial C_1} e + \frac{\partial P}{\partial C_2} c \\ \frac{dP}{dw} &= \left(\frac{\partial P}{\partial C_1} + \frac{\partial P}{\partial C_2}\right) 2\cos\mu \end{aligned} \quad (11)$$

Now concerning the shock curvature K_s,

$$K_s = -\frac{d\alpha}{ds} = -\frac{\dfrac{d\delta}{ds}}{\left(\dfrac{d\delta}{d\alpha}\right)_s} \quad (12)$$

But from Eqs. (2)–(4),

$$\delta_D - \delta_A = \frac{d\delta}{ds} b = \left(\frac{d\delta}{dP}\right)_{C_1}\left(\frac{\partial P}{\partial C_1} a - \frac{\partial P}{\partial C_2} c\right)$$

whence

$$\frac{d\delta}{ds} = \left(\frac{d\delta}{dP}\right)_{C_1} \frac{\sin(\mu - \alpha + \delta)}{\sin 2\mu} \times \left[\frac{\partial P}{\partial C_1} - \frac{\partial P}{\partial C_2} \frac{\sin(\mu + \alpha - \delta)}{\sin(\mu - \alpha + \delta)}\right] \quad (13)$$

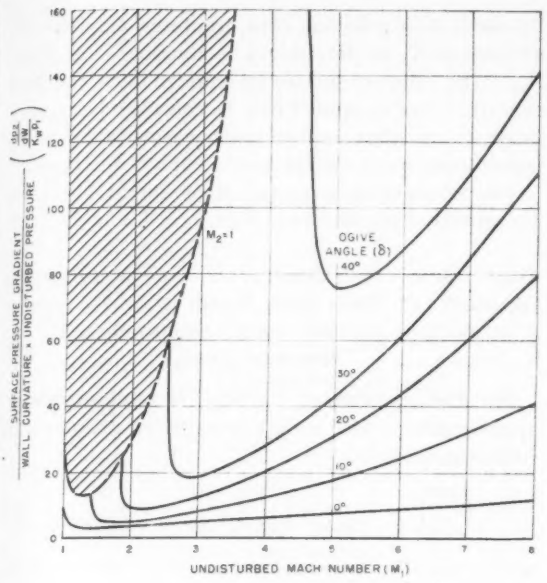

FIG. 2.

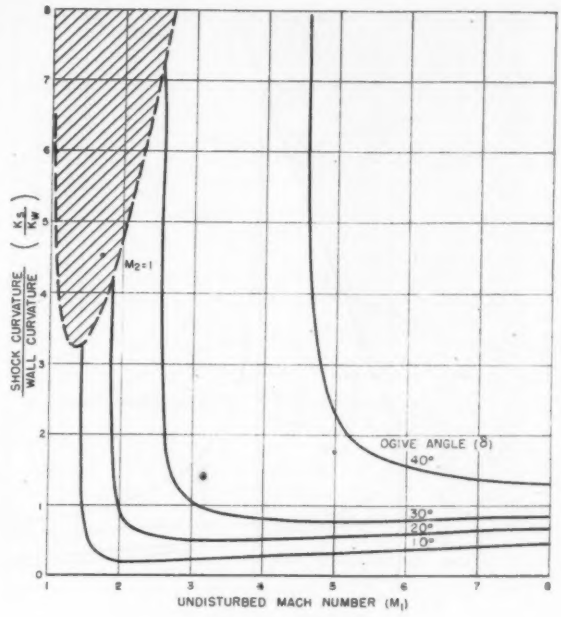

FIG. 4.

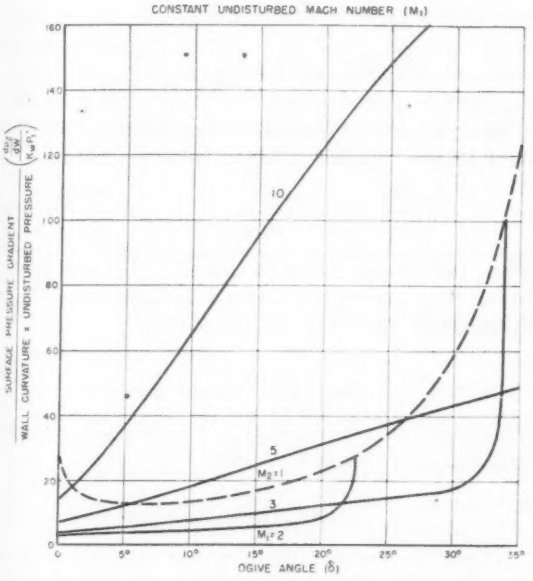

FIG. 3.

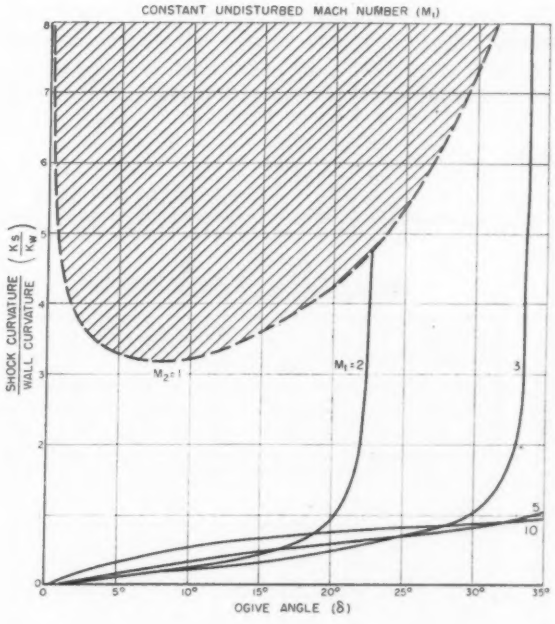

FIG. 5.

and

$$K_s = -\frac{(d\delta/dP)_{C_1}}{(d\delta/d\alpha)_s}\frac{\sin(\mu-\alpha+\delta)}{\sin 2\mu}\times\left[\frac{\partial P}{\partial C_1}-\frac{\partial P}{\partial C_2}\frac{\sin(\mu+\alpha-\delta)}{\sin(\mu-\alpha+\delta)}\right] \quad (14)$$

Now Eqs. (7) and (10) determine $\partial P/\partial C_1$ and $\partial P/\partial C_2$ in terms of $(\partial P/d\delta)_s$, $(d\delta/dP)_{C_1}$, μ, α, δ, and K_w. By specifying δ and K_w (fixing the problem geometrically), μ, α, and P can be readily obtained from the well-known solutions for the supersonic wedge flow as functions of the Mach Number of the oncoming flow. The basic characteristic equation yields for $(d\delta/dP)_{C_1}$

$$(d\delta/dP)_{C_1} = \sin 2\mu/2\gamma P \quad (15)$$

where γ is the adiabatic exponent, and $(dP/d\delta)_s$ can be found from differentiation of familiar relations for inclined shock fronts

$$(dP/d\delta)_s = (\partial P/\partial\alpha)_s/(\partial\delta/\partial\alpha)_s \quad (16)$$

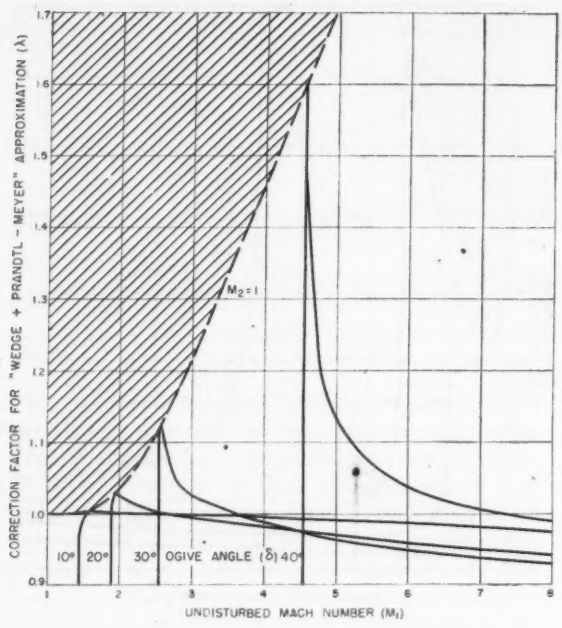

FIG. 6.

where

$$P = \frac{\gamma - 1}{\gamma + 1}\left(\frac{2\gamma}{\gamma - 1}\, M_1^2 \sin^2 \alpha - 1\right)$$

and

$$\delta = \alpha - \tan^{-1}\left\{\frac{[2/(\gamma - 1)] + M_1^2 \sin^2 \alpha}{[(\gamma + 1)/2(\gamma - 1)]M_1^2 \sin 2\alpha}\right\}$$

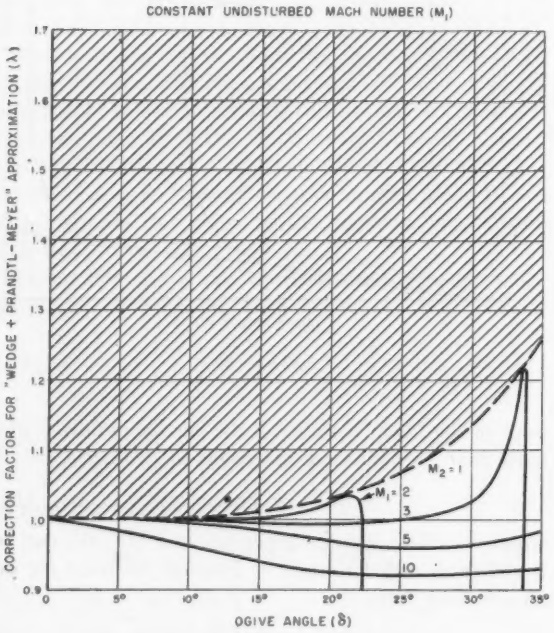

FIG. 7.

By use of these relations, then, from Eqs. (11) and (14), dP/dw and K_s are determined as functions of M, δ, and K_w. The values of surface-pressure gradient and shock curvature thus computed may be considered as approximate values that approach the exact values as the régime considered shrinks to the edge of the ogive.*

The results of these computations (for air $\gamma = 1.405$) are presented graphically in Figs. 2, 3, 4, and 5.

Comparison of Corrected Surface-Pressure Gradient at Edge with Results of "Wedge + Prandtl-Meyer" and "Tangent-Wedge" Approximations

For the uncorrected "Wedge + Prandtl-Meyer" approximation, the surface-pressure gradient at the edge is given by

$$\left(\frac{dP}{dw}\right)_{\text{"W + P-M"}} = \left(\frac{dP}{d\delta}\right)_{c_1}\frac{d\delta}{dw} = -\frac{K_w}{(d\delta/dP)_{c_1}} \tag{17}$$

where $(d\delta/dP)_{c_1}$ is given by Eq. (15). By use of Eq. (17) and the exact value of dP/dw computed in the previous section, a correction factor λ (a function of M and δ) can be computed such that

$$(dP/dw)_{\text{exact}} = \lambda\left(\frac{dP}{dw}\right)_{\text{"W + P-M"}} \tag{18}$$

Similarly, the surface-pressure gradient at the edge given by the "tangent-wedge" approximation

$$\left(\frac{dP}{dw}\right)_{\text{"T-W"}} = \left(\frac{dP}{dS}\right)_s\frac{d\delta}{dw} = -K_w\left(\frac{dP}{d\delta}\right)_s \tag{19}$$

where $(dP/d\delta)_s$ is computed from Eq. (16), can be used to compute a correction factor Ψ (a function of M_1 and δ) such that

$$\frac{dP}{dw_{\text{exact}}} = \Psi\left(\frac{dP}{dw}\right)_{\text{"T-W"}} \tag{20}$$

The results of computation of λ and Ψ are presented graphically in Figs. 6, 7, 8, and 9.

Comments on Results

It will be observed that limiting lines appear in the graphs of the results because steady flow with attached shock is possible only in a certain régime of combinations of Mach Numbers and wedge angles. For any given value of half-wedge angle δ ($< \sin^{-1} 1/\gamma$) there exists a minimum Mach Number for which detachment of the shock does not occur. Also, for any given Mach Number, there exists a maximum half-wedge angle for which detachment of the shock does not occur. The maximum possible half-wedge angle for which flow with attached shock is possible is

$$\delta = \sin^{-1} 1/\gamma \qquad (\delta = 45.38° \text{ for } \gamma = 1.405)$$

* For a more general derivation of relations involving curved shocks see "On Curved Shock Waves," by T. Y. Thomas, *Journal of Mathematics and Physics*, Vol. XXVI, No. 1, April, 1947.

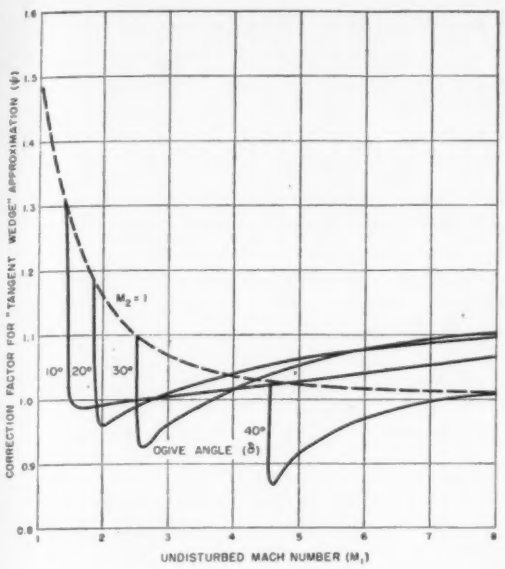

FIG. 8.

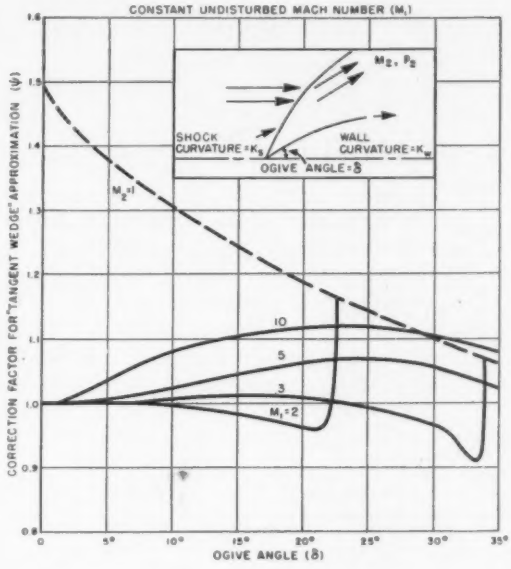

FIG. 9.

which requires an infinite Mach Number to maintain the attachment.

Since the correction factors λ and Ψ take on values both greater than unity and less than unity, it is difficult to make any simple generalizations concerning ranges of Mach Numbers or wedge angles for which either approximation method should be safe to use. From Figs. 6 and 8, however, it would appear that generally the "tangent-wedge" approximation is better at low Mach Numbers and the "wedge + Prandtl-Meyer" approximation is better at high Mach Numbers.

Announcing a New Department . . . Readers' Forum

It has been suggested by several members of the I.A.S. Editorial Committee that the *Journal* open a special department to fill the need for the more immediate communication of essential results of research in the greatly expanded and accelerated fields of the aeronautical sciences. Therefore, it has been decided to establish a new department, the "Readers' Forum," which will include letters to the editor for the quick publication of (1) brief reports of important findings in aeronautical sciences and (2) discussions of papers published in the *Journal*.

Specifications for Submission of Material

(1) All letters should be accompanied by a suggested short title, giving some indication to the reader of the subject under discussion.

(2) These letters should not exceed 800 words in length.

(3) Publication will be completed 6 to 8 weeks after receipt of the material.

(4) The Editorial Committee will not hold itself responsible for the opinions expressed by the correspondents, and no proofs will be sent to the authors.

(5) All letters should be double-spaced.

It is hoped that the new department may be started with the January, 1949, issue of the *Journal*. Contributions should be sent to:

Editor, Journal of the Aeronautical Sciences
2 East 64th street
New York 21, New York

SUGGESTIONS *for* CONTRIBUTORS

to the Publications of the

INSTITUTE *of the* AERONAUTICAL SCIENCES

The Institute of the Aeronautical Sciences invites both members and nonmembers from any country to submit papers for publication in the JOURNAL OF THE AERONAUTICAL SCIENCES and the AERONAUTICAL ENGINEERING REVIEW. The Institute, following the practice of other societies, does not pay for contributions.

The following directions for the preparation of papers, if followed by authors, will save correspondence, avoid the return of papers for changes, minimize the work of preparation for the printer, and save the expense due to the charges made for "author's corrections."

MANUSCRIPTS: The original typewritten copy of the paper is desired, double or triple spaced on one side of white paper sheets, consecutively numbered. There should be wide margins to allow for the marking of directions to the printer. Correcting, changing, or adding to papers after they are in type is costly. It is, therefore, imperative that papers submitted be in final form. Typographical errors may be corrected on proofs, but if authors wish to add material, they may do so at their own expense. In mailing, drawings may be rolled, but manuscripts should be sent flat. Send by first class mail (register, if you wish, for your own protection) to the Editorial Office, Institute of the Aeronautical Sciences, 2 East 64th Street, New York 21, N.Y. All manuscripts will be examined by the Editorial Committee and by the Editor. Authors will be advised as promptly as possible whether the paper is acceptable for publication.

TITLES: The title of the paper should be brief. The name and initials of the author should be written as he prefers. The use of the full name of an author is advocated because of the frequent duplication of initials and surnames which sometimes makes it difficult to establish the identity of the author. This is particularly important for large annual indexing and abstracting services. All titles and degrees or honors are omitted. The name of the organization with which the author is associated should be placed after his name on a separate line. The date on which the paper is received will be inserted by the Editor. The author's title should be indicated in a footnote.

SUMMARIES OR ABSTRACTS: An abstract to be printed at the beginning should accompany each article. It should be adequate as an *index* and as a *summary*. It should contain a statement of major conclusions reached, since summaries in many cases constitute the only source of information used in compiling scientific reference indexes. Abstracts printed in other journals, especially foreign, in most cases, consist of summaries from printed papers. The summary should explain as adequately as possible the major conclusions to a nonspecialist in the subject and should contain from 100 to 300 words, depending on the length of the paper.

SUBHEADINGS: Subheadings should be inserted by the author at frequent intervals. The work of editorial preparation will be simplified by the author providing many subheadings.

MATTER USUALLY DELETED: Photographs or illustrations of little technical interest and not showing advances in general practice. Too detailed tabular matter (general results of such tables may be included in the text). Lengthy descriptions of materials or processes or of preliminary experiments or theories that preceded final results; salient features only are of interest.

REFERENCES AND FOOTNOTES: References should appear as footnotes only, numbered consecutively, grouped together at the end of the manuscript. The arrangement should be as follows: (for books)—[1] Durand, W. F., *Aerodynamic Theory*, 1st Ed., Vol. 1, p. 23; Julius Springer, Berlin, 1934. (For magazines)—[1] Englund, C. R., Crawford, A. B., and Mumford, W. W., *Some Results of a Study of Ultra-Short-Wave Transmission Phenomenon*, Proc. I. R. E., Vol. 20, No. 12, pp. 481 and 482, March, 1933. Please give author, title, edition, volume, page, publisher, and date of publication as indicated. Omission of one required fact causes much extra editorial work and possible inaccuracies.

ILLUSTRATIONS: Illustrations should accompany manuscripts and each should always be referred to in the text, by number. Drawings or graphs should not be larger than 12 × 16 inches, and must be made with jet black India Ink on white paper or tracing cloth, the latter being preferred. *Do not use typewriter for lettering.* The smallest lettering on 8 × 10 inch figures should be no less than 1/4 inch high. Cross-section paper (white with black lines) may be used, but should not have more than 4 lines per inch. If finer ruled paper is used, the major division lines should be drawn in with black ink, omitting the finer divisions. In the case of finely ruled paper, only blue-lined paper can be accepted. *Tracing paper and blueprints* are not acceptable. Lettering and all markings must be large enough to be readable after reduction. Mail rolled or flat, never fold. Drawings that cannot be reproduced (including pencil drawings) will be returned to the author for redrawing, thus delaying publication of the paper. Photographs should be distinct and show clear black and white contrasts. They must be on glossy white paper. Avoid round and oval photographs.

CAPTIONS AND LEGENDS: Legends or captions must accompany each drawing or photograph submitted. If written on the drawing or photograph, they should be placed below and well outside the part to be reproduced. Each table should have a caption such as Table 1, Table 2, Table 3, etc. Captions should be complete in themselves so as to make the data intelligible to the reader without reference to the text. A duplicate list of captions for figures should be included as the last page of the manuscript. Use "Fig. 1" (not Figure 1), Figs. 3 and 4, etc., in both the text and the numbering of illustrations. In the text, "Eq. (1)," or "Eqs. (1) and (2)" are preferable to "Equation (1)." In captions and legends, except for "Fig." and "Eq.," and in table headings, write all words in full; do not abbreviate.

MATHEMATICAL WORK: Only the simplest formulas should be typewritten, all others should be carefully written in pen and ink, the writing to be large enough so that ample room is provided to mark mathematical matter for the printer. A considerable space for marking should be allowed above and below all equations. All complicated equations should be repeated on separate sheets with plenty of space left for marking. The solidus should be used for simple fractions appearing within the text. Make all expressions clear to the typesetter. Greek letters used in formulas should be clearly designated by name on the margin of the manuscript. All symbols should be clearly written and carefully checked. The difference between capital and lower-case letters should be clearly distinguished and care taken to avoid confusion between zero (0) and the letter (o), between the numeral (one) and the letter (ell) and the prime (′), between alpha and a, kappa and k, u and mu, v and nu, n and eta. All subscripts and exponents should be clearly marked and dots and bars over letters or mathematical expressions should be avoided. Avoid complicated exponents and subscripts. When it is necessary to repeat a complicated expression, it should be represented by some convenient symbol.

NOMENCLATURE AND ABBREVIATIONS: Standard abbreviations should be used, and it should be noted that most abbreviations are lower case such as m.p.h., b.m.e.p., i.hp., b.hp., hp., . . . etc.